OBJECT PROPERTIES AND GENERALISATION: DEVELOPMENTAL PSYCHOLOGY TO DEVELOPMENTAL ROBOTICS

SURESH KUMAR[1], MUHAMMAD WAQAS[1, 2], RAMEEZ AKBAR[3], SAEED AHMED KHAN[1] JAMSHED A. ANSARI[1]

[1]Department of Electrical Engineering, Sukkur Institute of Business Administration, Sindh, Pakistan
[2]School of Energy Science and Engineering, University of Electronic Science and Technology, Chengdu, Sichuan, P. R. China
[3]Department of Electrical Engineering, Quaid-e-Awam University of Science Engineering and Technology, Nawabshah, Sindh, Pakistan
Correspondence and requests for materials should be addressed to Muhammad Waqas & Suresh Kumar (email: mwaqas@iba-suk.edu.pk; suresh@iba-suk.edu.pk)

***ABSTRACT*— Having curiosity by nature, humans start to explore surrounding environment at very early age. Such exploration starts by interacting with objects in immediate reach, like toys. Human infants have been observed to make generalisation about their actions on objects and related outcomes by learning from interactions with them. In psychology, it has been found that these generalisations are strongly influenced by objects' visual properties. In this study we present simulation of generalising object properties based on interaction and visual features. The results show that object shape is more reliable than other object visual feature for generalising outcome.**

Keywords: artificial intelligence, developmental robotics, behavioural learning, schema system

1. INTRODUCTION

Humans have curiosity of understanding the world, even universe, by nature. Curiosity is found in most living species, however, humans, being capable of reasoning and developing the knowledge, are involved most to explore and satisfy their curiosity. Humans start to explore the world at very beginning of the life, early infancy, even when they have poor sensory and motor capabilities [1].

Visual experiences are very important to learn about the objects, along with the manual explorations. In fact, visual ability helps to learn motor capabilities and without visual ability infants have been found with delayed motor developments [2-4]. Piaget, in his famous theory of cognitive development, had represented human age into six different learning stages [5]. The very first stage starts from right after the birth up-to two years of age. He labelled this stage as "Sensorimotor" stage, because he believed that at this stage infants' leaning and knowledge is associated with their sensorimotor experiences with the surrounding environment and objects. His theory suggests that object exploration, visually and manually, helps infant to understand about the object physics, its properties and affordability. Infants remember actions on objects, and related outcomes, and have been observed to use those actions on the other, novel, objects to obtain identical outcome [6-8]. However, they extend their expectation to novel objects which have similar visual features to the one/those they experienced before.

Extending expectations or actions/situations to novel objects having particular set of similarities with the objects/situations experienced in previous time can be labelled as "Generalisation". Shepard believes that human as well as non-humans species posses this generalising capability [9], which helps to learn and extend the learning. In generalising object, objects features, form (e.g. shape, size) & surface (e.g. colour, texture) features, are very important.

Understanding about object properties in early age using visual and manual experiences have been widely studied in the developmental psychology. In those studies, psychologists have found that infants rely on object's form features, rather than the surface features, to generalise and extend actions, and expectations, to novel objects [6-8, 10]. In particular, they rely on object shape for making general conclusions and expect that object of similar shape will give same outcome or show similar behaviour when acted upon them.

Infants have been found to associate and generalise non-obvious properties, such as squashy sound, with objects. Baldwin et al. found that 9-16 months old extend their experience to novel objects which have similar shape to one they experienced before. They presented an object to infants which produced some noise while grasping. Infants were allowed to interact with such object only for 20 seconds and later they were presented similar and different shaped objects, some of them possessed same non-obvious property (squashy noise). In these experiments infants have been found to explore, manually, more those objects which have shape similarity but did not produced the sound as they experienced before. The objects of different shape were explored less, irrespective of having non-obvious property. More manual exploration was observed in surprise state as infants expected the object to produce noise and failure to produce such outcome they tried to explore more.

From above experiment, it seems that infants; 1) generalise very quickly, even with one and 20 seconds experience. 2) Rely on shape for generalisation. Graham & Poulin [7] and Welder & Graham [8] found very similar results in similar experiments, and same two points (generalising quickly and reliance on shape for generalising) are evident from their experimental results.

In practical robotics, robots may need to observe and act upon different objects. These actions, on objects, can be similar in term of kinematics or outcome. For an efficient robotics application, a robot or robotic system should learn from as less experiences as possible and extend the learning to new and novel situations/objects, irrespective of learning environment. This can be possible if robot is able to generalise objects/situations based on the sensory features, especially visual features, as humans do. Various robotist have been working on this topic and we can see some fascinating results as well.

In this paper we are proposing an mechanism for generalising non-obvious object properties related to the visual properties using an adaptive learning tool, Dev-PSchema, for artificial agents. We will evaluate our mechanism using very similar experiment about generalising object properties, performed by Baldwin [6], but in a simulated robotic environment. In section-2 we will discuss about the robotics studies on this topic. In section-3 we will discuss about the tool PSchema and its extended version Dev-PSchema. In section-4, experiment and related results will be discussed. In section-5 well will look into the developmental psychology to validate the results and in section-6 we will end with the conclusions and future work.

2. RELATED STUDIES

Achieving human like intelligence in artificial agents is aim of the researchers in the field of Artificial Intelligence (AI). Researchers, in AI, are working different aspects of learning. Here we are interested in object learning leaning and particularly generalisation. Sinopov & Stoytchev in [11] presented a mechanism for learning and generalising tool use. Learning in this system was performed by the demonstration and using visual features system generalises the outcome of the tool with particular actions. They used compact decision tree model for generalisation and evaluated the system by extending the learning to novel (never experienced before) tools. This system shows good accuracy for predicting outcome for familiarized (experienced before) tools but achieved accuracy 56% in predicting the outcome for novel tools.

Similarly Pastor et. al. developed another learning mechanism for generalising “Grasp-Move-Place” task [12]. This system was trained to perform this task by demonstration. Motion libraries were developed while performing the task by human demonstrator wearing exo-skeleton robotic arm. The motion libraries were then transferred into 7 Degree of Freedom (DoF) robotic arm and system was evaluated by performing same task on novel objects. The position for placing the grasped object was generalised by the system and was able to successfully perform the task. A very similar study was performed in [13]. In this study, researchers demonstrated the generalising capability of the system for reach and transport task. Task was generalised after three demonstrations by finding the common elements in the topological sequence of the action for the given task.

These learning systems, described above, show a good degree of accuracy for generalisation. However, in these studies systems were trained to perform these tasks either by demonstrations [12, 13] or supervised learning [11]. In the field of

developmental robotics, it is aimed to develop learning mechanisms inspired from the developmental psychology. In developmental psychology, it is considered that early object learning and actions associated with those are related by sensorimotor experiences [5]. Robotists are also developing system having learning mechanism based on senosrimotor experiences.

Geib et. al. [14] proposed a high level learning mechanism named as Objec-Action-Complexes (OACs). Proposed system is able to learn from the high level sensorimotor experiences and plan actions according to learning experiences. System uses high level representation and authors claimed that system is able to bridge the gap between low level robotic control and high level representation and action planning system. The OACs are learning outcome containing high level sensory states before and after the action and action itself. System uses multiple OACs to find the common elements between them for generalisation. The generalised OACs are referred as Instantiated State Transition Fragment (ISTF), which are used for action planning and prediction. Kruger et. al. [15] implemented this system in their work. Action prediction has been demonstrated in this work using ISTFs, however, system was trained for prediction using supervised learning mechanism in neural networks.

Hermans et. al. demonstrated affordance prediction model in [27]. The prediction model is based on visual attributes of the objects, such as size, shape etc, and physical attributes (e.g. weight) perceived through visual information. This model was trained with Support Vector Machine (SVM) and K-Nearest Neighbour (k-NN) networks to predict the affordances for the novel objects. The prediction for novel objects can be considered as generalisation of attributes for affordance.

Recently, Aguilar proposed another high level learning system for artificial agents termed as "Dev-ER" [16]. This system also uses high level knowledge representation of world and actions. Learning outcomes are in shape sensor motor schemas, containing context and actions. System is also able to create generalised schemas based on the experiences. Generalisation in this system is based on the deductive inference, by creating very abstract to content specific schema. Moreover, in the study, this system was provided with basic action schemas to act in the environment.

The robotic models discussed above, have shown significant results in this area of research. However these models, except [16], are trained with neural networks for learning predictions and generalisations. Model presented in [16] uses deductive inference for generalisation, by creating very generalise learning and develop it to specific learning with experiences. In our proposed mechanism inductive generalisation is used. By which non-generalised learning (schemas) are created initially, which are used create generalised learning with experiences.

3. METHODOLOGY

Piaget believed that human knowledge is stored in shape schemas in the memory and at first stage these schemas are sensor motor experiences only [5]. Further, he believed that infants reason the situations in the world using schemas. This process is referred as "Assimilation". If infant's knowledge is unable to deal with the situations in the world, he/she created new schema accordingly and process is referred as "Accommodation".

Although, Piaget's work has been argued by many psychologists, especially Spelke's core knowledge concept [17], yet it is considered an influential study of infant psychology. AI researchers, also, have developed and implemented learning systems for artificial agents based on the sensorimotor experiences. To the best of our knowledge Drescher [18] was the first one who proposed schema based learning system for artificial agents. He referred such systems as schema mechanism, where learning involved with experiences.

In this work we are using an extended version of adaptive learning tool, PSchema [19], which offers continual, online learning. Inspired from the Piaget's sensorimotor stage of learning from Cognitive theory and Drescher's [18] proposed system, this tool uses sensorimotor experiences for building knowledge and learning are presented in the shape of schemas containing action and context. Fig. 1 shows a simple action schema.

Grasp Schema		
Preconditions	Action	Postconditions
Colour 'Red/Green' at 2,1 Shape 'Cube' at 2, 1 Touching at 2, 1	Grasp	Colour 'Red/Green' at 2, 1 Shape 'Cube at 2, 1 Sound Observation

Fig. 1: A simple action (grasp) schema

Action schemas contain sensory states before and after actions, known as preconditions and post conditions. System uses excitation calculator to select a schema, based on the similarity with current state and novelty, for execution. Schema building mechanism decides and builds schemas after execution, using "Assimilation & Accommodation" process. We extended this system and named as "Dev-PSchema". In sections 3.1 we will discuss about the extensions that we made in the system.

3.1 DEV-PSCHEMA

We extended schema building and generalisation mechanisms. In schema building mechanism of PSchema, we extended the system to undergo the accommodation process and create new schema when system get new state or subset of the post-conditions of executed schema. In original version of "PSchema" system did not created new schema when outcome of an action schema was subset of post-conditions of any of the stored schemas, having the same actions and preconditions. Schema building routine is called every time sensory state is updated in the system, usually before and after execution of an action. The extended schema building mechanism is described in simple form in Algorithm 1.

***Algorithm 1*: Updating State & Create Schema**

Procedure Update_state(State New)
  if *Last schema* **OR** *Last state is Null* **then**
    Return
  end if
  if *New state different from Last state* **then**
    Preconditions = Last state
    Action = Last schema action
    Postconditions = New state
    make new schema(Preconditions; Action; Postconditions)
  end if
  if *New schema not in memory* **then**
    Add New schema in memory
    Generalise(New schema)
  end if
    Return
  end procedure
end

Schema, for action execution, is selected using excitation calculator which finds the similarity between the sensory state in the environment and schemas in memory. Here, most salient schema (post-conditions matching with new state) is selected for execution. Here we are using same algorithm for excitation as it is in PSchema. Algorithm for excitation calculator can be found in [20].

We extended generalisation algorithm as well. Generalisation in PSchema was decided on number of schemas that have similar action and context (preconditions and post-conditions). If a property appears in different values in similar schemas then that property will be generalised, replaced with dollar sign "$" including a random, unique alphabetic character. With "$" sign system indicates that property is generalised, whereas alphabetic character represent any value of that property. Generalisation algorithm in PSchema can be obtained from [20]. A simple generalised schema is shown in Fig. 2.

Complete Generalised Schema		
Preconditions	Action	Postconditions
Colour '$a' at $b, $c Shape '$x' at $b, $c Touching object	Grasp	Colour '$a' at $b, $c Shape '$x' at $b, $c Holding object

Fig. 2: A simple generalised grasp schema

Fig. 2 shows that properties, such as object colour, shape and position, are generalised. This generalise schema can be used to grasp any object (if graspable) when end affecter is touching the object and will result in holding the object.

In Dev-PSchema, we made changes in generalisation algorithm and now systems generalises those properties, as well, which appeared in bootstrap schema (see IV-B.1). These changes enable the system to identify the properties which appeared in result of action and reaming will be generalised even if they appeared once in similar schemas. Simplified, extended algorithm for generalisation is shown in Algorithm 2.

Algorithm 2: **Generalisation Algorithm**

Procedure GENERALISE *(New Schema; Schema Memory)*

if *New don't have preconditions* **then**

return

end if

for *each schema S in Memory* **do**

if *S not generalised AND have similar context* as *New* **then**

Add \S" in List similars

end if

if *action in S and New are similar AND postconditions in S are less than postconditions in New* **then**

Add postcondition properties in old props

end if

end for

trial schema = copy of new

for *each property* ***P*** *and* ***P2*** *in precondition and postconditions respectively of schema*

S from List similars **do**

if *Value of* **P** *and* **P2** *is same OR* **P** *in old props* **then**

Replace value of each property P in trial schema with random unique alphabet

end if

end for

add trial schema in memory

end procedure

end

This mechanism will help to learn the system about the dependencies for an schema and the common properties in the schema will be generalised. In the work we get two types of generalised schemas. In one type all the properties are generalised, named as complete generalised schema. In other type, named as partial generalised schema, one or more than one property will not but generalised but at least one property will be generalised.

4. EXPERIMENT AND RESULTS

To evaluate the system we will perform experiments and observe generalised schemas. We expect that system will create complete generalised schema when it finds dependent properties with different values and partial generalised schema when dependent property is only available in one value. Here we considered object shape as dependent property for a particular grasp schema. If system finds similar schemas in memory with different types of shape then it will generalise the shape, else it will give partial or non generalised schemas, depending upon the state.

4.1 EXPERIMENTAL SET-UP

We used a simple simulator to evaluate the system. Simulator contains end effector, a hand, to perform actions in the environment. Simulator is able to perform two basic actions, reach and grasp. These actions are defined at high level, without low level kinematics of the agent, robot. Simulator also contains objects of different shape and colour. Objects are defined with their high level sensory information, colour, shape and position. In this experiment we are using two types of objects. One, which provides some non obvious property e.g. sound, when grasped. Spheres and cubes are of this category, irrespective of their colour. Cylinders, irrespective of colour, are objects of the second category which does not produce any non-obvious property when grasped. Fig. 3 shows the environment of the simulator.

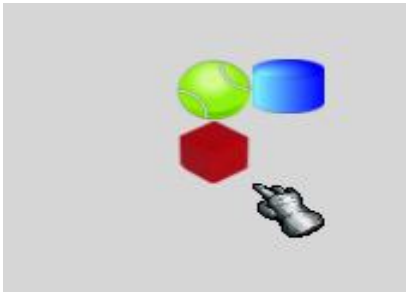

Fig. 3: Simulator environment

4.2 EXPERIMENTAL STAGES AND RESULTS

Experiment is started with the "Boot strapping" process. After this, first object is introduced to interact with. To evaluate the system, we divided further experiment into four different paths(A-D), where object of same/different shape and colour, with respect to first object, are introduced. All of the objects at this stage are of same category as first object which produced sound when grasped. At later stage an object of different category, cylinder, is presented at each path. Fig. 4 shows the experimental flow diagram.

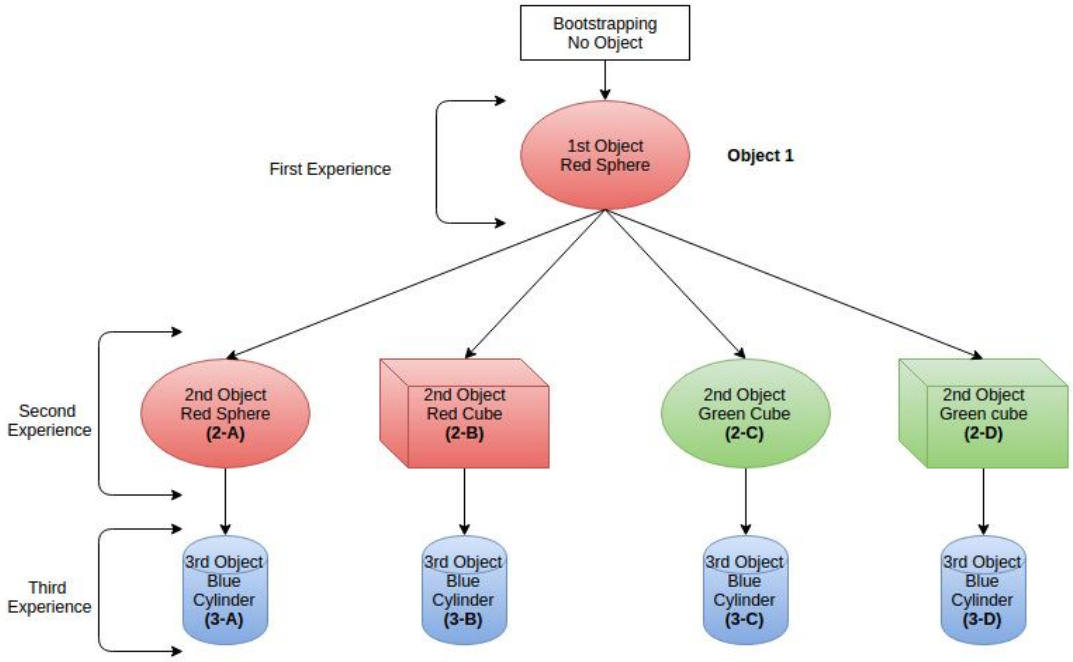

Fig. 4: Experimental stages

It should be noted that object is represented with separate colour and shape observations, considering as separate sensory channels. Each of the stage mentioned in the Fig. 4 is discussed bellow.

1) Bootstrapping: At this stage system is allowed to perform all the basic actions. In this case reach and grasp. Simulated end effecter, Hand, will reach at each space a finally grasp action in the environment and store schema for the action. We refer these schemas as bootstrap schemas, which generated without any object in the environment. These schemas do not have preconditions. It should be noted that grasp action without any object in the environment will result in hand close, which give touch simulation generated by touching own hand. Fig. 5 shows reach and grasp bootstrap schemas.

Reach Schema		
Preconditions	**Action**	**Postconditions**
	Reach	Colour 'Hand' at 1, 1

Grasp Schema		
Preconditions	**Action**	**Postconditions**
	Grasp	Colour 'Hand' at 1, 1 Touching object at 1, 1

Fig. 5: Experimental Stages

This process provides the basic set of schema for basic actions. Which will be used to interact with objects and higher level of action schemas will be created.

2) First Experience: At this stage object is introduced in the environment. First introduced object is red sphere, which produces sound when grasped. Introducing an object, in the environment at any reachable position, triggers the reach schema for that position by calling memory of own hand at that position. When object reaches that position, it touches the object, which results simulated touch sense. This touch sense excites the grasp schemas, as it is the only schema that contains the touch sense. System executes the grasp schema and object produces sound. This new observation, sound, triggers the system undergo schema building process and creates new schema. Fig. 6 shows the step by step process at this stage. After system completes the schema building process, object is removed from the environment and moved to next stage.

3) Second Experience: At this stage, four different learning paths are produced by introducing different objects of same category but at different positions. The change in object shape, colour or position triggered the system novelty and system

interacts with the object. This stage resembles the four different individual babies at same learning age, having same experience of first object.

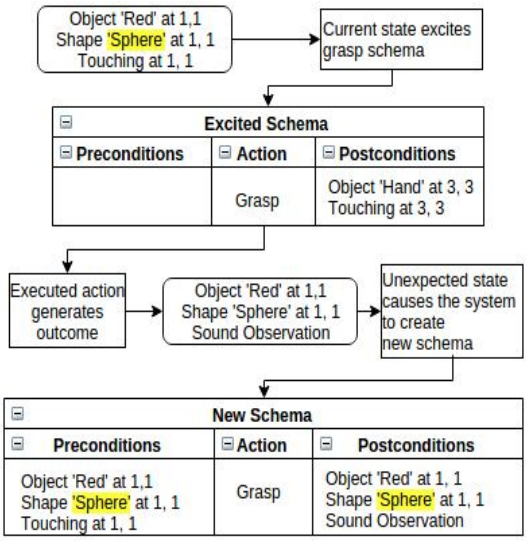

Fig. 6: First object experience

Reach and grasp schemas are selected and executed, respectively, at all four paths when object is introduced. At path A and C where object of same shape but same and different colour from the one experience before, are introduced. After creating new grasp schema, for either of these objects, system undergoes through generalisation process as two schemas with same action and similar context are present in memory. Schema building process for paths 2A or 2C is shown in Fig. 7.

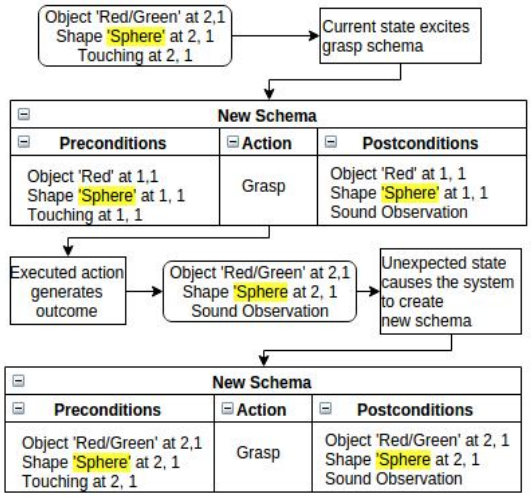

Fig. 7: Second object, same shape same/different colour

Similarly for paths 2B and 2D system undergoes the same process as shown Fig. 7, except objects are of different shape. At every path at this stage system undergoes for generalisation process and creates generalised schemas. For paths 2A and 2C system creates partial generalised schema and for 2B and 2D system creates complete generalised schemas. Both of these schemas are shown in Fig. 8.

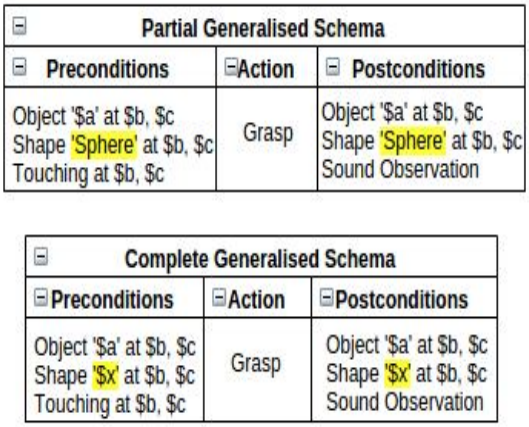

Fig. 8: Partial (top) & complete (bottom) generalised schemas

From Fig. 8 it is clear that system creates partial generalised schema, not generalising shape, when object of same shape with same/different colour is grasped. For object having different shape, system creates complete generalised schema, generalising shape, colour and position.

4) Third Experience: To evaluate the changes we made in schema building, we introduced another object of different category. This object, cylinder, when grasped produces no sound, unlike the last two object experiences. Introducing this object in the environment triggers the system to use generalised grasp schema to grasp this object. From the post conditions of the schema, system expects that this object will also respond with sound when grasped. However, failure to get such observation, system undergoes the "Accommodation" and create schema for this object.

This new schema confirms the two processes; 1) System is able to deal with over- generalisation. 2) System creates new schema even outcome is subset of the schema post conditions. The results produced in this experiment are further discussed in the section 5.

5. DISCUSSION

We started our experiment with bootstrapping process, where system builds basic set of schemas. It can be argued that system learns about these actions in supervisory learning mechanism. However, the system performs random motor actions in unsupervised environment and without any object present to interact with. This resembles to the motor babbling in infants. Where infants learn about own movements and control them while observing and acting randomly [5]. Goldstein also believes that humans learn own motion observing changes in environment and linking proprioceptive information with it [21].

From the results of the second experience of the object, we obtained partial generalised schema for object having same shape and complete generalised schema for objects of different shape. This output is similar to experimental results has been reported in [6, 8]. In their experiment researchers found that infants expected same non-obvious property from the object of same shape, from the one they experienced earlier. These results shows that colour of the object have no effect on this. Object having same shape, irrespective of colour, were expected to posses the non-obvious property. However, objects of different shapes, even same colour, were not considered as same and non-obvious property was not expected.

In various other experiments it has been found that infants rely on shape, rather than the colour, to recognise and identify the object [7, 22-25]. These evidences from the psychology show that shape is more important feature than colour when it is associated with certain situations or conditions. So the question arises why shape of the object is more important than the colour? Psychologists have different theories on this matter. Researchers in [7] believe that shape feature is easily perceivable, which does not require more experiences for recognition. They also believe that shape is an integral part of the representation used for objects. However, Nicholson & Keith [23] argues that colour information is also used in representation but shape information is more influential. They believe colour information speeds up the recognition process but, yet, shape is most reliable information and both are encoded separately in representation. Similarly Wilcox [25] believes that infants link shape information with the event outcome, hence they use same information to perform predictions.

These evidences clearly supports that shape is more important in object representation and it is separately represented from colour. This validates our object representation, separately in colour and shape. Our findings are also in-line with these evidences as we obtained partial generalised schemas for same shape objects but complete generalised for different shapes. The generalised schemas represent a concept that schema systems builds with experiences. At stage 2A or 2C system builds concept that spherical object of any colour will produce sound when grasped. Similarly for stages 2B or 2D it builds the concept that object of any shape and colour will produce sound when grasped. These concepts are in the shape partial and complete generalised schemas respectively.

At stage 3A-D, system experience third object and creates new schema. System initially uses its concept to deal with this new object. For stage 3A or 3C system believes that only spherical object will produce the sound, which is verified. However, system doesn't have experience with new object it undergoes schema building process. Similarly, at stage 3B or 3D system expects that new object will produce sound when grasped. But failure triggers the system to create a new memory, schema, about this experience.

At third stage system creates new schema, no matter at which path it is (A-D). The information, no sound, while grasping ends up with new schema. This what expected from infants as well when they fail to deal new information with their existing knowledge. Piaget [5] believes that using "Accommodation", human builds up new knowledge when failed to deal using existing. In one of recent study, Stahl and Feigenson found that infants' learning is affected by the expectation of their actions and related outcomes [26]. Their findings support Piaget's thought about "Accommodation" process in learning.

6. CONCLUSION

Considering human learning model, in developmental robotics it is aimed that a learning model should be continuous, adaptive, domain independent and extending learning in novel

environment. This learning model has ability to learn continuously and use the past learning in novel situations. Learning bootstrap schema and using those in novel situation when objects were introduced, shows the capability of the system for continuous, adaptive learning, irrespective of the environment. System is also able to build hierarchical structure of knowledge, as it uses bootstrap schema for actions on the objects and develops next level of knowledge for those actions by creating new schemas.

Generalising capability helps the system to learn and build concepts. These concepts may not fit every situation, however this is what have been observed in humans as well, where humans generalise very quickly and then learn from their mistakes. Experiment in this study demonstrated that system makes generalisations which may fails, as in case of 3B and 3D. Failure generalisation triggered system to explore further and develop new knowledge.

We believe this system provides a way to investigate the learning capability in early infancy in humans by incorporating representation of knowledge at that age. This system works with high level representation and abstract actions. Thus system need to work with low level sensory information processing such as visual libraries and low level kinematics system of an artificial agent for abstract actions. In future we are looking to extend this mechanism for considering failure in more specified way and develop different levels of generalisations. We will also like to integrate this system with a robotic platform in near future.

REFERENCES

[1] Slater A.,"Introduction to Infant Development", Oxford University Press, 2007.

[2] Adelson E. and Fraiberg S., "Gross Motor Development in Infants Blind from Birth", Child Development, Vol. 45, pp 114–126, 1974.

[3] Corbetta D. and Snapp-Childs W., "Seeing and Touching: The Role of Sensory Motor Experience on the Development of Infant Reaching" Infant Behaviour and Development, Vol. 32(1), pp 44–58, 2009.

[4] Prechtl H. F., Cioni G., Einspieler C., Bos A. F., and Ferrari F.," Role of Vision on Early Motor Development: Lessons from the Blind", Developmental Medicine & Child Neurology, Vol.43(03), pp 198–201, 2001.

[5] Piaget J., Cook M., and Norton W., "The Origins of Intelligence in Children", International Universities Press New York, Vol.8, 1952.

[6] Baldwin D. A., Markman E. M., and Melartin R. L., "Infants' Ability to Draw Inferences about Non Obvious Object Properties: Evidence from Exploratory Play", Child Development, Vol. 64(3), pp 711–728, 1993.

[7] Graham S. A. and Poulin-Dubois D., "Infants' Reliance on Shape to Generalize Novel Labels to Animate and Inanimate Objects", Journal of Child Language, Vol. 26(02), pp295–320, 1999.

[8] Welder A. N. and Graham S. A., "The Influence of Shape Similarity and Shared Labels on Infants Inductive Inferences about Non Obvious Object Properties", Child Development, Vol. 72(6), pp 1653–1673, 2001.

[9] Shepard R. N., "Toward a Universal Law of Generalization for Psychological Science", Vol. 237(4820), pp 1317–1323, 1987.

[10] Gershkoff-Stowe L., Connell B., and Smith L., "Priming Over Generalizations in Two-and Four Year Old Children", Journal of Child Language, Vol. 33(03), pp 461–486, 2006.

[11] Sinapov J. and Stoytchev A., "Learning and Generalization of Behavior Grounded Tool Affordance", IEEE 6th International Conference on Development and Learnin ICDL, pp 19–24, 2007.

[12] Pastor P., Hoffmann H., Asfour T., and Schaal S., "Learning and Generalization of Motor Skills by Learning from Demonstration", In ICRA'09. IEEE International Conference on Robotics and Automation, pp 763–768, 2009.

[13] Nicolescu M. N. and Mataric M. J., "Natural Methods for Robot Task Learning: Instructive Demonstrations, Generalization and Practice", In Proceedings of the Second International Joint

Conference on Autonomous Agents and Multiagent Systems, ACM, pp 241–248, 2003.

[14] Geib C., Mourao K., Petrick R., Pugeault N., Steedman M., Krueger N., and Worgotter F., "Object Action Complexes as an Interface for Planning and Robot Control", IEEE RAS International Conference on Humanoid Robots, 2006.

[15] Kruger N., Geib C., Piater J., Petrick R., Steedman M., Worgotter F., Ude A., Asfour T., Kraft D., and Omrcen D., "Object–Action Complexes: Grounded Abstractions of Sensory–Motor Processes", Robotics and Autonomous Systems, Vol.59(10), pp 740–757, 2011.

[16] Aguilar W. and Perez De Ver R. P. Y. Perez De Ver "A Computational Model of Early Cognitive Development as a Creative Process", Cognitive Systems Research, Vol.33, pp 17–41, 2015.

[17] Spelke E. S., Phillips A., and Woodward A. L., "Infants' knowledge of Object Motion and Human Action", 1995.

[18] Drescher G. L., "Made-Up Minds: A Constructivist Approach to Artificial Intelligence, MIT Press, 1991.

[19] Sheldon M. and Lee. Pschema M., "A Developmental Schema Learning Framework for Embodied Agents", IEEE International Conference on Development and Learning (ICDL), Vol.2, pp 1–7, 2001.

[20] Sheldon M. T., "Intrinsically Motivated Developmental Learning of Communication in Robotic Agents", PhD Thesis, Aberystwyth University, September 2012.

[21] Goldstein E. B., "Sensation and Perception", Cengage Learning, 2010.

[22] Belongie S., Malik J., and Puzicha J.," Shape Matching and Object Recognition using Shape Contexts", Pattern Analysis and Machine Intelligence, IEEE Transactions, Vol.24(4), pp 509–522, 2002.

[23] Nicholson K. G. and Humphrey G. K., "The Effect of Colour Congruency on Shape Discriminations of Novel Objects", Perception, Vol.33(3), pp 339–353, 2004.

[24] Tremoulet P. D., Leslie A. M., and Hall D. G., "Infant Individuation and Identification of Objects", Cognitive Development, Vol. 15(4), pp 499–522, 2000.

[25] Wilcox T., "Object Individuation: Infants Use of Shape, Size, Pattern, and Colour", Cognition, Vol. 72(2), pp 125–166, 1999.

[26] Stahl, A. E. and Feigenson L., "Observing the unexpected enhances infants' learning and exploration", Science, 348(6230), pp.91–94, 2015.

[27] Hermans, T., Rehg, J. M. and Bobick, A., "Affordance prediction via learned object attributes", IEEE International Conference on Robotics and Automation (ICRA): Workshop on Semantic Perception, Mapping, and Exploration, 2011.

DESIGN AND ANALYSIS OF WIND ACCELERATING AND GUIDING ROTOR HOUSE FOR A VERTICAL AXIS WIND TURBINE

Abdul Latif Manganhar*, Saleem Raza Samo**, Muhammad Ramzan Luhur*** and Altaf Hussain Rajpar****

ABSTRACT

The intermittent behavior and low wind speed (at sites) are major barriers to wind energy effective harness. Several efforts have been made to overcome these shortcomings; however, ducting or funneling of rotors has been proposed as good technique to achieve improvement over these deficiencies. Latter approach not only improves efficiency, but covers environmental concerns of wind power generators also. For the sites where wind speed is very low and turbulent, vertical axis wind turbines (VAWTs) remained the better choice. In this study wind accelerating and guiding rotor house (WAG-RH) is introduced to enhance the working range of a VAWT in low wind speed with improved efficiency. The WAG-RH collects the free stream wind parcel, directs and accelerates it towards the useful space left for VAWT to avoid the negative torque and generate more positive torque. In present study, multiple WAG-RH design concepts have been investigated, and favorable results have been achieved in terms of increase in velocity. Nevertheless, final configuration RH(4,45) gives the better performance over all proposed WAG-RH configurations. The numerical simulations are performed using design software Gambit and CFD software ANSYS Fluent 14.5 and compared with experimental results. The comparison of both approaches show good agreement.

Keywords: Ducting; vertical axis wind turbine; wind acceleration; rotor efficiency; ANSYS Fluent

1. INTRODUCTION

The power output of a wind turbine is proportional to cube of the wind speed that impinges on the rotor blades. Any technique, which can increase the upstream wind speed to the turbine, even by a small amount, can largely improve the power output of turbine. Converging diverging ducts have been used to increase the upstream wind speed striking the turbine to improve its power output [1-3]. Ducting of wind turbine rotors have been done mainly for three reasons. First, to improve the power of low-speed wind and enhance working range of wind power generators; second, to improve the efficiency of wind rotors through effective working of incoming wind; and third, to avoid the environmental effects of wind energy as reported in [4,7]. The maximum theoretical efficiency, a conventional wind turbine may extract, is 59.3% of the power available in a stream tube of wind with an area equal to the swept area of the rotor, known as Betz limit (Betz 1966). It has been reported by several researchers that improvement in efficiency beyond the Betz limit can also be achieved by placing a turbine inside a shroud [8-14]. The ducting of vertical axis wind turbine (VAWT) was first introduced by Webster [15] for a building integrated VAWT. In this concept wind enters horizontally and leaves the duct vertically after transferring its energy to vertical rotor. This approach was proved effective and robust in operation by [16]. In 2008, Hau and Cheng [17] developed a bucket-shaped duct for an in-house VAWT and reported 80% increase in rotor efficiency compared to its bare working efficiency.

Carcangiu and Montisci [18] introduced a roof top system suitable for wind power generation in urban areas and reported that the system can fulfill the energy demand of a common building. Corscadden [19] proposed an idea to investigate the improvement over potential performance possible with strategic placement of VAWT in the built environment.

* Assistant Professor, Department of Mechanical Engineering, Quaid-e-Awam University of Engineering, Sciences and Technology, Nawabshah, Pakistan

** Professor, Department of Energy and Environment Engineering, Quaid-e-Awam University of Engineering, Sciences and Technology, Nawabshah, Pakistan.

*** Assistant Professor, Department of Mechanical Engineering, Quaid-e-Awam University of Engineering, Sciences and Technology, Nawabshah, Pakistan

**** Professor, *Department of Mechanical Engineering, Quaid-e-Awam University of Engineering, Sciences and Technology, Nawabshah, Pakistan

In order to avoid the negative torque produced by VAWT, wind deflectors, curtains and concentrators have been introduced. A concentrator nozzle attached at rotor inlet can direct (wind flow only to the concave side of blade) and increase the wind speed at rotor inlet, leading to improved power coefficient of VAWT [20,21]. A wind-solar hybrid renewable energy harvester was introduced by Tong et al. [22], which overcomes the inferior aspect of low wind speed by guiding and increasing the speed of free-stream wind through fixed or yaw-able power-augmentation-guide-vane (PAGV) before approaching the wind turbine. Latter system was again verified by placing a Sistan wind turbine inside the PAGV and improved performance of rotor has been reported [6]. Nevertheless, both the concentrator nozzle and the PAGV concepts, eliminate the possibility of VAWT to receive wind from any direction and require yaw mechanism.

To overcome this deficiency, a rotor house design based on wind accelerating technique was proposed by Manganhar et al. [23], which can receive wind from all the directions, besides accelerating and concentrating the wind in the proposed rotor zone. Additionally, the proposed design can accommodate a solar air heater on upper surface of the house, which can further accelerate the wind inside the structure beside the use for space heating in winter. At the same time, Chong et al. [24] also introduced a shrouded wind-solar hybrid renewable energy and rain water harvester with an omni-directional-guide-vane (ODGV) for urban high-rise application, where authors claimed that ODGV guides the flow to an optimum flow angle before it interacts with the rotor blades. However, neither the flow angle nor the other design parameters are optimized as it is claimed. Authors only analyzed one design configuration for three wind directions.
The recent development of the technology sector of micro vertical wind systems is inclined to improve the performance of technology and versatility of its use. This can be achieved through the integration of new technologies such as magnetic levitation rotors to reduce friction, and the new Invelox turbine which relies on a wind acceleration duct immediately before the turbine itself and the funnel-shaped structure with multiple openings to catch breezes from any direction [24a].
In this work emphasis has been given to increase the wind speed by developing a novel wind accelerating and guiding rotor house(WAG-RH) system. The proposed WAG-RH is a simple and an economical design that can collect, guide, accelerate and concentrate free stream wind parcel of an area nearly equal to the projected area of the rotor house before interacting the rotor blades inside the house. The present design compared to complex design (with eight tapered walls and concave top surface) introduced by Chong et al. [24], uses four uniform walls and a flat top surface. The performance parameters of WAG-RH have been optimized by testing multiple-RH design configurations with four wall geometries using numerical simulations. Numerical methods compared to experimental methods are less expensive and less time consuming for testing of such systems[24b]. The final WAG-RH design gives good improvement over in-coming wind speed and guides it to pass through most useful location in the rotor zone. The simulated results have been compared with the experimental results and show good agreement.

The paper is structured in such a way that Section 2 describes the design parameters and the methods applied. Section 3 presents the results and discussions, and final Section 4 concludes the outcome of the work.

2. MATERIALS AND METHODS

The WAG-RH is a house for a VAWT, which improves the performance of a conventional vertical rotor. The geometrical features of the proposed WAG-RH design are shown in Fig.1, where D is the diameter of the rotor house and d the diameter of the rotor zone. The dimension H represents the height of the vertical wall and B its length.

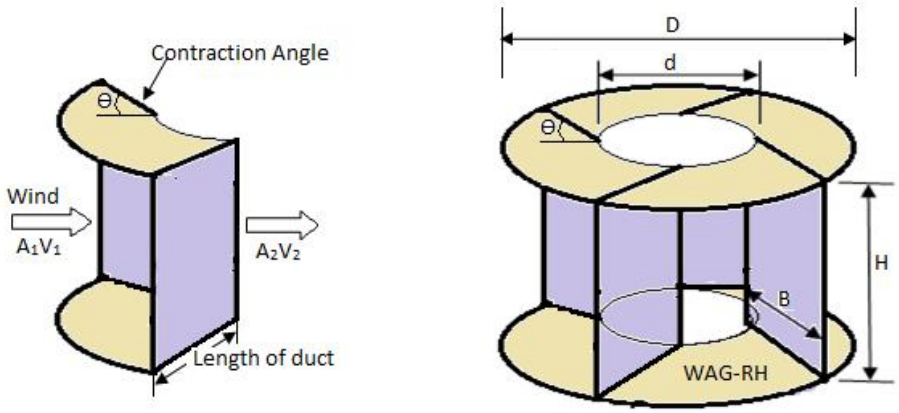

Fig. 1 Geometrical features of WAG-RH

The rotor house has four vertical walls, which constitute four converging channels towards the rotor zone. The parameters A_1V_1 describe the flow at inlet and A_2V_2 the flow at outlet of the channel, where A_1 and A_2 are the areas, and V_1 and V_2 the velocities at inlet and outlet of the channel, respectively. The convergence of each channel depends on the tilt angle (contraction angle) and the length of the channel wall. Both the contraction angle and the length of the channel, change the contraction ratio (A_1/A_2) of the channel, which cause variation in the velocity. The higher the contraction ratio, the higher the increase in velocity. The length of the channel also changes the diameter of the rotor house leading to change in the diameter ratio (D/d).

The initial design specifications (used for experimental analysis) for the walls were taken as 0.3 m length and 0.3 m height. Each wall was tilted at contraction angle of 45^o in clockwise direction about its origin at the circumference of circular rotor zone. This configuration gives the diameter ratio of 4 with 0.2 m diameter of the rotor zone.

2.1 SIMULATION OF WAG-RH GEOMETRY

The numerical simulations are performed by several experts such as [24-26] using CFD as an essential tool for analyzing wide-range of wind flows for the structures such as proposed in present study. The Navier-Stokes equations have been considered as the model equations for all CFD problems, which formulate the principles of conservation of mass, energy and momentum in the form of partial differential equations. In this study two-dimensional steady state Reynolds Averaged Navier-Stokes (RANS) equations are used as governing equations, which are solved through CFD educational version of ANSYS fluent 14.5. The RANS method is one of the most popular methods used by the CFD community [27] to solve the complex type flow problems.

The selection of a turbulence model in any CFD code is highly dependent on the nature of the flow considered [28]. The change in nature of flow, changes its mathematical nature that can directly or indirectly affect the computational resources, time and accuracy of results. For the present study SST k-ω turbulence model was selected, which is successfully applied by Chong et al. [24,6] and Shahizare et al. [28a] for such structures as adopted in these simulations. The SST k-ω model carries the combination of k-ω turbulence model (robust for near wall region) and the k-ε model (suitable for away from walls) [27]. Further, SST k-ω model behaves well in adverse pressure gradients and separating flow also [29]. Table 1 below contains the setup conditions used for present ANSYS Fluent computations.

Table 1 ANSYS Fluent Solver Setup Conditions

Solver type	: Pressure-based
Velocity formulation	: Absolute
Time	: Steady
Gravity	: -9.81 m/s^2 in Y
Models	: Viscous SST k-ω
Material	: Air
Scheme	: Simple
Gradient	: Least squares cell
Pressure	: Standard
Momentum	: Second-order upwind
Turbulent kinetic energy	: First-order upwind
Specific dissipation rate	: First-order upwind

2.2 WAG-RH PERFORMANCE ANALYSIS

2.2.1 PERFORMANCE PARAMETERS AND CONFIGURATION CODES

From Fig. 1 it is obvious that the performance parameters of WAG-RH to be optimized can be:

- Contraction angle (Θ)
- The ratio between house and rotor zone diameters (D/d)
- Angle of incidence (Φ)
- Wind velocity (V)

With change in the above parameters, various rotor house design configurations can be developed. For the identification of the configurations, a coding system has been introduced based on RH(D/d,Θ), where RH represents the rotor house. In the investigation, three variations to each parameter were found enough to understand the effect on the performance of the WAG-RH. For these variations, the values for diameter ratios and contraction angles were taken as D/d=4,3,2 and Θ=45^o,40^o,30^o. Based on this, nine RH configurations were developed and simulated, which are RH(4,30), RH(4,40), RH(4,45), RH(3,30), RH(3,40), RH(3,45), RH(2,30), RH(2,40), and RH(2,45).

2.2.2 MANUFACTURING OF WAG-RH AND EXPERIMENTAL SETUP

The WAG-RH geometry was finalized through numerical simulations carried out for nine configurations described in Section 2.2.1. The geometrical configuration RH(4,45) as shown in Fig. 2(a) delivered better results than all other configurations. In final design, the diameter of the WAG-RH D=0.8 m, diameter of the rotor zone D=0.2 m, height and length of the vertical walls are H=0.3 m and B=0.3 m, respectively, tilted at contraction angel of 45^o. Based on these dimensions, the experimental model was manufactured as shown in Fig. 2(b) at mechanical engineering workshop of Quaid-e-Awam University of Engineering, Sciences and Technology (QUEST), Nawabshah, Pakistan.

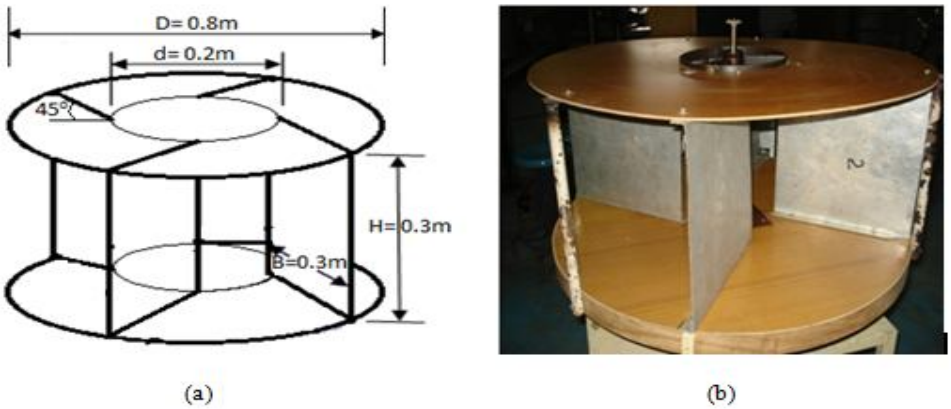

Fig. 2 (a) Optimized WAG-RH geometry and (b) manufactured model

The performance of WAG-RH experimental model in terms of wind speed amplification was studied by using subsonic open type wind tunnel of the QUEST shown in Fig. 3 and compared with numerically simulated performance. The WAG-RH was placed in front of the wind tunnel opening having dimensions of 0.5 m x 0.5 m. The measurements were performed at different inlet velocities, V_{in} =(1,3,5,7,9) m/s.

(a) (b)

Fig. 3 (a) Experimental setup and (b) experimental layout showing five important locations in the rotor zone in stream-wise direction where measurements were taken.

The velocity variations were measured at five fixed points in the stream-wise direction in the rotor zone, as shown in Fig. 3(b). The wind speed measurements were performed using TES-1340 Hot-Wire Anemometer having accuracy of ±3% of reading ±1%FS.

3. RESULTS AND DISCUSSIONS

3.1. EFFECT OF CONTRACTION ANGLE

Here, performance of each RH configuration is analyzed in terms of velocity variation along the stream-wise direction in the rotor zone. The configuration RH(4,30) contributes 20-25% increase in velocity for five selected inlet velocities as described in Section 2.2.2. Similarly, RH(4,40) gives 33-35% and RH(4,45) 41- 49% for the same inlet velocities as shown in Fig. 4(a).

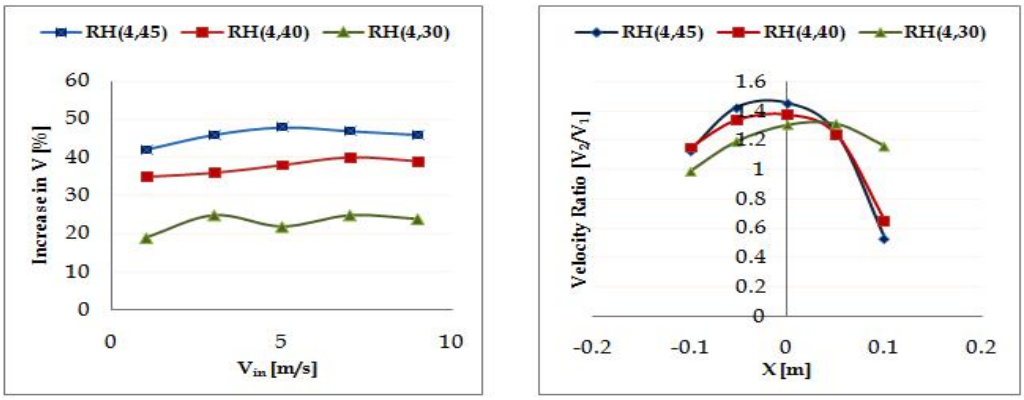

(a) (b)

Fig. 4 Performance comparison of three RH configurations in terms of. (a) Increase in inlet velocity for five different velocities and (b) velocity ratio at 5 m/s inlet velocity for five fixed points in the rotor zone in stream-wise direction

The comparison of velocities shows that the configuration RH(4,45) gives better performance in terms of velocity amplification than other two configurations. Fig. 4(b) presents the comparison of velocity ratio (V_2/V_1) for three RH configurations at inlet velocity of 5 m/s at five fixed points in the rotor zone in stream-wise direction. The results reflect 1.5 times increase in inlet velocity in case of RH(4,45), which is 14% greater than the increase contributed by RH(4,40) and 20% greater than the increase achieved with RH(4,30).

3.2 EFFECT OF WIND DIRECTION

It is clear from discussion in 3.1 that the performance of configurations RH(4,45) and RH(4,40) based on effects of contraction angle are better and close to each other. The performance of RH(4,30) is not up to the mark as compared to other two configurations; therefore, the investigation of wind direction effect can be limited to RH(4,45) and RH(4,40). The effect of wind direction on the performance of latter RH configurations is analyzed by changing the angle of incidence, as shown in Fig. 5.

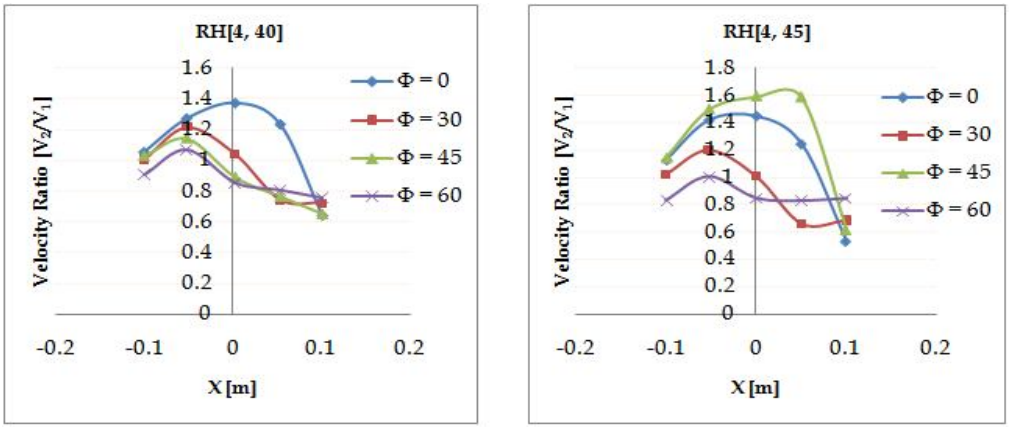

(a) (b)

Fig. 5 Performance comparison of two RH configurations in terms of velocity ratio contribution

The Fig. 5 indicates the change in velocity ratio in the rotor zone in stream-wise direction for RH(4,40) and RH(4,45) at inlet velocity of 5 m/s for angles of incidence Φ=0°,30°,45°,60°. According to Fig. 5(a), RH(4,40) configuration contributes maximum 1.38 times increase in inlet velocity at 0° and less or equal to 1.25 times for rest of angles of incidence. Looking at Fig. 5(b), it has been observed that RH(4,45) gives high velocity ratios at 0° and 45°, which are 1.5 times and 1.6 times increase in inlet velocity, respectively. The optimum values of velocity ratio at different angles of incidence for both configurations are summarized in Table 2.

Table 2. Optimum values of velocity ratio

RH Configurations	Angle of incidence (Φ)			
	0°	30°	45°	60°
RH(4,40)	1.38	1.2	1.2	1.15
RH(4,45)	1.5	1.25	1.6	1.12

3.3 EFFECT OF DIAMETER RATIO

The analysis of Sections 3.1.1 and 3.1.2 attributed that the configuration RH(4,45) gives better performance than the other configurations. Thus, further investigation are performed only for remaining configurations of this design such as RH(2,45) and RH(3,45) to optimize the diameter ratio. For this purpose, simulations are performed for these three configurations and results are shown in Fig. 6.

The fig. 6 demonstrates the contours of velocity magnitude developed for RH(2,45), RH(3,45) and RH(4,45) configurations at V_{in} =5 m/s and Φ=0°. It clearly indicates that each design configuration collects the free stream wind parcel of an area approximately equal to the projected area of that design configuration, concentrates and accelerates it in the rotor zone. It is also obvious that the walls divert and guide the flow to pass through half of

the rotor zone, which could be beneficial to minimize the generation of negative torque and generate more positive torque when the rotor will operate in this zone. Further, in comparison to RH(2,45) and RH(3,45) configurations, more stream-lined and concentrated flow pattern has been observed for RH(4,45) in the rotor zone.

In order to better understand the contour results, graphical representation of the flow patterns are presented in Fig. 7. The figure indicates that with the increase in diameter ratio (D/d), there is increase in velocity ratio inside the rotor zone.

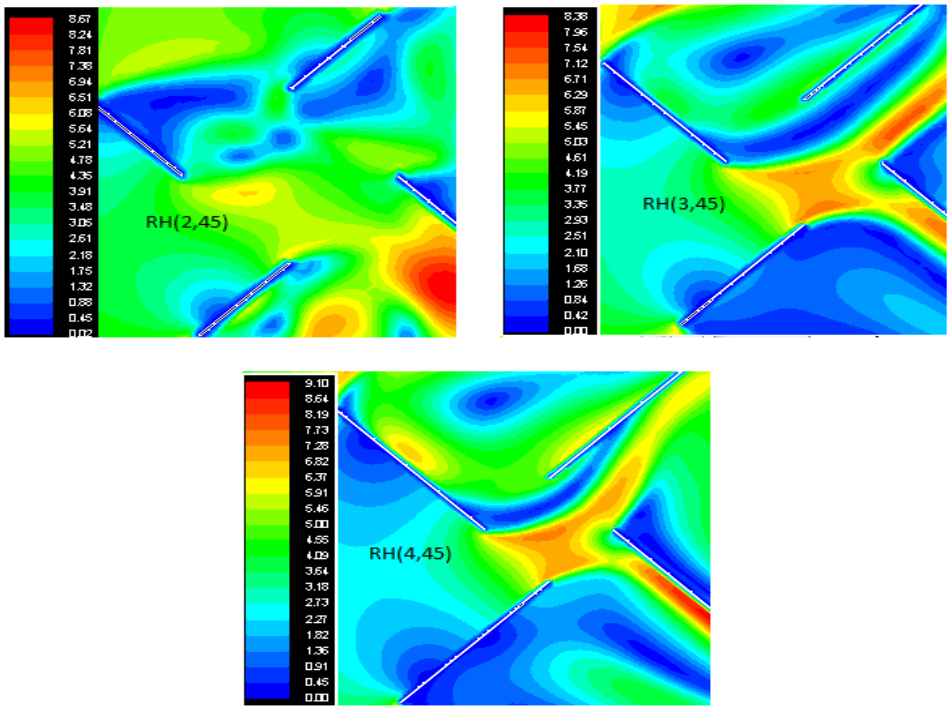

Fig. 6 Contour plots colored by velocity magnitude showing the flow pattern for three RH configurations based on diameter ratio

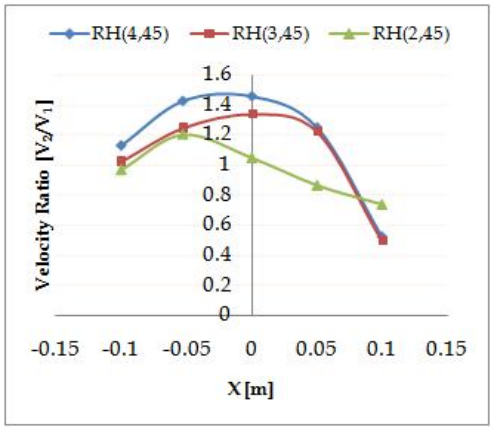

Fig.7 Performance comparison of three RH configurations based on diameter ratio

3.4 EFFECT OF WIND VELOCITY

In this section, the performance of optimal configuration RH(4,45) has been verified in the context of wind velocities V_{in}=(1,3,5,7,9) m/s at $\Phi=0^{o}$ as mentioned in Section 2.2.2. The variations in wind velocity magnitude and velocity ratio in the rotor zone in stream-wise direction are shown in Fig. 8.

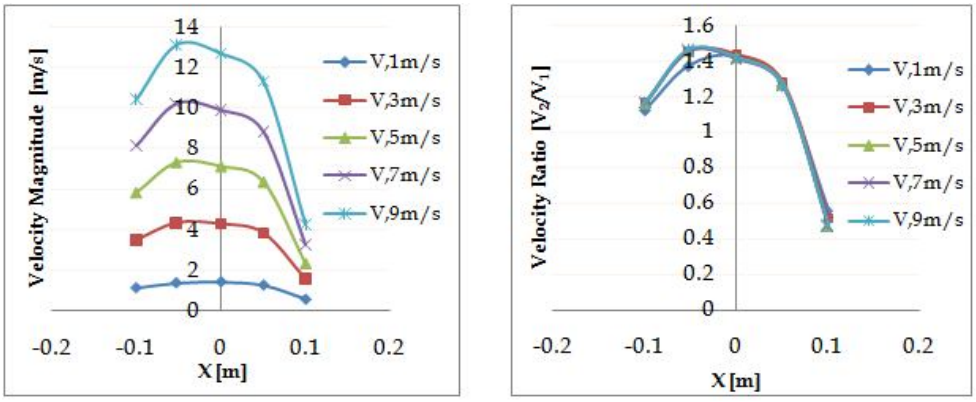

(a) (b)

Fig. 8 Contribution of RH(4,45) for change in velocity magnitude and velocity ratio at different inlet velocities in the rotor zone

The Fig. 8(a) demonstrates that with the increase in inlet velocity, the velocity magnitude in the rotor zone increases significantly. For the quantification of change in velocity magnitude, velocity ratio is estimated as given in Fig. 8(b). The figure indicates that for all inlet velocities, there is nearly 1.5 times increase in inlet velocity in the rotor zone.

3.5 EXPERIMENTAL RESULTS

The performance investigation of manufactured model for RH(4,45) configuration was conducted experimentally as described in Section 2.2.2. The results are shown in Fig. 9, which describes the change in velocity magnitude in the rotor zone in stream-wise direction at V_{in}=5 m/s and Φ=0°.

According to observations, the inlet velocity magnitude of 5 m/s increases to 7.7 m/s in the rotor zone (see Fig. 9(a)), which in terms of velocity ratio, is 1.54 times increase in the inlet velocity. Further, in Fig. 9(b), experimental and numerical results are compared for identical conditions, and show good level of agreement.

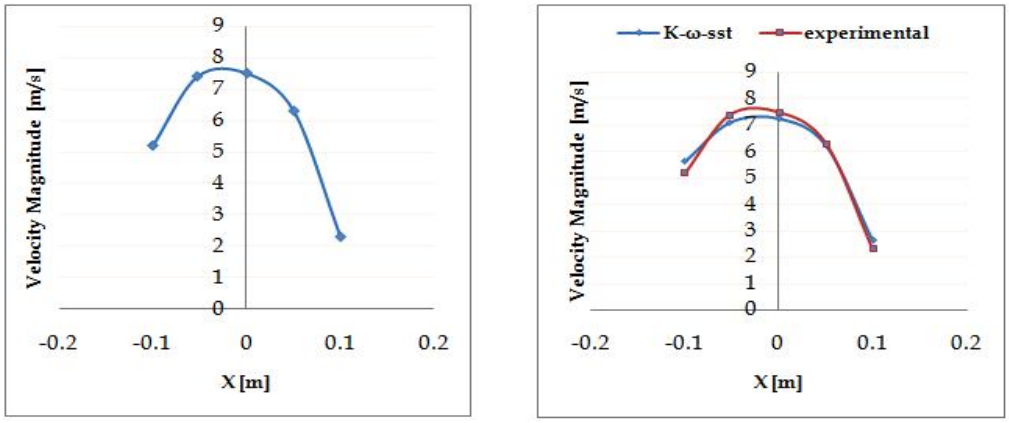

(a) (b)

Fig. 9 Performance of RH(4,45) configuration (a) Experimental results and (b) comparison of experimental and numerical results.

4. CONCLUSION

A wind accelerating and guiding rotor house (WAG-RH) has been developed to enhance the speed and working range of a conventional VAWT at low wind speed with improved efficiency. The WAG-RH collects the free stream wind parcel of an area nearly equal to the projected area of the rotor house, and directs and accelerates it towards the useful space left for VAWT to avoid negative torque and generate more positive torque.

Multiple WAG-RH design concepts have been investigated and favorable results have been observed in terms of increase in velocity. Nevertheless, final configuration RH(4,45) contributes better performance as compared to other proposed configurations. The optimized configuration RH(4,45) for any channel with any velocity at angles of incidence $\Phi=0^o$ and 45^o gives nearly 1.5 and 1.6 times increase in inlet velocity, respectively, in the rotor house. The increase in diameter ratio of WAG-RH(4,45) higher than 4 can further increase the performance, but the system may not be economical. The comparison of experimental and numerical results for identical conditions reflects good agreement.

The future aim is to investigate the performance of conventional VAWT in the designed WAG-RH as well as to integrate the rotor house with a solar air heating system that may further improve the performance of rotor, which is work in progress. The solar heater can also be used for space heating in winter.

ACKNOWLEDGEMENT

Authors would like to acknowledge the facilities provided by Quaid-e-Awam University of Engineering, Sciences and Technology, Nawabshah, Pakistan.

REFERENCES

[1] Lawn, C.J. (2003), " Optimization of the power output from ducted wind turbines", Proc. Instn. Mech. Engrs, Part A: J. Power and Energy, **217**, pp.107–117.

[2] Mertens, S. (2002), "Turby", Technical report 009, Delft University Wind Energy Research Institute (DUWIND), the Netherlands.

[3] Watson, S.J., Infield, D.G., Barton, J.P. and Wylie, S.J. (2007), "Modeling of the Performance of a Building-Mounted Ducted Wind Turbine", Journal of Physics: Conference Series, **75**, 012001 (10 pages).

[4] Anyi, M., Kirke, B. and Ali, S. (2010), "Remote community electrification in Sarawak, Malaysia", Renewable Energy., **35**, pp.1609-1613.

[5] Howell, R., Qin, N., Edwards, J. and Durrani, N. (2010), "Wind tunnel and numerical study of a small vertical axis wind turbine", Renewable Energy., **35**, pp.412-422.

[6] Chong, W.T., Pan, K.C., Poh, S.C., Fazlizan, A., Oon, C.S., Badarudinc, A. and Nik-Ghazali, N. (2013), "Performance investigation of a power augmented vertical axis wind turbine for urban high-rise application", Renewable Energy., **51**, pp.388-397.

[7] Bratley, J. (2014), " The impacts of wind turbines", Available: http://www.clean-energy-ideas.com/wind/wind-turbines/the-impacts-of-wind-turbines, accessed December 2014.

[8] Kogan, A. and Seginer, A. (1963), "Shrouded Aerogenerator Design Study II, Axisymmetrical Shroud Performance", Proc. 5th Ann. Conf on Aviation and Astronautics, Tel-Aviv, Israel.

[9] Igra, O., Kogan, A. and Seginer, A. (1963), "Shrouds for Aerogenerators", AIAA paper, pp.176-181.

[10] Oman, R.A., Foreman, K.M. and Gilbert, B.L. (1975), "A Progress Report on the Diffuser Augmented Wind Turbine", Proc. 3rd Biennial Conference and Workshop on Wind Energy Conversion Systems, Washington DC, USA, pp.826-829.

[11] Gilbert, B.L., Oman, R.A. and Foreman, K.M. (1978), " Fluid Dynamics of DAWT's", Journal of Energy, **2**, pp.368-374.

[12] Abe, K., Nishida, M., Sakurai, A., Ohya, Y., Kihara, H. and Wada E. (2005), "Experimental and numerical investigations of flow fields behind a small wind turbine with a flanged diffuser", J Wind Eng Ind Aerod., **93**, pp.951-970.

[13] Matsushima, T., Takagi, S. and Muroyama, S. (2006), "Characteristics of a highly efficient propeller type small wind turbine with a diffuser", Renewable Energy, **31**, 1343-1354.

[14] Ohya, Y., Karasudani, T., Sakurai, A., Abe, K. and Inoue, M. (2008), "Development of a shrouded wind turbine with a flanged diffuser", J. Wind Eng. Ind. Aerodyn., **96**, 524-539.

[15] Webster, G.W. (1979), "Devices for Utilizing the Power of the Wind", Patent No. 4154556, Glasgow, Scotland.

[16] Grant, A.D., Nasr, S.A. and Kilpatrick, J. (1994), "Development of a Ducted Wind Energy Converter", Wind Engineering., **18**, 297-304.

[17] Hua, S.Y. and Cheng, J.H. (2008), "Innovatory designs for ducted wind turbines", Renew Energ., **33**:1491–1498.

[18] Carcangiu, S. and Montisci, A. (2012), "Performance assessment of an aeolian roof for the exploitation of wind power in urban areas", International Conference on Renewable Energies and Power Quality, Santiago de Compostela, Spain.

[19] Corscadden, K.W. (2013), "Evaluating the Impact of Wind Speed Modification on the Performance of Vertical Axis Wind Turbines", IOSR Journal of Engineering (IOSRJEN)., **3**, 11-17.

[20] Deda, A.B. and Atilgan, M. (2010), "The use of a curtain design to increase the performance level of a Savonius wind rotors", Renew Energ., **35**, 821-829.

[21] RUSL.F. (2012), "Experimental Study on the Increase of the Efficiency of Vertical Axis Wind Turbines by Equipping Them with Wind Concentrators", Journal of Sustainable Energy, **3**, 30-35.

[22] Tong, C.W., Zainon, M.Z., Chew, P.S., Kui, S.C. and Keong, W.S. (2010), "Innovative Power Augmentation Guide Vane Design of Wind Solar Hybrid Renewable Energy Harvester for Urban High Rise Application", AIP Conf. Proc., **1225**, 507-521.

[23] Manganhar, A.L., Samo, S.R. and Rajpar, A.H. (2012), "Micro Vertical Axis Wind Turbine Design Integrated with Wind Accelerating Techniques", Journal of Basic Applied Sciences, **8**, 607-612.

[24] Chong, W.T., Poh, S.C., Fazlizan, A. and Pan, K.C. (2012), "Vertical axis wind turbine with omni-directional-guide-vane for urban highrise buildings", J. Cent. South Univ., **19**, 727-732.

[24a] Marco Casini, M.(2016), "Small Vertical Axis Wind Turbines for Energy Efficiency of Buildings", Journal of Clean Energy Technologies, Vol. 4, No. 1, pp.56-65

[24b] Dhoble, L.N and Mahalle, A.K.(2016), "Cfd Analysis of Savonius Vertical Axis Wind Turbine:A Review", International Research Journal of Engineering and Technology Vol.03, No. 01, pp.958-962

[25] Sezer-Uzol, N. and Long, L.N. (2006), "3-D time-accurate CFD simulations of wind turbine rotor flow fields", AIAA Paper 2006–394, American Institute of Aeronautics and Astronautics.

[26] Johansen, J. and Srensen, N.N. (2004), "Aerofoil characteristics from 3D CFD rotor computations", Wind Energ., **7**, 283-294

[27] Menter, F.R. and Rumsey, L.C. (1994), "Assessment of Two-Equation Turbulence Models for Transonic Flows", AIAA Paper 94–2343, 25th AIAA Fluid Dynamics Conference, Colorado Springs, Colo.

[28] Vermeer, L.J., Srensen, J.N. and Crespo, A. (2003), "Wind turbine wake aerodynamics", Progress in Aerospace Sciences, **39**, 467-510.

[28a] Shahizare, B, Nazri, N, Wen Tong Chong, W.T, Tabatabaeikia, S.S and Izadyar, N.(2016), "Investigation of the Optimal Omni-Direction-Guide-Vane Design for Vertical Axis Wind Turbines Based on Unsteady Flow CFD Simulation", Energies, 9, 146, pp.1-25

[29] Nobile, R., Vahdat, M., Barlow, J.F. and Crook, A.M. (2014), "Unsteady flow simulation of a vertical axis augmented wind turbine: A two-dimensional study", J. Wind Eng. Ind. Aerodyn., **125**, 168-179.

MULTI RELAY BEAMFORMING DESIGN FOR TWO-HOP SINGLE USER SYSTEM WITH PERFECT CSI

Abdul Sattar Saand[1], Ehsan Ali[1], Adnan Ahmed Arain[2], Abdul Rafay Khatri[1] and Varun Jeoti[3]

[1]Deparements of Electrical and Electronic Engineering, Quaid-e-Awam University of Engineering Sciences and Technology Nawabshah, Pakistan.[2]Deparements of Computer System Engineering, Quaid-e-Awam University of Engineering Sciences and Technology Nawabshah, Pakistan.[3] Department of Electrical and Electronic Engineering, Universiti Teknologi PETRONAS, Malaysia
Corresponding author: asattarsaand@gmail.com

ABSTRACT

The purpose of this research is to achieve maximum ergodic capacity of wireless MIMO relay assisted network by designing relay linear processing. A novel linear beamforming is developed for amplify-and-forward two-hop multi-relay wireless network. In this design matched-filter beamforming is applied as receive processing for multiple relays and leakage based beamforming is designed as the relay transmit beamforming. Each terminal of the network is fitted with multiple antennas for intra node array gain. The information of both links is exploited at the relay terminals. The link (direct) from the source to user terminal is avoided. The relay terminals operate in half duplex mode. Through Matlab® simulations, it is revealed that the proposed scheme out performs the existing conventional relay beamformings for multi-relay case in the two-hop network.

Keywords: Amplify-and-forward Relay, Capacity; Leakage; Multiple relays; Perfect CSI

I.INTRODUCTION

Wireless cooperative communication is getting high popularity due to cooperation in data transfer and is an emergent research area [1-3]. The incessant demand of high data rate for wireless multimedia services delivered by wireless technologies is increasing day-by-day due to the easy access and freedom of wireless system. The modern wireless communications technologies, are promising to meet high date rate demand on everywhere basis efficiently and cost effectively. The relaying transmission techniques have got much attraction over the solution of increasing the number of base stations due their implementation simplicity and low cost to extend the coverage and capacity of the existing macro cell based base station systems [4]. This is because, when the existing base station systems operating under high frequencies then the range of base stations is naturally limited and also suffers from the sever channel fading, multipath fading and high path loss which decrease the coverage, capacity and reliability of the system.

In terms of capacity and the endorsed transmit power, a limited amount of resources are assigned to a base station to serve a pre-defined quantity of customers in a cell. However with the growing number of customers the offered capacity becomes inadequate and consequences the substandard service and the systems becomes capacity limited. At the same time due to the limited transmit power of the base station, the users at the cell edge experience insufficient power level because of the weak signals from the base station [5].

The performance of the relaying networks can further be enriched by designing a suitable relay processing scheme that can control the relay transmission impairments and provide better quality of service with enhanced capacity. In existing literature several research works for AF relay beamforming design are presented that assume channel information at relay nodes for maximization of capacity [6-10] The capacity scaling of relay assisted network is designed in[6]. In [9] authors proposed linear processing for non-regenerative relays using matched filter (MF) at the receiver side for as the receive filter and design the multiple relay transmit precoding using regularized zero forcing a variant of zero forcing. The MF facilitated in increasing SNR at the relay terminals, whereas RZF scheme helped to mitigate interference among multiple antennas at the downlink of the relay network [9]. The MF-RZF technique presented in [9] using the non-zero percentage of parameter for RZF may not reduce the interference entirely. If it the parameter has very low value then the technique behaves like zero forcing technique and at high value an extra power would be consumed and more in interference [8]. Therefore the RZF technique permits definite quantity of interference [11]. This paper proposes a linear processing for relay terminals in MIMO network, the novelty design is reflected in MF and SLNR beamforming design using Fukunaga Koontz Transform (FKT) [12]. The idea of this design can provide the distributed array gain and intra-node array gain from the multiple antennas every node and distributed array gain from the multiple relay nodes.

The paper is outlined as: Section 2, describe the multi-relay assisted MIMO system model. In Section 3, the proposed

relay processing is formulated. Section 4 presents and discusses the numerical results. The conclusion is given in section 5.

II.SYSTEM MODEL

Here a two-hop relaying network witha source, multiple relays in cluster making parallel relay branches and one destination with multiple antennas is considered and illustrated in Fig.1. It consist of N_s the number of transmit antennas at MIMO source $N_r$arerelay receiving antennas and $N_d$are destination antennas. Spatial multiplexing is to be done at the source.

The communication between source to user is taken place through multiple relay terminals. Here the source sends signal $\boldsymbol{s}$to relay terminals that satisfy the source power constraint as $\mathbb{E}\{ss^H\} = \frac{P_s}{N_s}\boldsymbol{I}_{N_s}$. Where, P_s is the source transmission power and P_r is the relay transmission power. Therefore N_s is the number of source antennas and $\mathbf{I}_{N_s}$ is identity matrix of $N_s \times N_s$,$\boldsymbol{H}_k \in \mathbb{C}^{N_S \times N_r}$ is the channel from source to the relay terminals, k=1,2,…,K that is $\boldsymbol{H_1}, \ldots, \boldsymbol{H}_k$. Where, $\boldsymbol{H}_{rd}$ is the channel between k^{th} relay nodes (k=1, 2,…,K) and destination.

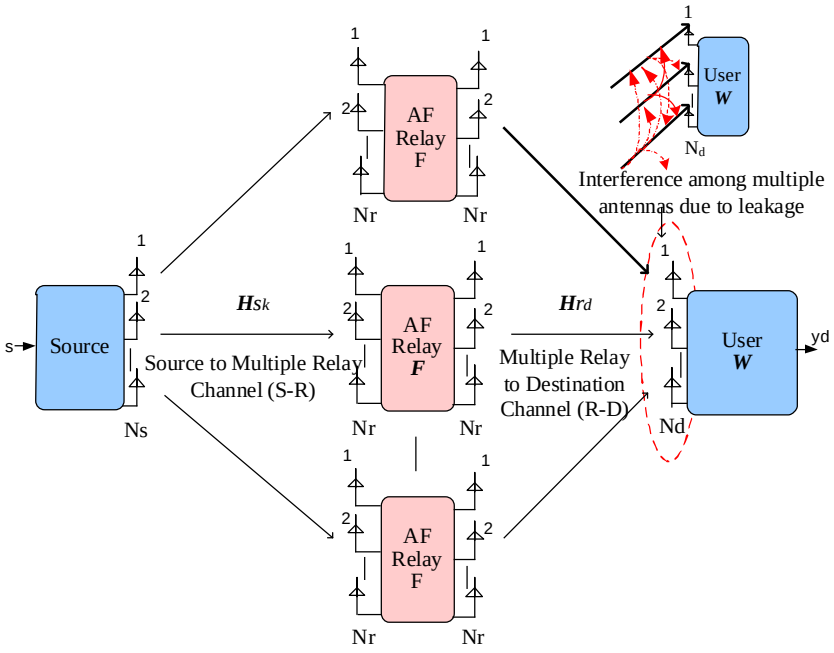

Fig.1. Atwo-hop multiple cascadedAF relay network

That is $\boldsymbol{H}_{rd} \in \mathbb{C}^{N_d \times N_r}$. Since $\boldsymbol{n}_d$ is $\boldsymbol{n}_d \in \mathbb{C}^{N_d}$ complex Gaussian noise with zero mean and covariance satisfying noise variance $\mathbb{E}\{\boldsymbol{n}_d \boldsymbol{n}_d{}^H\} = \sigma_d^2 I_{N_d}$ and σ_d^2 noise power at the destination. The corresponding received signals at thek^{th} relay terminals are given as;

$$\boldsymbol{s}_{rk} = \sum_{k=1}^{K} \boldsymbol{H}_k \boldsymbol{s} + \boldsymbol{n}_{rk} \quad (1)$$

Whereas,$\boldsymbol{n}_{rk}$ is zero mean additive Gaussian noise vector i-e $n_{rk} \sim CN(0, \sigma_r^2 \boldsymbol{I}_{M_r})$ independent across k^{th} relay terminals with noise covariance $\mathbb{E}\{\boldsymbol{n}_k \boldsymbol{n}_k{}^H\} = \sigma_r^2 \boldsymbol{I}_{N_r}$. Where σ_r^2 symbolizes the power at each relay terminal. The relays retransmit the signal to the user after multiplying amplifying matrix $\boldsymbol{F}_k$ that is termed as beamforming matrix. Let the$\boldsymbol{F}_k$ be beamforming matrix i-e $\boldsymbol{F}_k \in C^{N_r \times N_r}$ at relay nodes.

The relay precoded signal vector retransmitted by the k^{th} relays to the destination/user is written as;

$$\boldsymbol{r}_k = \boldsymbol{F}_k \sum_{k=1}^{K} \boldsymbol{F}_k \boldsymbol{H}_{s,k}\, \boldsymbol{s} + \boldsymbol{n}_k \quad (2)$$

Constraintof power at the relay satisfies as,

$$\mathbb{E}\{\boldsymbol{r}_k{}^H \boldsymbol{r}_k\} \leq P_r \quad (3)$$

The relay power constraint can be derived as;

$$P(\boldsymbol{r}_k) = tr\left\{\boldsymbol{F}_k \left(\frac{P_s}{N_s}\boldsymbol{H}_{sk}\boldsymbol{H}_{sk}^H + \sigma_r^2 \boldsymbol{I}_{N_r}\right)\boldsymbol{F}_k^H\right\} \leq P_r \quad (4)$$

The relay precoded and forwarded signal at destination is written as;

$$\boldsymbol{y} = H_{rd}\boldsymbol{r}_k + n_d$$

$$\therefore \quad \boldsymbol{r}_k = \boldsymbol{F}_k \boldsymbol{s}_{rk}$$

$$\boldsymbol{y} = \sum_{k=1}^{K} \boldsymbol{H}_{sk}\, \boldsymbol{F}_k \boldsymbol{H}_{rd} \boldsymbol{s} + \sum_{k=1}^{K} \boldsymbol{H}_{rd}\, \boldsymbol{F}_k \boldsymbol{n}_k + \boldsymbol{n}_d \quad (5)$$

III.RELAY PRECODING

The ergodic capacity of the AF relay assisted MIMO relay network is analyzed at the destination by applying QR decomposition and successive interference cancellation (SIC) detections [9]. Here QRD is exploited as detection scheme for destination node. Let in (5) the terms $\sum_{k=1}^{K} \boldsymbol{H}_{rd}\boldsymbol{F}_k\boldsymbol{H}_{sk} = \boldsymbol{H}_{sd}$is an effective channel and $\sum_{k=1}^{K} \boldsymbol{H}_{krd}\boldsymbol{F}_k\boldsymbol{n}_{rd} + \boldsymbol{n}_d = \boldsymbol{n}$ is effective noise. The equation (5) can be regenerated as $\boldsymbol{H}_{sk} = \lfloor \boldsymbol{H}_1, \dots, \boldsymbol{H}_k \rfloor$.

$$\boldsymbol{y} = \boldsymbol{H}_{sd}\boldsymbol{s} + \boldsymbol{n} \tag{6}$$

Where, $\boldsymbol{H}_{sd}$ is effective channel from source to user and $\boldsymbol{n}$is the effective noise vector.

The QRD implementation at the effective channel $\boldsymbol{H}_{sd}$ is given as;

$$\boldsymbol{H}_{sd} = \boldsymbol{Q}_{sd}\boldsymbol{R}_{sd} \tag{7}$$

Whereas, $\boldsymbol{Q}_{sd}$ is an$N_s \times N_d$ unitary matrix and $\boldsymbol{R}_{sd}$ is $N_s \times N_d$ right upper triangular matrix.

Therefore the QR detection at destination is selected as;

$$\boldsymbol{W} = \boldsymbol{Q}_{sd}^{H} \tag{8}$$

Then after detection the received signal vector becomes;

$$\hat{\boldsymbol{y}} = \boldsymbol{R}_{sd}\boldsymbol{s} + \boldsymbol{Q}_{sd}^{H} \tag{9}$$

The optimal relay precoder design is formulated as;

$$\widehat{\boldsymbol{F}}_k = \underset{\boldsymbol{F}_k}{\operatorname{argmax}} SLNR_k(\boldsymbol{F}_k)$$

$$\text{s.t } P(r_k) \leq PQ_k \tag{10}$$

It is assumed that a power coefficient ρ_k is used with k^{th} relay precoder $\boldsymbol{F}_k$ in (2) to confirm that transmit power of each relay equal to Q_k the total power of k^{th} relay terminals. After applying precoding and power coefficient the relay forward signal is written as;

$$\hat{r}_k = \rho_k\boldsymbol{F}_k r_k \tag{11}$$

From (3) the factor P_k that controls power is written as;

$$P_k = \left(\frac{Q_k}{tr\left\{F_k\left(\frac{P_s}{N_S}H_{sk}H_{sk}^{H} + \sigma_r^2 I_{N_r}\right)F_k^{H}\right\}}\right)^{\frac{1}{2}} \tag{12}$$

IV.MATCHED FILTER-PER ANTENNA SLNR BASED MULTI-RELAY PROCESSING (MF-PASLNR)

In this relay transceiver design for amplify-and-forward multiple relay aided network, MFis used as multiple relay receive beamforming while leakage based relay transmit beamforming. In this scheme the matched filter remove the noise effect [13] at the relay reception for the multi-relay network, whereas the leakage based relay transmit beamforming tries to control the interference due to leakage signal at the user end. Here each relay beamforming is segregated into two components a relay receive beamforming based matched filter and transmit precoder based on SLNR maximization.

The matched filter beamforming matrix for the k^{th}relay for first hop of the network is set to,

$$\boldsymbol{F}_{sk}^{MF} = \boldsymbol{H}_{sk}^{H} \tag{13}$$

Here receive precoder is $\boldsymbol{H}_{Sk}^{H}$ is optimal weighting matrix that maximize SNR received at relays.

The interference caused by the leakage signal cannot be cancelled by using conventional techniques like regularized zero-forcing and zero forcing. Though, leakage based downlink precoding can show robustness against interference among multiple antennas at the destination. In this design, interference due to leakage at the destination side is taken into account for multi-relay downlink precoder design as [14]. The proposed technique reduces interference (leakage) among multiple antennas. In Fig 1 the channel from multiple relay terminals to the destination is represented by notation$\boldsymbol{H}_{rdc}$.

$$\boldsymbol{H}_{rdc} = \lfloor \boldsymbol{H}_1^{H}\boldsymbol{H}_2^{H}, \dots, \boldsymbol{H}_K^{H} \rfloor^{H} \tag{14}$$

The matrix for k relay terminals to the destination for j^{th} antennas is given as;

$$\boldsymbol{H}_{rdc}^{j} = \lfloor \boldsymbol{H}_{k-1}^{H}\boldsymbol{H}_{k+1}^{H}, \dots, \boldsymbol{H}_K^{H} \rfloor^{H} \tag{15}$$

Under the relay power constraints the transmit precoding is designed as;

$$\widehat{\boldsymbol{F}}_k^{j} = \arg\max_{F_k^{j} \in C^{N_r \times 1}} SLNR_k^{j}\left(\boldsymbol{F}_k^{j}\right)$$

$$\text{s.t } P(r_k) \leq PQ_k \tag{16}$$

where, $\boldsymbol{F}_k^{j}$ is the k^{th} relay transmit precoding for j^{th} destination antennas. For multiple relay network the signal to leakage and noise ratio is given as;

$$PASLNR_k^{j} = \frac{\left\|h_{rd}^{j}f_k^{j}\right\|_F^2}{\sum_{\substack{i=1 \\ j\neq k}}^{L}\left\|\boldsymbol{H}_{rd}f_k^{j}\right\|_F^2 + \sum_{\substack{i=1 \\ j\neq k}}^{N_d}\left\|\mathbf{h}_{\mathrm{rd}}f_k^{j}\right\|_F^2 + \sigma_d^{j^2}} \tag{17}$$

Equation (17) is the relationship between wanted signal to the leakage and noise power, here,$\boldsymbol{h}_k^{j}$ shows row vector of the j^{th}receive antennas $j = 1, \dots, N_d$, $\sigma_d^{j^2}$ is the destination

noise variance, i.e $\sigma_d^{j^2} = \sigma_1^{j^2}, \ldots, \sigma_d^{j^2}$ and $f_k^j = f_1, \ldots, f_{N_d}$ is vector wise k^{th} relay transmit precoding for j^{th} antenna elements is generated as;

$$\boldsymbol{f}_k^j = \arg \max_{\boldsymbol{F}_k^j \in C^{N_T \times 1}} \frac{\boldsymbol{f}_k^{j^H} (\boldsymbol{h}_k^{j^H} \boldsymbol{h}_{rd}^j) \boldsymbol{f}_k^j}{\boldsymbol{f}_k^{j^H} (\boldsymbol{H}_{rd}^{j^H} \boldsymbol{H}_{rd}^j + \sigma_{rk}^{j^2} \boldsymbol{I}_{N_T}) \boldsymbol{f}_k^j} \quad (18)$$

$$\boldsymbol{F}_k^j = [\boldsymbol{f}^1, \ldots, \boldsymbol{f}^{N_d}].$$

Here, $\boldsymbol{F}_k^j$ is the k^{th} relay transmit precoding matrix for j^{th} receive antennas at the destination that helps to maximize the SLNR. After multiplying relay receive beamforming matrix (13) with (18) we get;

$$\boldsymbol{F} = \boldsymbol{F}_k^j \times \boldsymbol{H}_{sk}^H \quad (19)$$

The optimization problem in (18) for k relays transmit beamforming mapped to Fukunaga Koontz Transform as follows;

$$\hat{T}_1 = h_k^{l^H} h_k^l \quad (20)$$

$$\hat{T}_2 = \boldsymbol{H}_{rdc}^H H_{rdc} + \sigma_d^2 I_{N_d} \quad (21)$$

Now,

$$T = \hat{T}_1 + \hat{T}_2 = \boldsymbol{H}_{rdc}^H \boldsymbol{H}_{rdc} + \sigma_d^2 I_{N_d} \quad (22)$$

Then signal received at destination is given by;

$$\boldsymbol{y}_d = \sum_{\substack{j=1 \\ k \neq j}}^{N_d} \rho \boldsymbol{H}_{rd} \boldsymbol{F} \boldsymbol{H}_{sk} \boldsymbol{s} + \sum_{\substack{j=1 \\ k \neq j}}^{N_d} \boldsymbol{H}_{rd} \boldsymbol{F} \boldsymbol{s}_i + \boldsymbol{H}_{rd} \boldsymbol{F} \boldsymbol{n}_k + \boldsymbol{n}_d \quad (23)$$

In (23) $\boldsymbol{G}_{sd} = \rho \boldsymbol{H}_{rd} \boldsymbol{F} \boldsymbol{H}_{sk}$ is an equivalent channel, whereas $\boldsymbol{I} = \boldsymbol{G} \boldsymbol{F} \boldsymbol{s}_i$ is the interference of the leakage signal and $\boldsymbol{n} = \boldsymbol{H}_{rd} \boldsymbol{F} \boldsymbol{n}_k + \boldsymbol{n}_d$ is the destination equivalent noise. The notation $\boldsymbol{s}_i$ symbolizes the interference signal. The QR decomposition operation of channel $\boldsymbol{G}_{sd}$ gives $\boldsymbol{Q}$ and $\boldsymbol{R}$ the unitary and upper right triangular matrix. The receiver filter using QRD [9]is given as;

$$\boldsymbol{W} = (\boldsymbol{Q}_{sd})^H \quad (24)$$

The effective SINR in terms of power of relay beamforming is given by;

$$SINR = \frac{\left(\frac{P_s}{N_d}\right) r_{j,j}^2}{\left\| (\rho (\boldsymbol{Q}_{sd})^H \boldsymbol{H}_{rd} \boldsymbol{F})_j \right\|^2 \sigma_k^{l^2} + \sigma_d^{j^2}} \quad (25)$$

In in above equation $r_{j,j}^2$ are j^{th} entries of $\boldsymbol{R}$. The ergodic capacity for multi-relay network is given as;

$$C_{erg} = E_{\{H_{sk}, H_{rd}\}} \left\{ \frac{1}{2} \sum_{\substack{j=1 \\ k \neq j}}^{N_d} \log_2 (1 + SINR) \right\} \quad (26)$$

V.RESULTS AND DISCUSSION

The simulation is conceded out for corroborating the performance supremacy of the proposed relay precoding approaches. The ergodic capacities of proposed relay processing scheme MF-PASLNR-Max with the scheme MF-RZF proposed in [9], MF-ZF and ZF-ZF. The mode of transmission is supposed as half duplex for AF relay protocol in dual-hop MIMO multi relay network system. The capacity upper bound set in [6] is taken as baseline. All relay processing designs are assessed under the condition of many factors. The equal power P_s is assumed from source to the all relay nodes. The entries of all links are flat fading and H_{sk} and H_{rd} are i.i.d with complex Gaussian. The same power constraint is considered for all the cascaded relay terminals. The both channel knowledge is assumed as perfect. The outcome of the projectedarrangement is compared with the available traditional relay processing schemes.

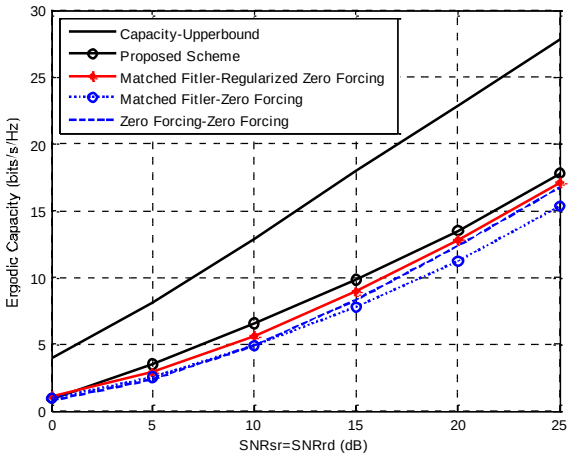

Fig. 2: Performance of the beamforming schemes in b/s/Hz versus SNR ranges (0-25 dB)

The graphs in Figure 2 represent performance comparisons of the proposed technique with other conventional scheme for AF relay in multi-relay network scenario. The performance is obtained at under system configuration $N_s = N_r = N_d = 3$antennas and the number of relay terminals=3.

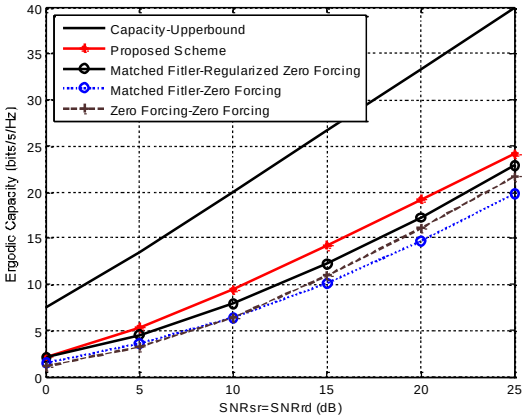

Fig. 3.Performance of the beamforming schemes in b/s/Hz versus SNR ranges (0-25 dB).

The graphs represent performance comparisons of the proposed technique with other conventional scheme for AF relay terminals. The performance is obtained under system configuration of $N_s = N_r = N_d =$ 4antennasand the relay terminals=5.

The result of MF-PASLNR-Max using FKT is shown in Fig.2 and Fig.3. The capacity of the newly designed relaying strategy approximately grows linearly with SNR values and outperforms other schemes. The Fig.3 shows the outcome of the proposed design with the increased quantity of antennas at each node of the network that is 4 antennas at each node of the network including each relay.

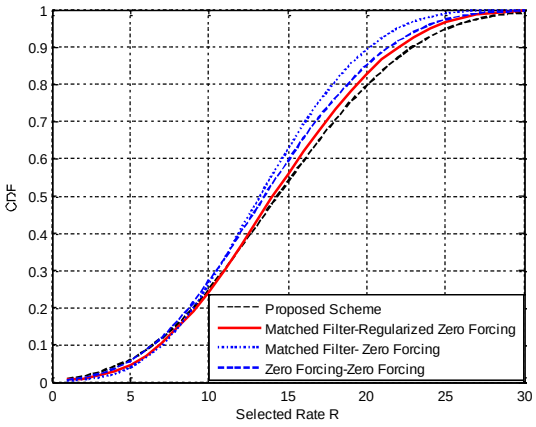

Fig.4. Outage capacity comparison of the proposed relay processing technique other available techniques, the system is configured with 3 antennas at each terminal and 5 relay are connected in parallel in dual-hop MIMO system

Figure 4, compares the outage capacity enactment of the proposed relay linear processing for multi-relay MIMO system. The outage performance of the proposed MF-PASLNR-FKT technique is compared with the MF-RZF, MF-ZF and ZF-ZF. The proposed technique out performs the other available conventional relay processing techniques

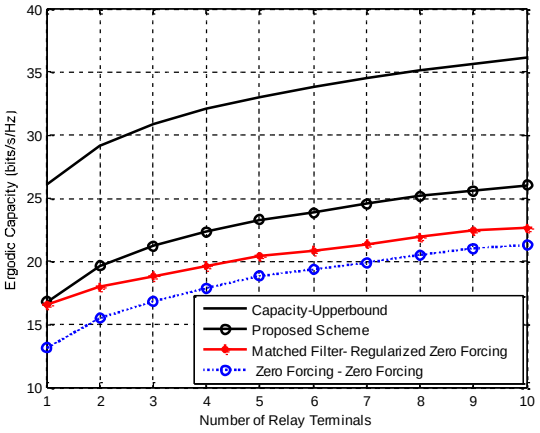

Fig.5. Maximum ergodic capacity versus number of AF relay terminal with configuration of 3 antennas at each terminal and SNR= 40 dB.

The ergodic capacity is to be examined with various relay precoding schemes and presented in Fig.5 that shows that, an apparent variation in the capacity with the increasing number of relay terminals in the two-hop network, with 3 antennas at each terminal, SNR=40 dB and *K*=1-10 relay terminals. Note that, the proposed relay processing scheme out performs the other conventional schemes for AF relay terminals at every number of the relay terminal from 1 to 10.

The simulation reveals that, by considering the criterion for amplify-and-forward relay processing using matched filter and SLNR criterion at the multiple relay terminals, the SNR is maximized at the relay terminals by controlling the noise, whereas due to leakage control at the relays downlink SLNR is maximized. Increasing relay terminal in parallel the system performance is improved that results and multiple antennas at each node increase the capacity.

CONCLUSION

A new beamforming scheme based on MF and SLNR techniques is developed for multiple MIMO AF relay terminals in two-hop MIMO network. The network design delivers both the intra node and distributed array gains contributed by the multiple antennas and multiple relay terminals. Simulation results obtained under various network parameters validate that the projectedsystem outperforms the conventional relay beamforming techniques in terms of ergodic capacity. The above mentioned results and discussion concludes that the proposed technique is more efficient technique.

REFERENCES

[1] A. Chakrabarti, A. Sabharwal, and B. Aazhang, "Cooperative communications," in Cooperation in Wireless Networks: Principles and Applications, ed: Springer, 2006, pp. 29-68.

[2] Y.-W. Hong, W.-J. Huang, F.-H. Chiu, and C.-C. J. Kuo, "Cooperative communications in resource-constrained wireless networks," Signal Processing Magazine, IEEE, vol. 24, pp. 47-57, 2007.

[3] K. R. Liu, Cooperative communications and networking: Cambridge university press, 2009.

[4] X. Tao, X. Xu, and Q. Cui, "An overview of cooperativecommunications," Communications Magazine, IEEE, vol. 50, pp. 65-71, 2012.

[5] M. Iwamura, H. Takahashi, and S. Nagata, "Relay technology in LTE-Advanced," NTT DoCoMo Technical Journal, vol. 12, pp. 29-36, 2010.

[6] H. Bolcskei, R. U. Nabar, O. Oyman, and A. J. Paulraj, "Capacity scaling laws in MIMO relay networks," Wireless Communications, IEEE Transactions on, vol. 5, pp. 1433-1444, 2006.

[7] Z. Wang and W. Chen, "Relay Beamforming Design with SIC Detection for MIMO Multirelay Networks with Imperfect CSI," Vehicular Technology, IEEE Transactions on, vol. 62, pp. 3774-3785, 2013.

[8] Z. Wang, W. Chen, and J. Li, "Efficient beamforming for MIMO relaying broadcast channel with imperfect channel estimation," Vehicular Technology, IEEE Transactions on, vol. 61, pp. 419-426, 2012.

[9] Y. Zhang, H. Luo, and W. Chen, "Efficient relay beamforming design with SIC detection for dual-hop MIMO relay networks," Vehicular Technology, IEEE Transactions on, vol. 59, pp. 4192-4197, 2010.

[10] Z. Wang, W. Chen, F. Gao, and J. Li, "Capacity Performance of Relay Beamformings for MIMO Multirelay Networks With Imperfect-CSI at Relays," Vehicular Technology, IEEE Transactions on, vol. 60, pp. 2608-2619, 2011.

[11] D. Senaratne and C. Tellambura, "Performance analysis of channel inversion over MIMO channels," in Global Telecommunications Conference, 2009. GLOBECOM 2009. IEEE, 2009, pp. 1-5.

[12] K. Fukunaga and W. L. Koontz, "Application of the Karhunen-Lo? ve Expansion to Feature Selection and Ordering," IEEE Transactions on Computers, vol. 19, pp. 311-318, 1970.

[13] M. Qingyu, A. Osseiran, and J. Gan, "MIMO amplify-and-forward relaying: spatial gain and filter matrix design," in Communications Workshops, 2008. ICC Workshops' 08. IEEE International Conference on, 2008, pp. 26-30.

[14]A. S. Saand, V. Jeoti, M. Saad, and M. Naufal, "Relay precoding for dual-hop MIMO network using per antenna SLNR maximization," in Wireless Technology and Applications (ISWTA), 2014 IEEE Symposium,2014, pp. 41-46.

ELLIPTIC CURVES WITH MANY POINTS OVER A SMALL FINITE FIELD

M. A. Soomro*, A.H. Sheikh** and S. H. Sandilo*

ABSTRACT

This note contains examples of elliptic curvs with maximal possible number of rational points over a finite field F_q. More precisely this is done for every $q = p^n$ with $p \leq 19$ a prime number and $1 < n \leq 5$ and also for all $q = p \leq 97$ a prime number. The examples were computed using the computer algebra package Maple and the free mathematics software system Sage.

Keywords: *Elliptic Curves, Finite fields*

1. INTRODUCTION

We denote by $N_q(1)$ the maximal number of rational points that an elliptic curve E over a finite field F_q of cardinality q can have. A result of Deuring and Waterhouse (see [4, Thm. 4.1]); for an exposition see also [1, p. 15-16]) states that

$$N_q(1) = \begin{cases} q+m \text{ if } q = p^e \,\&\, e \geq 5 \text{is odd} \,\&\, p \mid m; \\ q+m+1 \qquad\qquad otherwise. \end{cases}$$

Here p is the characteristic of F_q and m is the largest integer less than or equal to $2\sqrt{q}$.

In this research, we present, for many small q, an elliptic curve over F_q attaining this bound.

2. THE PRIME FIELDS

Over F_2 the equation $y^2 + y = x^3 + x$ defines an elliptic curve with $N_2(1) = 5$ rational points. For odd prime numbers p, we search over equations $y^2 = x^3 + ax + b$ satisfying $4a^3 + 27b^2 \neq 0$ in order to find an example with $N_p(1) = p + 1 + \lfloor 2\sqrt{p} \rfloor$ rational points. Using Maple, this is very simple for small p. The result is given in the Table (1).

3. FIELDS OF CARDINALITY p^2

To find examples of elliptic curves over F_{p^2} having $N_{p^2}(1) = p^2 + 1 + 2p$ rational points, we use the following lemma.

Lenmma 3.1 Suppose E / F_q is an elliptic curve. Then

$$\#E(F_{q^2}) = q^2 + 1 + 2q \Leftrightarrow \#E(F_q) = q + 1.$$

Proof

By Chap.V, Sec. 2 in [3] and Chap. IV, Sec. 3 in [5].

Let $\#E(F_q) = q + 1 - a$. Write $X^2 - aX + q = (X - \alpha)(X - \beta)$ with $\alpha, \beta \in \mathbb{C}$. Then

$$\#E(F)_{q^n} = q^n + 1 - \alpha^n - \beta^n$$

for all $n \geq 1$.

So in particular one has $\#E(F_{q^2}) = q^2 + 1 - \alpha^2 - \beta^2$. This implies

$$\begin{aligned} \#E(F_{q^2}) = q^2 + 1 + 2q \\ \Leftrightarrow \ \alpha^2 + \beta^2 = -2q, \\ \Leftrightarrow \alpha^2 + \beta^2 + 2\alpha\beta = 0, \\ \Leftrightarrow (\alpha + \beta)^2 = 0 \\ \Leftrightarrow \alpha + \beta = 0 \\ \Leftrightarrow \#E(F_q) = q + 1, \end{aligned}$$

which proves the lemma.

q	$N_q(1)$	Elliptic Curve
2	5	$y^2 + y = x^3 + x$
3	7	$y^2 = x^3 + 2x + 1$
5	10	$y^2 = x^3 + 3$
7	13	$y^2 = x^3 + 3$
11	18	$y^2 = x^3 + x + 3$
13	21	$y^2 = x^3 + 4$
17	26	$y^2 = x^3 + 3x$
19	28	$y^2 = x^3 + 8$
23	33	$y^2 = x^3 + x + 11$
29	40	$y^2 = x^3 + 4x$
31	43	$y^2 = x^3 + 3$
37	50	$y^2 = x^3 + 2x$
41	54	$y^2 = x^3 + 2x + 4$
43	57	$y^2 = x^3 + 9$
47	61	$y^2 = x^3 + x + 38$
53	68	$y^2 = x^3 + x$
59	75	$y^2 = x^3 + 2x + 22$
61	77	$y^2 = x^3 + 6x + 29$
67	84	$y^2 = x^3 + 1$
71	88	$y^2 = x^3 + x + 9$
73	91	$y^2 = x^3 + 5$
79	97	$y^2 = x^3 + 3$
83	102	$y^2 = x^3 + 2x + 19$
89	108	$y^2 = x^3 + x + 8$
97	117	$y^2 = x^3 + 2$

Table 1: List of Curves over prime fields

More generally, any elliptic curve over F_q, having precisely $q + 1$ rational points, will have $N_{q^{2s}}(1) = q^{2s} + 1 + 2q^s$ rational points over the field $F_{q^{2s}}$, with s any odd integer.

For $q = p$ prime the existence of such an elliptic curve (i.e. having precisely $p + 1$ rational points) over F_p follows, as before, from the results of Deuring and of Waterhouse (see [4, Thm. 4.1]).

To have explicit examples, first note that for $p = 2$, the equation $y^2 + y = x^3$ defines an elliptic curve with exactly $3 = p + 1$ rational points over F_2. Next, for every prime number $p \equiv 5 \bmod (6)$ the equation $y^2 = x^3 + 1$defines an elliptic curve with precisely $p + 1$ rational points over F_p. (This is well-known; compare, e.g., Exer. IV-4.10 in [3].)

Similarly (see Exer. IV-4.8 in [3]) for every prime number $p \equiv 3 \bmod (4)$ the equation $y^2 = x^3 + x$ defines an elliptic curve whose number of rational points over $F_p$equals $p + 1$. With these remarks, we have examples for every prime $p \leq 19$ except $p = 13$.

One has $\#E(F_{13}) = 14$ for the elliptic curve E: $y^2 = x^3 + x + 4$.

This discussion is summarized in the Table 2.

p	$N_{p^2}(1)$	Elliptic Curve
2	9	$y^2 + y = x^3$
3	16	$y^2 = x^3 + x$
5	36	$y^2 = x^3 + 1$
7	64	$y^2 = x^3 + x$
11	144	$y^2 = x^3 + x$
13	196	$y^2 = x^3 + x + 4$
17	324	$y^2 = x^3 + 1$
19	400	$y^2 = x^3 + x$

Table 2

4. FIELDS OF CARDINALITY p^3

Most of the curves given in the following Table 3 are found by a simple trick given in Section 7 and other by using the free mathematics software system Sage.

Write $F_{p^3} = F_p[z]$ in which z satisfies $g(z) = 0$ for a monic irreducible $g \in F_p[X]$ of degree 3.

Note that if E is defined over F_{p^3}, then the p-power Frobenius map defines an isomorphism $E(F_{p^3}) \simeq E^{(p)}(F_{p^3})$. Here $E^{(p)}$ denotes the elliptic curve obtained from E by raising the coefficients of its equation to the power p. In particular, in an equation involving z the number of points does not depend on

which zero of g in $F_p[z]$ is taken.

p	$N_{p^3}(1)$	Elliptic Curve	Minimal Polynomial of z
2	14	$y^2 + xy + y = x^3 + 1$	
3	38	$y^2 = x^3 + 2x^2 + 2x$	
5	148	$y^2 = x^3 + x + 2$	
7	381	$y^2 = x^3 + z^2$	$X^3 + 6X^2 + 4$
11	1404	$y^2 = x^3 + x + 4$	
13	2291	$y^2 = x^3 + z^2x + z^{75}$	$X^3 + 2X + 11$
17	5054	$y^2 = x^3 + x + 4$	
19	7025	$y^2 = x^3 + z^2x + z^9$	$X^3 + 4X + 17$

Table 3

5. FIELDS OF CARDINALITY p^4

If an elliptic curve E over a finite field F_q satisfies $\#E(F_q) = q + 1$, then as in Lemma 3.1, $\#E(F_{q^4}) = q^4 + 1 - 2q^2$. This implies that a quadratic twist E^{tw} of E over F_{q^4} satisfies $\#E^{tw}(F_{q^4}) = q^4 + 1 + 2q^2 = N_{q^4}(1)$, by the following two lemmas.

Lemma 5.1 Suppose q is odd, and let C/F_q be the hyperelliptic curve corresponding to an equation $y^2 = f(x)$ with $f \in F_q[X]$ square free. Suppose $\alpha \in F_q^*$ is not a square and define the hyper-elliptic curve C^{tw}/F_q corresponding to the equation $\alpha\, y^2 = f(x)$. Then

$$\#C(F_q) + \#C^{tw}(F_q) = 2q + 2.$$

Proof For $x_0 \in F_q$. If $f(x_0) = 0$, then this contributes one point to both curves. If $f(x_0) \in F_q^{*2}$, then this contributes 2 points to C and 0 points to C^{tw}. If $f(x_0) \in F_q^* \backslash F_q^{*2}$, then this contributes 0 points to C and 2 points to C^{tw}. Finally, consider points at infinity.If f has odd degree, then both C and C^{tw} have one rational point at infinity. If f has even degree and leading coefficient in F_q^{*2}, then C has 2 points at infinity while C^{tw} has no point at infinity. In the remaining case C^{tw} has 2 points and C has none. Therefore $\#C(F_q) + C^{tw}(F_q) = 2q + 2$.

Now if $E: y^2 = x^3 + Ax + B$ is an elliptic curve over odd finite field $F_q$and satisfies $\#E(F_q) = q + 1$, then $\#E(F_{q^4}) = q^4 + 1 - 2q^2$. Take an $\alpha \in F_{q^4}^*$, not a square, we make another curve

$$E^{tw}: \alpha\, y^2 = x^3 + Ax + B$$

equivalently $E^{tw}: y^2 = x^3 + \alpha^2 Ax + \alpha^3 B$ (see Exer. 2.23 and 4.10 in [5]). Then

$$\#E(F_{q^4}) + \#E^{tw}(F_{q^4}) = 2q^4 + 2,$$

Therefore,

$$\#E^{tw}(F_{q^4}) = q^4 + 1 + 2q^2,$$

hence E^{tw} is the required maximal elliptic curve over F_{q^4}.

Lemma 5.2 Suppose $q = 2^n$. Then a generalized Weierstrass equation for an elliptic curve over F_q is

$$E: y^2 + (a_1x + a_3)y = f(x) \tag{1}$$

with $f(x)$ monic of degree 3. The quadratic twist isomorphic to (1) over $F_{q^2} = F_q(\beta)$, where β satisfies an irreducible polynomial $X^2 + X + a = 0$ for some $a \in F_q$, is

$$E^{tw}: \eta^2 + (a_1x + a_3)\eta = f(x) + a(a_1x + a_3)^2. \tag{2}$$

It satisfies

$$\#E(F_q) + \#E^{tw}(F_q) = 2q + 2.$$

Proof Take $x_0 \in F_q$. Let $a_1x_0 + a_3 = \xi$ and $f(x_0) = \delta$. First suppose $\delta = 0$. If $\xi = 0$ we obtain one point on both E and E^{tw}. If $\xi \neq 0$ then the equations (1) and (2) at x_0 give

$$y^2 + \xi y = 0, \tag{3}$$

$$\eta^2 + \xi\eta = a\xi^2. \tag{4}$$

Clearly (3) has precisely 2 solutions, namely $y = 0$ and $y = \xi$. The equation (4) has no solution $\eta \in F_q$, since if $\eta \in F_q$ would be a solution then $\frac{\eta}{\xi} \in F_q$ would be a zero of $X^2 + X + a = 0$, which is assumed to be irreducible.

Now suppose $\delta \neq 0$. If $\xi = 0$ we obtain one point on both E and E^{tw}. If $\xi \neq 0$ then the Equations (1) and (2) at x_0 give

$$y^2 + \xi y = \delta, \tag{5}$$

$$\eta^2 + \xi\eta = \delta + a\xi^2. \tag{6}$$

If both Equations (5) and (6) would have a solution $y$and $\eta \in F_q$ respectively, then $\frac{y+\eta}{\xi} \in F_q$ would be a zero of $X^2 + X + a = 0$ which is not possible.

Now Suppose the Equation (5) has no solution in F_q. Then it has 2 solutions in $F_{q^2} = F_q(\beta)$. Let $y_0 = y_1 + y_2\beta$, where $y_1, y_2 \in F_q$ and $y_2 \neq 0$, be one of the solutions of the Equation (5) in F_{q^2}. Hence

$$(y_1 + y_2\beta)^2 + \xi(y_1 + y_2\beta) = \delta,$$

which can be written as

$$y_1^2 + y_2^2\beta + y_2^2 a + y_1\xi + y_2\beta\xi = \delta, \tag{7}$$

comparing coefficients of β shows

$$y_2^2 + \xi y_2 = 0$$

so $y_2 = \xi$. So the equation (7) gives

$$y_1^2 + \xi y_1 = a\xi^2,$$

hence y_1 is a solution of the Equation (4).

Finally, both the curves have one point at infinity. Therefore $\#E(F_q) + \#E^{tw}(F_q) = 2q + 2$.

For instance, for $q = p$ odd we have the curves over F_p, with precisely $p + 1$ rational points, in the table of Section 3. Take a curve $E: y\text{^}2 = x^3 + x$ having $\#E(F_3) = 4$ and $\alpha = z \in F_{3^4}\}$ satisfying $z^4 + 2z^3 + 2 = 0$. Then z is not square in F_{3^4}, since $X^8 + 2X^6 + 2 \in F_3[X]$ is irreducible. Hence $E^{tw}: zy^2 = x^3 + x$ equivalently $E^{tw}: y^2 = x^3 + z^2 x$ is the required elliptic curve over F_{3^4} with $\#E(F_{3^4}) = N_{3\text{^}4}(1) = 100$. For $q = 2$, the curve $E: y^2 + y = x^3$ has $\#E(F_2) = 3$. Write $F_{2^4} = F_2[z]$ in which z satisfies $z^4 + z + 1 = 0$. Then quadratic twist of this curve $L = F_{2^4}(\beta)$, where β satisfies irreducible polynomial $X^2 + X + z^3$, will be

$$E^{tw}: y^2 + y = x^3 + z^3.$$

and it has the maximum possible number of point over $K = F_{2^4}$. This discussion is summarized in the Table 4.

p	$N_{p^4}(1)$	Elliptic Curve	Minimal Polynomial of z
2	25	$y^2 + y = x^3 + z^3$	$X^4 + X + 1$
3	100	$y^2 = x^3 + z^2x$	$X^4 + 2X^3 + 2$
5	676	$y^2 = x^3 + z^3$	$X^4 + 4X^2 + 4X + 2$
7	2500	$y^2 = x^3 + z^2x$	$X^4 + 5X^2 + 4X + 3$
11	14884	$y^2 = x^3 + z^2x$	$X^4 + 8X^2 + 10X + 2$
13	28900	$y^2 = x^3 + z^2x + 4z^3$	$X^4 + 3X^2 + 12X + 2$
17	84100	$y^2 = x^3 + z^3$	$X^4 + 7X^2 + 10X + 3$
19	131044	$y\text{^}2 = x\text{^}3 + z\text{^}\{2\}x$	$X^4 + 2X^2 + 11X + 2$

Table 4

6. FIELDS OF CARDINALITY p^5

From the elliptic curves over the field with cardinality p^5 in the following Table 5 some are found by using the trick given in Section 7 and some by using free mathematics software system Sage.

p	$N_{p^5}(1)$	Elliptic Curve	Minimal Polynomial of z
2	44	$y^2 + xy + y = x^3 + x^2 + x$	
3	275	$y^2 = x^3 + 2x^2 + x + 1$	
5	3237	$y^2 = x^3 + z^{97}x + 1$	$X^5 + 4X + 3$
7	17066	$y^2 = x^3 + x + z^{601}$	$X^5 + X + 4$
11	161854	$y^2 = x^3 + x + 1$	
13	372512	$x^3 + zx + z^{333760}$	$X^5 + 4X + 11$
17	1422241	$y^2 = x^3 + \frac{3}{4}x^2 + z^{1351944}x + z^{198311}$	$X^5 + X + 14$
19	2479247	$y^2 = x^3 + \frac{1}{4}x^2 + z^{508237}x + z^{1608725}$	$X^5 + 5X + 17$

Table 5

7. A TRICK

By Chap. 4, Sec. 3 in [5], if we have a curve E / F_q with $\#E(F_q) = N$, then we can find the number of point of the same curve over F_{q^n}. Namely write $N = q + 1 - a$ and $\alpha, \beta \in C$ be the zero's of $X^2 - aX + q$. Then $\#E(F_{q^n}) = q^n + 1 - \alpha^n - \beta^n$.

Example 7.1 The curve $E: y^2 = x^3 + 2x^2 + 2$ has $\#E(F_3) = 2$, then we can write $\#E(F_3) = 3 + 1 - 2$, therefore $a = 2$, then by [Chap. 4, Sec. 3 in [5], we have $\alpha = 1 + i\sqrt{(2)}, \beta = 1 - i\sqrt{2}$. Then

$$\#E(F_{3^3}) = 3^3 + 1 - (1+i\sqrt{2})^3 - (1-i\sqrt{2})^3 = 38 = N_{3^3}(1).$$

By this trick we can find some maximal curves over F_{p^3} and F_{p^5} with coefficients from F_p.

p	$\#E / F_p$	$N_p^3(1)$	equation
2	2	14	$y^2 + xy = x^3 + x^2 + x$
3	2	38	$y^2 = x^3 + 2x^2 + 2$
5	4	148	$y^2 = x^3 + x + 2$
11	9	1404	$y^2 = x^3 + x + 4$
17	14	5054	$y^2 = x^3 + x + 3,$

Table 6

Also

p	$\#E / F_p$	$N_{p^5}(1)$	equation
2	4	44	$y^2 + xy + y = x^3 + x^2 + x$
3	5	275	$y^2 = x^3 + 2x^2 + 1$
11	14	161854	$y^2 = x^3 + x + 1.$

Table 7

REFERENCES

[1] J. P. Serre, Rational points on curves over finite fields. Unpublished Notes by F.Q. Gouvea of lectures at Harvard University, 1985.

[2] J.H. Silverman, The arithmetic of elliptic curves. Graduate Texts in Mathematics 106, Springer Verlag, New York, 1986.

[3] J.H. Silverman and J. Tate, Rational points on elliptic curves. Undergraduate Texts in Mathematics, Springer-Verlag, New York, 1992.

[4] W.C. Waterhouse, Abelian varieties over finite fields, Ann. sci. de

[5] Lawrence C. Washington, Elliptic Curves Number Theryoy and Cryptography, by Taylor & Francis Group, LLC, University of Maryland College Park, Maryland, U.S.A, second edition (2008).

ASSESSMENT OF WATER QUALITY OF LBOD SYSTEM AND ENVIRONMENTAL CONCERNS

Ali Asghar Mahessar[1], Kishan Chand Mukwana[2], Abdul Latif Qureshi[3]
Muhammad Ehsan ul Haq leghari[4] Abdul Latif Manganhar[2]

[1]Deputy Director, Sindh Barrages Rehabilitation Project, Irrigation Department, Government of Sindh, Hyderabad, Sindh, Pakistan,
[2]Assistant Professor, Energy & Environment Engineering Department, QUEST, Nawabshah
[3]Professor, U.S-Pakistan Center for Advanced Studies in Water, Mehran University Engineering & Technology, Jamshoro, Sindh, Pakistan
[4]Managing Director, Sindh Irrigation & Drainage Authority (SIDA), Hyderabad

ABSTRACT

The system of Left Bank Outfall Drain (LBOD) is one of the major drainage projects ever carried out in Pakistan and World. This system has developed a positive impact on the productivity over large areas of land within its catchment areas, twin problem of salinity and waterlogging in these areas have reduced considerably. However, much of the positive effects in the upper reaches of the drainage catchment have been set off by negative impacts in the tail reaches. Here wetland areas were salinised and a landscape of small lakes interconnected with densely grown wetland vegetation was changed to one large water body with saline and infertile fringes. Drainage System nowadays is facing serious problem of industrial, agricultural, pesticide and municipal effluents by disposal of different pollution sources. The TDS values of collected samples range from 1500 to 23000 mg/L. Similarly the results of other water quality parameters like; calcium, sodium, chloride and magnesium are also higher than the permissible national standards. These contaminants caused degradation of LBOD system and placed serious environmental and health threats. Apart from causing degradation of drainage water quality and the large water bodies' also causing health threat to the local population through waterborne and vector diseases such as malaria have been on a steady rise. It is argued that much of these negative effects could have been avoided by just applying sound engineering principles. This paper presents adverse environmental impacts, such as pollution of the drainage waters, groundwater, and destruction of wetlands.

Keyword: LBOD system, Industrial Effluent, Waterlogging, Salinity, Drainage water

1. INTRODUCTION

The province of Sindh has faced salinity and waterlogging menace since long together with flooding and drainage. This has hampered the efforts for poverty reduction and economic development of the region. The province of Sindh has inadequate drainage capacity to smoothly dispose off rain, escape and drainage water to dispose off such waters away from command areas. Consequently the extended flooding lasts considerably longer and destroys the standing crops and raises the ground water-table rapidly to the surface. Deterioration of surface water quality also takes place when agricultural and industrial toxic wastes substances and effluents are discharged into irrigation canals and drains [1]. The absence clean drinking water is attributed to release of untreated wastewater and dumping of effluent in fresh water bodies [2]. It is estimated that 75 % of the population of developed nations lack clean drinking water and wastewater along with solid wastes are dumped into fresh water bodies [3].

The catchment area served by the mega drainage project of Left Bank Outfall Drain (LBOD) was initiated because of the acute problems of salinity and waterlogging. Hence, the LBOD has been constructed to control twin problem of salinity and waterlogging, and dispose off saline drainage water from an area of 1.275 million acres of Nawabshah, Sanghar and Mirpurkhas components and Badin component area (Culturable Command Area of 0.458 Million Acres). The sub-drains and drains discharge their saline effluent into the Spinal drain right from Nawabshah (Shaheed Benazirabad district) downwards mostly

carry agricultural and industrial effluents almost round the year [5]. However, in many parts of district Badin; the system has failed to give the desired results and has caused severe problems of land degradation and submergence of the area by saline water [6].

Drainage is nowadays identified as the forgotten factor in sustaining irrigated agriculture [7]. In the past drainage systems were designed for continuous operation and very little consideration was given to the environmental impact of the drainage water on surface water quality [8] with the resultant loss of water and an excessive load of salt being transported to surface water [9] along with any dissolved agricultural chemicals. The problem with accumulation of salts highlights the environmental concerns associated with drainage from arid irrigated lands [10].

The daily life human activities cause the pollution of fresh water bodies particularly the run-off from agricultural fields in agricultural countries. It is estimated that about 1.5 billion population around the world have no safe clean drinking water and about five million deaths per year are attributed to waterborne diseases [11]. It is estimated that 70 percent effluent from industries are disposed off without treatment into fresh water bodies and that contaminates the receiving water supplies in the developing countries [12].

The main sources of water contamination in the system of LBOD include; discharge of untreated wastewater, dumping of urban solid waste into drainage system, discharge of untreated industrial wastewater into freshwater bodies, seepage of fertilizers and pesticides from agriculture fields and soil, disposal of toxic sugar mills effluents into surface drains of the main drainage system and seawater intrusion into Tidal Link carrying [13]. Such water pollution is injurious to both the human health and biodiversity. Thus, the downstream population particularly in southern Sindh is exposed to adverse health effects due to both biological and chemical contamination of water bodies. The use of fertilizers and pesticides has increased over the years and are also causing the water pollution [14]. In addition to this the water pollution is also caused by the release of hazardous industrial wastes like persistent toxic synthetic organic chemicals, heavy metals, municipal wastewater and municipal solid wastes [15].
The wastewater generated by this way leaches down into the ground and add with ground water aquifers resulting in the contamination of the prevailing groundwater quality by changing its chemical composition [16]. The untreated effluent released from such industrial operations contaminates surface and ground water equally. It also harms the prevailing eco-system of fresh water bodies and affects the bio-diversity [17].

2. RESEARCH STUDY AREA

The LBOD drainage system as shown in Fig. 1 was launched to manage groundwater table levels and enhance the collection and disposal of drainage water from an area of 1.275 million acres on the Left Bank of the river Indus. The drainage effluent of about 1240 cusecs generated from these systems is disposed off through network of sub-drains, branch drains, main drains, spinal drain, out fall drains and Tidal Link into the Arabian Sea. The saline effluent from the LBOD system flows from the Kotri Barrage command area carried through the Spinal Drain, Dhoro Puran Outfall Drain (DPOD), Kadhan Pateji Outfall Drain (KPOD), and the Tidal Link, to the Arabian Sea

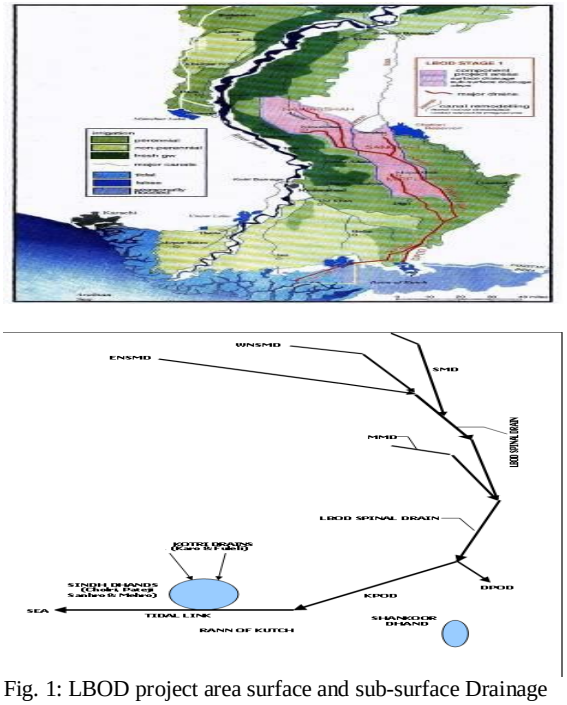

Fig. 1: LBOD project area surface and sub-surface Drainage

3. MATERIAL AND METHODS

The water samples were collected from different sample locations of the main and sub drains of LBOD system. The water samples were collected in clean sterilized plastic bottles and brought to Pakistan

Council of Research in Water Resources (PCRWR) laboratory Tando Jam for analysis. However, pH and Dissolved oxygen (DO) values were observed and recorded at the site. The results of analyzed water samples for physical and chemical characteristics are described below one by one.

4. RESULTS AND DISCUSSION

The pH value ranges from 6.2 to 8.5 according to permissible limits of NEQS. The analyzed results of pH values of 2007 and 2008 are varying from 6.2 to 7.8. Fig. 2 shows that pH values in some drains are close to threshold 7.8 which may degrade drainage water. This water is source of aquatic life and used for irrigating agricultural lands frequently. Moreover, the analyzed results of pH value of 2012 ranging from 6.2 to 7.8. Fig. 3 reveals that the values of eight locations are up to 7.8 while remaining values are lower from 7.8. However, these samples have been collected post floods 2011 from catchment area of LBOD system as shown in Fig.3 in 2012. The pH level should have reduced but concentration of alkalinity is showing increase with respect to time and could not dilute with high flood water 2011. The abrupt variations in pH (acidity and alkalinity) levels can bring stress conditions or eliminate aquatic life. This drainage water is not only room for aquatic life but also source of application water to agricultural crops. Hence, critical value of pH is not only harmful for aquatic life but also cause of degradation of fertile land.

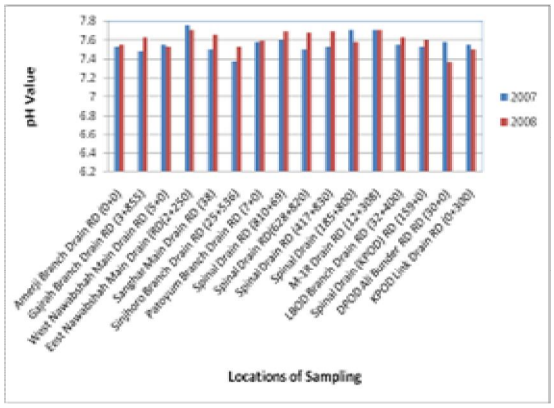

Fig. 2: pH value of years 2007 and 08

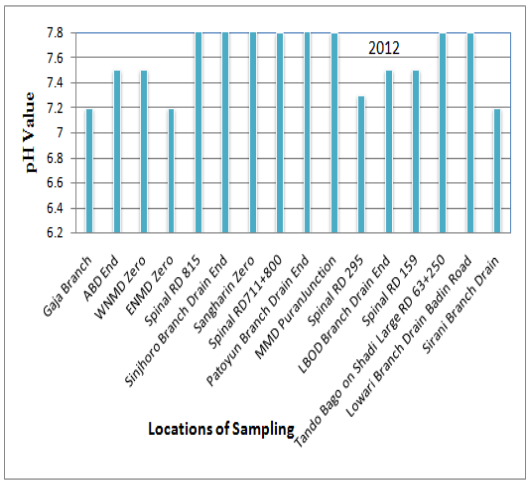

Fig. 3: pH value of year, 2012

The determined TDS values of collected samples range from 1500 to 23000 mg/L and shows a considerable variation of pollution level in the drains of LBOD as shown in Fig.4. The values of TDS of most of the samples are higher than permissible (1000 mg/L) NEQS limit. A high concentration of TDS is an indicator of possibly high value of contamination. Figure4 shows drains water is not only unfit for aquatic, drinking but also for application of agricultural cropping. However, Fig. 5 exhibits that TDS level varies from 500 to 5500 mg/L. this sample was collected after heavy rainfall in watershed area of LBOD system. Hence, TDS levels of drains have been reduced due to dilution of saline water with flood water 2011. If values of TDS in Fig. 4 and Fig. 5 are compared they demonstrate much variation between them.

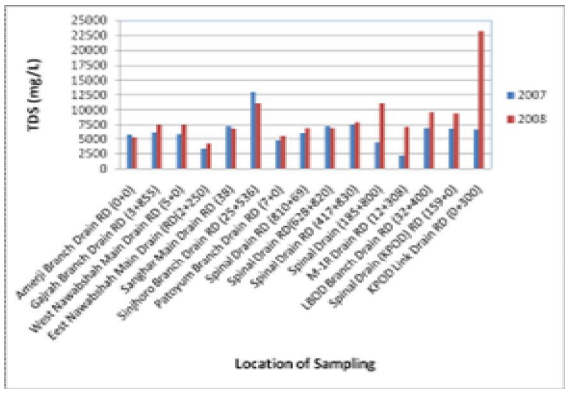

Fig. 4: TDS of years 2007 and 08

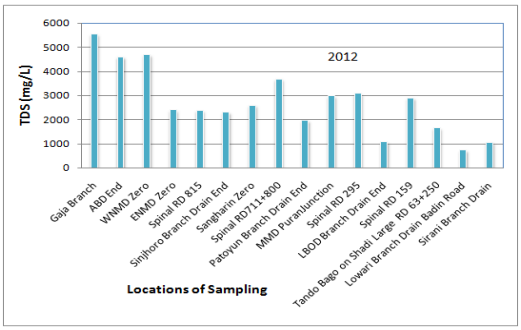

Fig. 5: TDS of year, 2012

The electrical conductivity (EC) of the analyzed water samples range from 2500 to 31000 µS/m as shown in Fig. 6. It is evident from the results that there is no any single drain whose value is within permissible levels as the acceptable level is 680 µS/m NEQS. The Fig. 7 reveals that the value of EC varies from 1000 to 8500. The comparison of values of EC is shown in Fig.6. The value of figure 6 is low due to dilution of drains' water in flood water 2011.

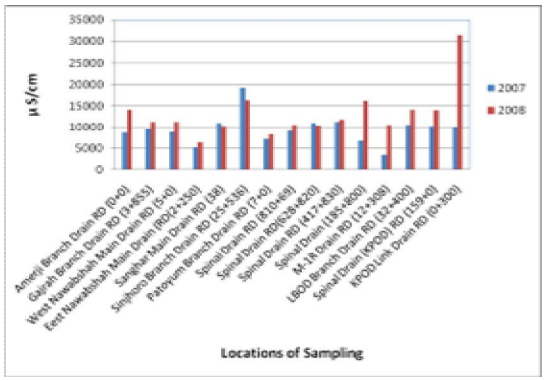

Fig. 6: Electric Conductivity of years 2007

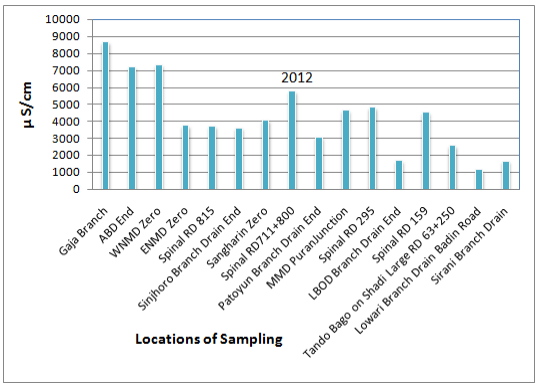

Fig. 7: Electric Conductivity of year, 2012

The collected samples were analyzed for calcium (Ca). The results were found higher than permissible NEQS values. Fig. 8 shows that calcium levels almost all drains are higher due to disposal of waste water from various sources i.e. industrial, municipal and agricultural effluents. The source of increasing calcium is due to sugar mills which are located in catchment area that are disposing off waste directly into drains without any treatment. This level of calcium is very detrimental for aquatic life while irrigating fertile lands. The comparison of Fig. 8 and Fig. 9 which demonstrates that calcium levels in Fig 9 low due to dilution with flood water 2011.

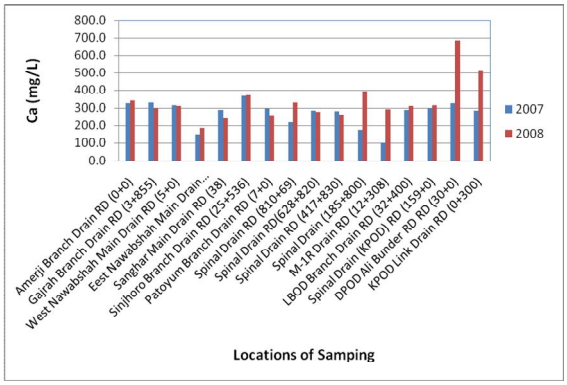

Fig. 8: Calcium of years 2007 and 08

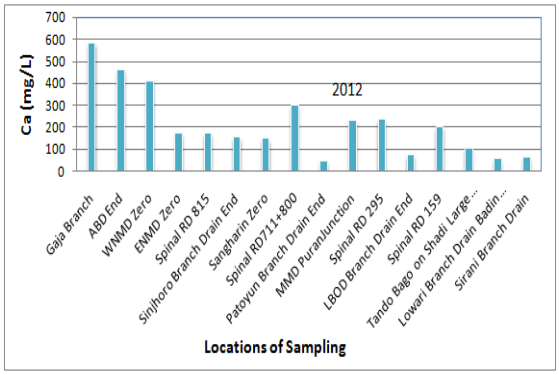

Fig. 9: Calcium of year, 2012

All the samples indicate that there is higher concentration of magnesium (Mg) in the drain water. It is due to the high quantity of ingredients containing magnesium used during the manufacturing process of the industrial units. Comparatively Fig. 10 represents larger concentration than Fig. 11. The Fig. 11 shows less concentration of magnesium due to dilution with flood water 2011.

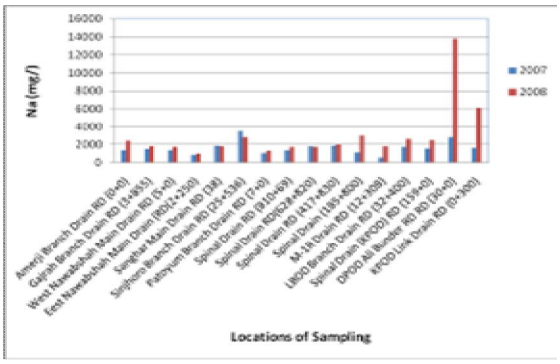

Fig. 10: Magnese of years 2007 and 08

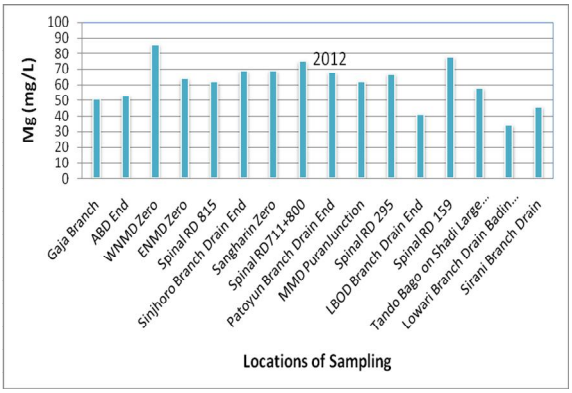

Fig. 11: Magnese of year, 2012

The presence of sodium (Na) in the samples is due to release of wastewater from various sugar mills in the watershed area of LBOD system. Therefore, the Fig. 12 and Fig. 13 indicate that there is larger quantity of sodium. Comparatively it was recorded that Fig. 12 represents larger concentration of sodium than Fig. 13. There is less concentration in figure 13 because the samples were collected post flood 2011.

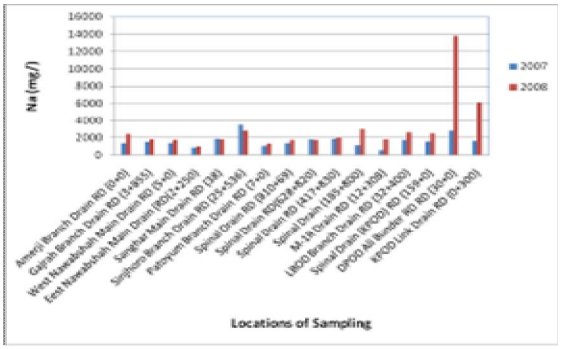

Fig. 12: Sodium of years 2007 and 08

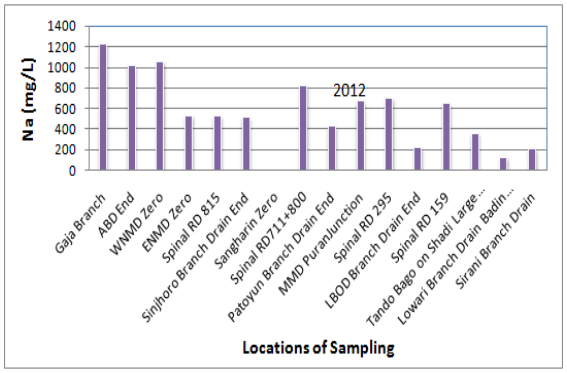

Fig. 13: Sodium of year, 2012

The chloride (Cl_2) concentrations are showing higher values than the permissible levels of NEQS as shown in Fig.14 and Fig. 15. Comparatively it was observed as shown Fig 14 the higher concentration of chloride because of combined effluent generated from units of sugar mills as they use of the higher quantities of the ingredients containing chlorides during the manufacturing process.

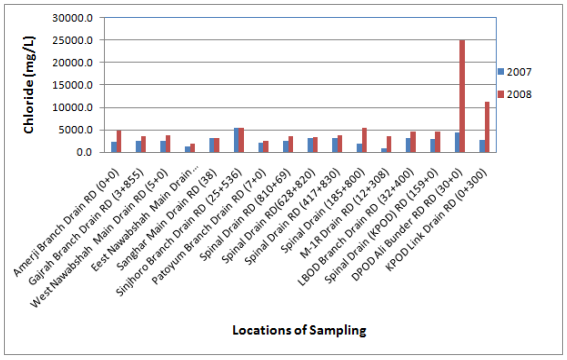

Fig. 14: Chloride of years 2007 and 2008

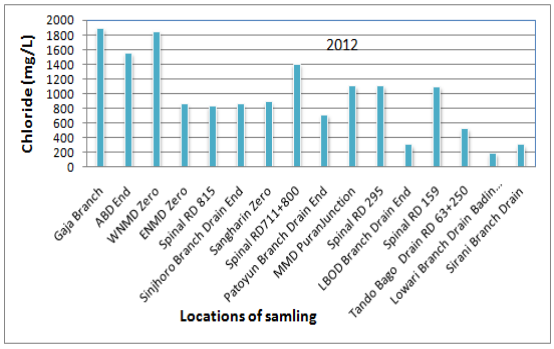

Fig. 15: Chloride of year, 2012

The hardness of all the samples as shown in Fig.16 and Fig. 17 are not within the limits of NEQS, whereas of hardness of sample obtained from West branch Nawabshah drain is too high than the permissible limits. The higher value was found at all locations as shown in Fig. 16 and its comparison is shown in Fig. 17. The higher level is due to the operational activity of sugar mills units.

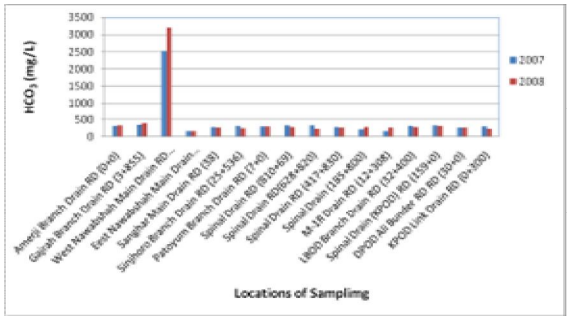

Fig. 16: Bicarbonate of years 2007 and 08

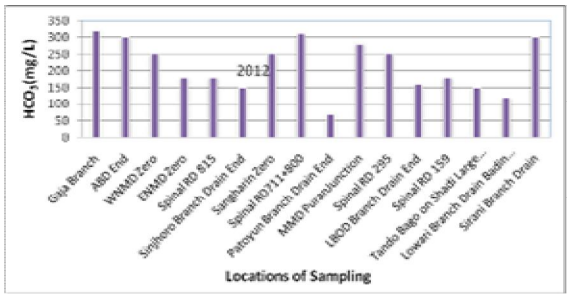

Fig. 17: Bicarbonate of year, 2012

The results of sulphate (SO_4) of analyzed samples as shown in Fig. 18 and Fig. 19 are higher than the permissible NEQS levels. Comparatively it was observed that as in Fig. 18 and Fig. 19 higher concentration of Sulphate because of combined effluent being discharged from different types of industrial units of Sugar mills.

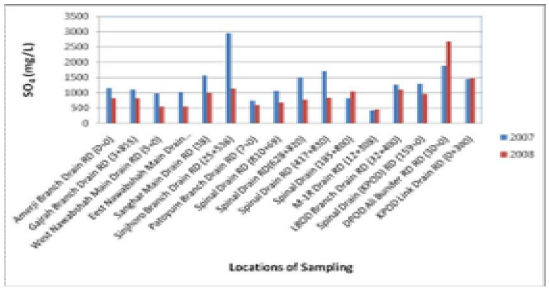

Fig. 18: Sulphate of years 2007 and 2008

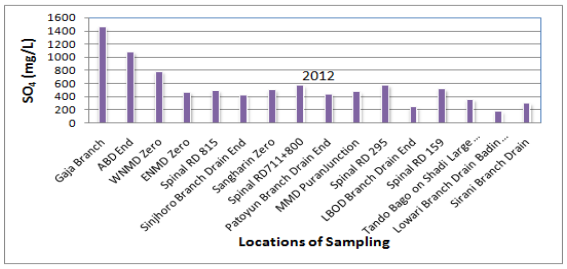

Fig. 19: Sulphate of year, 2012

Sodium in irrigation water can adversely affect the soil beneath the plant canopy. The water quality parameter known as sodium adsorption ratio (SAR) is useful when assessing the likelihood that sodium will be a problem in that regard. Water high in salinity as well as sodium may present additional problems. There are limits of SAR low sodium water SAR 0 to 10, medium sodium water SAR 10 to 18, High sodium water SAR 18 to 26 and very high sodium SAR above 26. Fig. 20 shows results of analyzed samples collected from different drains of LBOD system the values vary from 8 to 55 but frequently to close to 20. However, such water quality of drains is harmful all types of soils and requires good drainage, high leaching, gypsum addition.

Soil minerals such as calcite ($CaCo_3$) has low solubility and contribute to water only small increase in salanity as shown in Fig. 21.

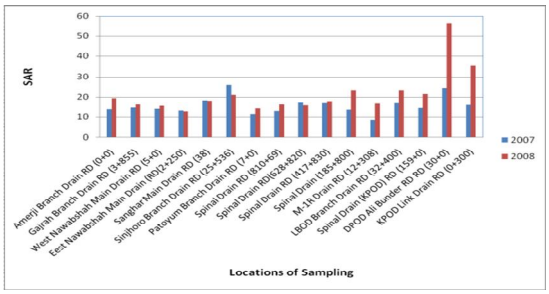

Fig. 20: Sodium Adorpation ratio

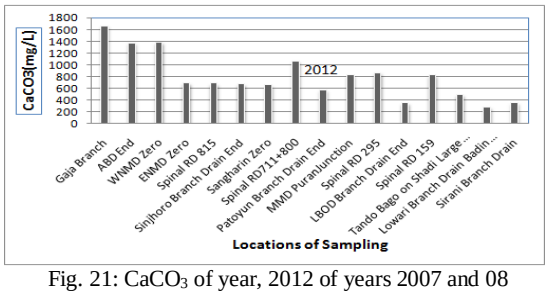

Fig. 21: $CaCO_3$ of year, 2012 of years 2007 and 08

The analyzed values for ortho phosphate (PO_4) indicates that there is high quantity of phosphate available in the wastewater sample, which shows the wastewater generated from factories is also mixing in drain water. Therefore the value of the Ortho phosphate become higher in all collected samples. The maximum value was recorded at Gaja drain and MMD as shown in Fig. 22.

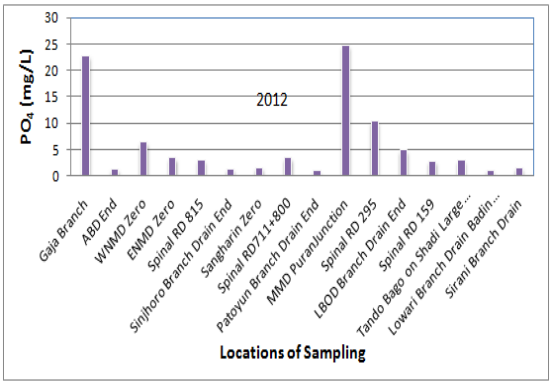

Fig. 22: PO_4 of years 2007 and 08

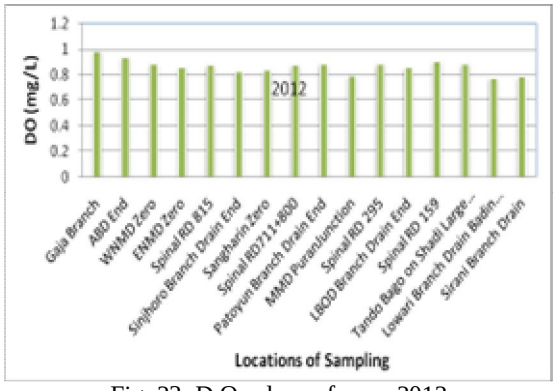

Fig. 23: D.O values of year, 2012

These analyzed results of dissolved oxygen (D.O) also indicate that there is low oxygen for aquatic life in water bodies which may cause death of ecological habitat and aquatic life as shown in Fig. 23. The lower levels of D.O indicate presence of higher quantities of organic related impurities. The organic load consumed D.O for its decomposition. The fish cannot survive at such low D.O level in water bodies if it is less than 2 mg/l as against a permissible threshold of 4.0 mg/l. The reduced D.O levels are detrimental for fish and it is almost impossible for the fish to survive under this environment having low D.O level in the water.

5. ADVERSE ENVIRONMENTAL IMPACT

The soils in the nearby drainage system have been found degraded due to the application of contaminated water of drains for growing crops due to irregular availability of canal water in catchment area of drainage network.

The contaminated drain water effects the livestock Fig. 24, such as buffalos, cows and goats suffer from diseases and die due to consumption of the effluents discharged into drains.

Fig. 24: LBOD in 2010

Fig. 25: LBOD during flood 2011

The birds and other aquatic fauna heavily rely on fish present in the drainage system as shown Fig 25. These big water bodies get significant attraction from the local as well migratory birds particularly in the winter season. However such contaminated water may cause threat to this aquatic life and consequently may affect the food chain system.

The agricultural and industrial wastewater in-filtrating through the soil from drains may contaminate the ground water. The human population living in the close vicinity has to depend only on ground water but that ground water may severely contaminate.

6. CONCLUSIONS

The untreated wastewater from industrial units as well as from domestic sources into drains of LBOD system is highly contaminated and contains pH, EC, TDS, sodium, calcium, magnesium, hardness, SAR calcium carbonate and lower limits of DO. Hence, this water is unfit for drinking and its application for irrigation is harmful for the fertility of soil. Additionally that wastewater from industrial units particularly from sugar mills without treatment was found harmful for ecosystem in the catchment area of LBOD system.

The poor water quality of drains is not only degrading fertile soil, surface water but it is also contaminating groundwater. Hence, without treatment of wastewater causes toxic water quality for aquatic life and ecological habitat. The results of collected samples in 2007 and 2008 are of very nature which shows that drain water is not fit for drinking and irrigation. Whereas, the analyzed result of collected samples in 2012 reveals better than 2007 and 2008 because the drain water was diluted with floodwater, during the year 2011 flood.

ACKNOWLEDGMENT

Authors are thankful to Sindh Irrigation and Drainage Authority, Hyderabad, Sindh, and Sindh Barrages Improvement Project, Irrigation department for their support and facility for completing this research work.

REFERENCES

1. Sohag Mumtaz Ahmed, Mahessar Ali Asghar, Memon Masroor Nabi, "Participation of Farmers in the Management of Drainage System", 4th Asian Regional Conference & 10th International Seminar on participation Irrigation Management Tehran-Iran, 2007.
2. Sohag Mumtaz, Ahmed and Mahessar Ali Asghar, "Pollution of Indus Waters and the Drainage system of Sindh", proceedings of Environmentally Sustainable Development in International Conference, COMSATS Institute of Information Technology Abbotabad, 2005.
3. Memon, Abdul Aziz, "Devastation of the Indus River Delta", Proc. World Water & Environmental Resources Congress, American Society of Civil Engineering (ASCE), 2005.
4. World Bank report, "Left Bank Outfall Drain Project and Pakistan's Waterlogging and Salinity problems" 1997.
5. Qureshi Abdul Latif, Mahessar Ali Asghar, Leghari Muhammad Ehsan-Ul-Haq, Lashari Bakhshal Khan, and Mari Fateh Muhammad. "Impact of Releasing Wastewater of Sugar Industries into Drainage System of LBOD, Sindh, Pakistan", International Journal of Environmental Science and Development, Vol. 6, No. 5, May 2015.
6. Schultz, E. International, Proceedings 5th International drainage Workshop WAPDA, February 8-15, 1992, Lahore, Pakistan.
7. Scheumann, W., and C. Freisem, "The Forgotten Factor: Drainage Its Role for Sustainable Agriculture", German Development Institute, Bonn 2001.
8. Doering, E. J., L. C. Benz. "Shallow water table concept for drainage design in semiarid and sub humid regions: Advances in Drainage", Proceedings of the Fourth National Drainage Symposium. American Society of Agriculture. St Joseph, Mich., American Society of Agricultural Engineers. ASAE Publication 12-82: 34-41, 1982.
9. Christen, E. W., J. E. Ayars, "Subsurface drainage design and management in irrigated areas of Australia", Irrigation Science 21: 35-43, 2001.
10. San Joaquin Valley Drainage, "The problem, In U. S. D. of. Interior and California Department of Water Resources: A Management Plan for Agricultural Subsurface Drainage and Related Problems on the west side San Joaquin Valley", California Department of Water Resources, Sacramento, California. p. 183, 1990.
11. K. A. Onsdorff, "What the Weitzenhoff Court got wrong?" Journal on Water and Environment Law and Practice, Vol. 4, No. 1, pp. 14-18, 1996.
12. United Nations-Water, "World Water Day brochure. [Online]. Available: http://www.unwater.org/ worldwaterday/ downloads/wwd09brochureen LOW.pdf, 2009.
13. Leghari, M. E., "Developing Sustainable Management Plan for Water Supply and Sanitation in Coastal Area of Badin" Masters diss., Mehran University of Engineering and Technology, Jamshoro, Pakistan, 2013.
14. Mahessar, A.A., Memon, N.A, Leghari, M.E.H., Qureshi, A.L. Arain, G.M, "Assessment of Source and Quality of Drinking Water in Coastal Area of Badin, Sindh, Pakistan", IOSR Journal of Environmental Science, Toxicology and Food Technology (IOSR-JESTFT) e-ISSN: 2319-2402, ISSN: 2319-2399. Volume 9, Issue 1 Ver. I, PP 09-15, 2015.
15. WHO report, "The right to water," United Nation World Water Development, 2003
16. M. C. Agale, N. G. Patel, and A. G. Patil, "Impact of sugar industry effluents on the quality of groundwater from Dahiwad village, District Dhule (M.S.)," Archives of Applied Science Research, Vol. 5, No. 2, pp. 58-60, 2013.
17. Habib, M. E., "Environmental Study of Seawater Intrusion around Tidal Link" Masters diss., Mehran University of Engineering and Technology, Jamshoro, Pakistan, 2013.

AN IMPLEMENTATION OF EXPERT SYSTEM FOR ORTHOPEDIC PATIENT DIAGNOSIS

FATIMA TUL ZUHRA*, ADNAN AHMED ARAIN**, MOHSIN ALI TUNIO***

ABSTRACT

An expert system is computer-based and knowledge-based systems that utilize expert knowledge experience of a qualified person in a restricted area. In this work, the ES_Buider 3.0 tool was used to incorporate expert knowledge and expert system technologies. This expert system tool allows the creation of Internet accessible expert systems to address many problematic domains. The developed expert system is able to assist (a) orthopedic doctors, nurses, and students in dealing with diseases associated with symptoms, and (b) orthopedic patients in the form of first-aid diagnosis and provide a repository of information vis-à-vis multiple diseases.

Keywords: Artificial intelligence, expert system, orthopedic, knowledge base, inference engine.

I. INTRODUCTION

Artificial Intelligence (AI) is an artificial brain with the capability of behaving similar to humans. Expert system (ES) is one of the applications of AI. ES aim to solve problems, make decisions, and provide consultations that normally require a human expert. An ES can be defined as a set of programs that use human expertise as knowledge, which is stored, encoded in knowledge base, and manipulated to solve problems within a specialized domain [1]. From the 60's, ES have evolved towards new techniques and applications from first systems such as PROSPECTOR, MYCIN, or DENDRAL, to the modern decision support systems [9-11]. ES had been applied to multiple problem domains, such as medical diagnosis, industrial issues, business, applied mechanics, and materials, especially aeronautics [2-6, 12-15, 24-33]. For example, ES now help diagnose illnesses (like mental disorder, diabetes, and heart), classify diseases, unit the component problem, design and develop software, and utilize fuzzy expert system via video surveillance [12-13, 16-17].

Basically, there are two types of expert system, which are (i) conventional and (ii) fuzzy logic based system. Conventional expert systems are typically symbolic reasoning engines, while fuzzy expert systems are oriented towards numerical processing, which handles uncertain or imprecise information [1]. However, there are three main components of an ES (as shown in Figure 1 & 2), which are (a) the user interface, showing questions and acquires answers from the user, showing the conclusions, and describes reasoning, (b) the knowledge or rule base (KB or RB), comprising of the facts and rules signifying the domain of knowledge, where the knowledge from specialists is transformed by a knowledge engineer into a set of rules [7], and (c) the inference engine (IE), applies the rules in order to acquire a conclusion and defines the method of reasoning used by ES. There are two main approaches of speculation used by expert system with production rules, which are forward (deductive) and backward (inductive) chaining. Depending on the project of the expert system, the inference engine performs either forward or backward chaining, or a combination of both. In deductive IE, the system begins with facts provided by the user, and then draws conclusions from those facts; there is no goal to prove, while in inductive IE, the system begins with some given goals that they need to prove. Generally, there are four people that contributed to the development of ES, who are (a) the domain expert, whose information and skills has to be gained to design and construct the expert system, (b) the knowledge engineer, who performs knowledge acquisition or the elicitation process involving a range of interview and non-interview approaches to extract knowledge from domain experts, (c) the programmer, who stores and encodes the expert knowledge into the knowledge base, and (d) the user (client or end user). Figures 1, 2 and 3 described the components and overall process of accessing valuable information from expert system through the user interface. After collecting information from the medical expert, the knowledge engineer transformed and programmed all the gathered information in knowledge base (in the form of facts and rules). When the user asks any query, the inference engine matches the user query with the stored rules in knowledge base and gives feedback to the user with appropriate explanations. The process of building an expert system is known as knowledge engineering process. The main stages in the knowledge engineering process (dialog process) are shown in Figure 3. Referring to Figure 3, this process will iterate until

*fatimatulzuhra86@gmail.com, PhD Scholar, UTM Malaysia
** Department of Computer Systems Engineering, QUEST, Nawabshah, Pakistan
*** Department of Electrical Engineering, MUET, Shaheed Zulfiqar Ali Bhutto Campus, Khairpur, Pakistan

the human expert finds the ES satisfactory for the envisaged purpose.

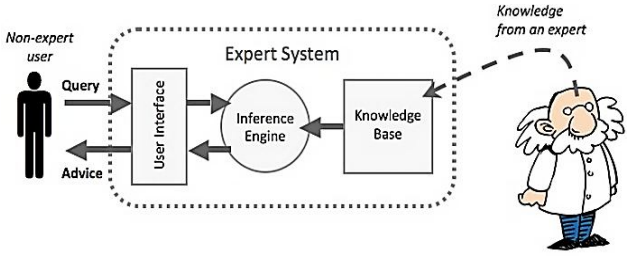

Figure 1: Interaction between expert system and user [23].

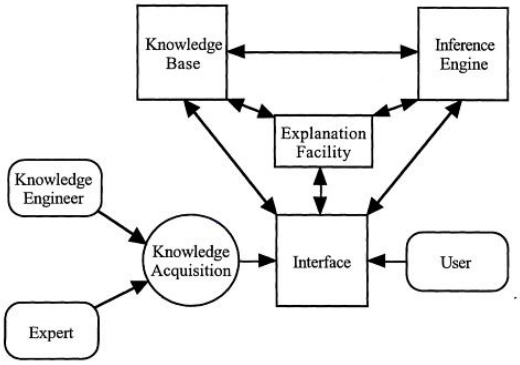

Figure 2: Architecture of expert system development and operational environment [8].

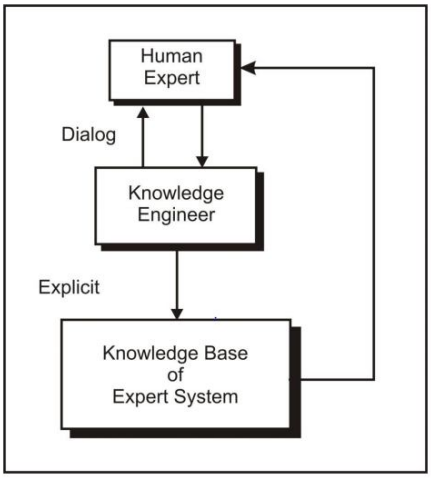

Figure 3: Knowledge engineering process [22].

Expert systems have some advantages over humans, some of them being the fact that they can possess knowledge from multiple experts, can be used in any risky environment where humans cannot work, is cheaper, permanent, unemotional, and respond relatively quickly. However, the development process of an expert system is quite a time consuming process, and it needs to be applied in an organized manner. This paper deals with the development of an expert system that (a) solve real world orthopedic problems, (b) comprises the expert knowledge of skillful human; this proficient knowledge is in a form that others may use to solve complications in a particular domain, (c) brings the user with diagnosed diseases via consultation, and (d) can enlighten the diagnoses it provides, and why it is asking particular questions. This paper is subdivided into five sections. The first section of this paper discussed the expert system, while the second describes the notion of the orthopedic field. The third section describes the expert system shell, while the fourth details its implementation. The final section concludes the paper.

II. AN OVERVIEW

A. ORTHOPEDIC FIELD

Orthopedic is a medical domain that focuses on the diagnosis, care, and treatment of patients with disorders of the ligaments, bones, nerves, joints, muscles, tendons, and skin [18]. These elements create a musculoskeletal system that helps us stand, sit, move, play, and work. Doctors who specialize in this domain are called orthopedic surgeons. Orthopedic specialists are involved in all aspects of heath care pertaining to the musculoskeletal system. They use medical, physical, and rehabilitative methods, as well as surgery. Orthopedic surgery addresses and attempts to correct problems associated with the skeleton and its corresponding attachments, ligaments, and tendons. It may also include some problems associated with the nervous system, such as those resulting from spinal injuries. These problems can occur at birth, via injury, or as the result of aging. They may be acute, as in an accident or injury, or chronic, as in many problems related to aging.

Orthopedic surgeons treat an extensive range of problems, ranging from dislocations and fractures, sciatica and low back pain, tendon injuries and ligament, bone tumors, osteoporosis and arthritis, and clubfoot [20]. Orthopedic specialists treat peoples of all age groups [21], such as (a) newborns and children with deformities, such as congenital dislocation of the hip, scoliosis, and club foot [19], (b) young people who need joint preserving surgery, such as osteotomy or arthroscopic surgery, and (c) older people with irreversible degenerative joint problems, such as joints replacement.

B. EXPERT SYSTEM SHELL

Most ES are developed using an expert system called 'shell'. An ES shell is a development tool that permits the entry of expert knowledge, and delivers the reasoning capability and user interface. An ES shell possesses a vacant inference engine, knowledge base, and a user interface. There are many tools available in the market. The ES_Buider 3.0 is user friendly, motivating, and compatible with Microsoft Windows from 98 to XP. It is used to create an ES that may be retrieved dynamically as web pages, and incorporated as a knowledge base into any website. It allows the user to generate complex, limitless decision tree, and it can be easily verified at every phase of the data entry. The purpose of the ES-Builder program is to promote expert system designers by providing a simple interface to implement prototypical ES that may have been pre-designed using appropriate design procedure. This type of ES was developed using a procedure of deductive reasoning. Thus, the expert system delivers an interface to test a series of attributes, which through the process of deduction, permits the user to arrive at a conclusion that is logically correct, based on the values selected by the user for each attribute. Built-in exporting functions include the flexibility to create web pages for (a) searching the expert system, (b) displaying the knowledge base, decision tree, and decision table, and (c) listing the attributes and values.

III. IMPLEMENTATION OF EXPERT SYSTEM

The development process of ES is time consuming. Taking this into account, this work has implemented an ES using an ES _builder expert system shell to diagnose orthopedic diseases. It consists of four phases, such as (i) domain selection, (ii) knowledge acquisition, (iii) knowledge representation, and (iv) system validation. Figure 4 (a&b) shows the output interfaces of the developed ES, where users can access the valuable information regarding a particular disease based on their symptoms. The development cycle of an expert system is shown in Figure 5. Referring to Figure 5, after selecting the orthopedic domain, knowledge was acquired by interviewing an orthopedic surgeon. The knowledge is all about the different patient's problems, such as shoulders, knees, hips, feet, thumbs, and wrists. The knowledge base is incomplete, and has six different problem areas and 370 rules with certain orthopedic diseases, but it could be updated with new symptoms and diseases. After obtaining knowledge from experts, it should be encoded and stored in the knowledge base, and transformed into one or more knowledge representation techniques. The knowledge base consists of the most widely used form of knowledge representation, such as (a) decision tree, which is a graphical depiction of the knowledge, and (b) production rules. Figure 6 represents the projected decision tree consists of some problem areas and symptoms along their specified diseases.

(a)

(b)

Figure 4(a-b): Developed orthopedic expert system where users can search any disease by identifying their problems.

Whereas the Figure 7 shows a knowledgebase consists of production rules. The production rule is typically expressed as IF (condition or premise), THEN (action or conclusion) keywords, and could have more than one condition. Conditions can be merged by OR and AND keywords. Once knowledge (initial facts) has been symbolized in some form, the inference engine will use this knowledge to draw conclusions (new facts). The ES_Buider shell has produced conclusions using the forward chaining method, where the system begins with facts provided by the user, then draws conclusions from those facts. All initial and new facts are stored in the working memory. Finally, in order to validate the ES, (a) the user is asked to answer problem-related questions, if a certain symptom appears, then the ES diagnoses the name of the disease, and post it on the screen with some satisfactory explanation, and (b) the diagnosis presented by the system was compared to the diagnosis presented by domain experts.

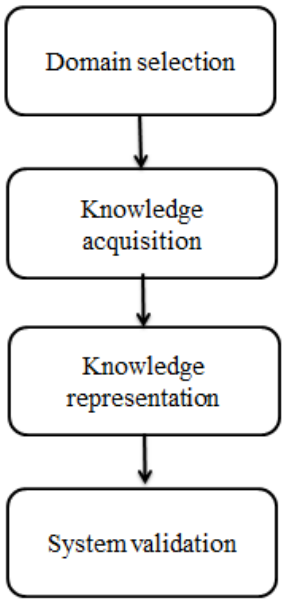

Figure 5: Expert system development cycle.

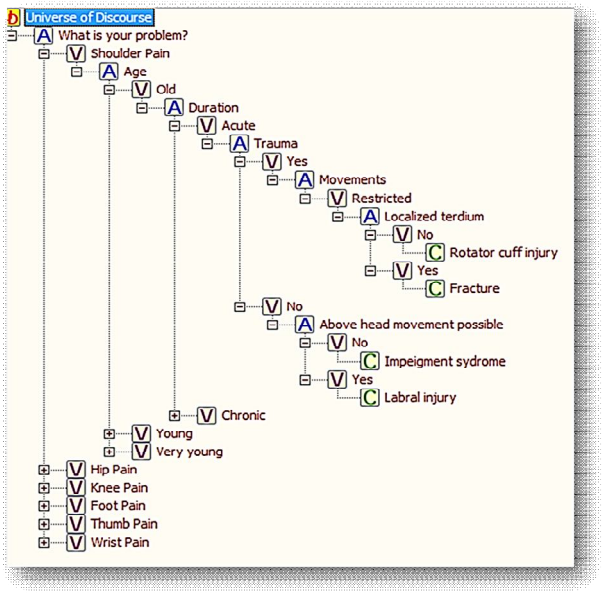

Figure 6: Decision tree of expert system.

Production rules in knowledge base

Rule 1:
IF patient has shoulder pain
AND if age is old
AND if duration is acute
AND if trauma
AND if movement restricted
AND if no localized terdium
THEN **rotator cuff injury**.

Rule 2:
IF patient has shoulder pain
AND if age is old
AND if duration is acute
AND if trauma
AND if movement restricted
AND if localized terdium
THEN **fracture**.

Rule 3:
IF patient has shoulder pain
AND if age is old
AND if duration is chronic
AND if normal movement
AND if range of movements restricted movement
THEN **adhesive capsulitis**.

.
.
.

Rule n

Figure 7: Samples of production rules in knowledge base of expert system.

IV. CONCLUSION

This paper proposed an ES that diagnoses orthopedic diseases with reasonable explanation based on their respective symptoms. The information obtained from the expert system is similar to the information specified by a skilled doctor in a particular domain. The used information in the knowledge base is incomplete, but could be updated with new symptoms and diseases.

REFERENCES

[1] Patel, M., Virparia, P., & Patel, D. 'Web based Fuzzy Expert System and Its Applications–a Survey' International Journal of Applied Information Systems, Vol. 7, No. 1, 11-15, 2012.

[2] McCauley, N., Ala, M., 'The use of expert systems in the healthcare industry' Information & Management, Vol. 22, 227–235, 1992.

[3] Johnston, M.E., Langton, K.B., Haynes, R.B., Mathieu, A., 'Effects of computer-based clinical decision support systems on clinician performance and patient outcome' A critical appraisal of research, Annals of internal medicine, Vol. 120, No. 2, 135–142, 1994.

[4] Velicer, W.F., Prochaska, J.O.,'An expert system intervention for smoking cessation' Patient education and counseling, Vol. 36. No. 2, 119–129, 1999.

[5] Leonard, K.J., 'The development of an expert system for fraud alert in consumer credit' European journal of operational research, 80 (2), 350–356, 1995.

[6] Schwuttke, U., Quan, A.G., Angelino, R., Veregge, J.R,. 'Combining real-time monitoring and knowledge-based analysis in MARVEL' Proceedings of the Second International Symposium on Ground Data Systems for Space Mission Operations, 453–458, 1993.

[7] Sagheb-Tehrani, M., 'Expert systems development: some issues of design process' Association for computing machinery (ACM), Special Interest Group on Software Engineering (SIGSOFT) Software Engineering Notes, Vol. 30, No. 2, 1–5, 2005.

[8] Medsker, L.R., 'Hybrid intelligent systems' Springer Science & Business Media, 2012.

[9] Tzafestas, S.G., 'Knowledge-based system diagnosis, supervision, and control' Springer Science & Business Media, 2013.

[10] Anderson, R.; Raeburn, S. & Beddie, L., 'Information and Knowledge Based Systems: an introduction' Prentice Hall International, New York, 1992.

[11] Giarratano J. & Riley G., 'Expert systems: principles and programming' PWS Publishing, Boston, 1998.

[12] Ali Adeli, Mehdi Neshat. 2010. 'A Fuzzy Expert System for Heart Disease Diagnosis' Proceedings of the International Multi Conference of Engineers and Computer Scientists 2010 Vol I, IMECS 2010, March 17 - 19, 2010, Hong Kong, 2010.

[13] Nursazwina Binti Ahmad Shapawi, 'Development of Web Based Fuzzy Expert System for Disease Diagnosis: Diabetes Diagnosis System, 2006.

[14] Jian Rong Wang, Yang Zhang, Tian Yu You, Shou Ming Hou, Wan Shan Wang, 'Constructing a Web-Based Fuzzy Expert System for Aeroengine Fault Diagnosis' Applied Mechanics and Materials, Vol. 16, 2009.

[15] Lopez-Cuadrado, J.L., Gonzalez-Carrasco, I., Garcia-Crespo, A., & Ruiz-Mezcua, B., 'A fully web oriented expert system tool' In IADIS International Conference, 2006.

[16] Sanz, J.A., Galar, M., Jurio, A., Brugos, A., Pagola, M., & Bustince, H., 'Medical diagnosis of cardiovascular diseases using an interval-valued fuzzy rule-based classification system' Applied Soft Computing, Vol. 20, 103-111, 2014.

[17] Muthukaruppan, S., & Er, M. J., 'A hybrid particle swarm optimization based fuzzy expert system for the diagnosis of coronary artery disease'. Expert Systems with Applications, Vol. 39, No.14, 11657-11665, 2012.

[18]Magee, D.J., Quillen, W.S., Manske, R.C., & Zachazewski, J.E., 'Pathology and intervention in musculoskeletal rehabilitation' Elsevier Health Sciences, 2015.

[19] Morelli, I., Sabbadini, M.G., & Bortolin, M., 'Orthopedic injuries and their treatment in children during earthquakes: a systematic review' Prehospital and disaster medicine, Vol. 30, No.05, 478-485, 2015.

[20]…https://en.wikibooks.org/wiki/Orthopaedic_Surgery /Introduction.

[21]…http://www.nhs.uk/conditions/orthopaedics/Pages/ Introduction.aspx.

[22]…http://shodhganga.inflibnet.ac.in/bitstream/10603 /5651/8/08_chapter%203.pdf.

[23]…https://sjhobbs.wikispaces.com/Robotics,+AI+and+ Expert+Systems.

[24] Gath, S.J., and Kulkarni, R.V., "A Review: Expert System for Diagnosis of Myocardial Infarction." arXiv preprint arXiv:1401.0245 , 2014.

[25] Jadhav, M.V., and Sattikar, A., "REVIEW of Application of Expert Systems in the Medicine." Sinhgad Institute of Management and Computer Application (SIMCA). 2014.

[26] Hyeon, Jonghwan, Kyo-Joong Oh, You Jin Kim, Hyunsuk Chung, Byeong Ho Kang, and Ho-Jin Choi. "Constructing an initial knowledge base for medical domain expert system using induct RDR." In 2016 IEEE International Conference on Big Data and Smart Computing (BigComp), 408-410, 2016.

[27] Norouzi, Jamshid, Ali Yadollahpour, Seyed Ahmad Mirbagheri, Mitra Mahdavi Mazdeh, and Seyed Ahmad Hosseini. "Predicting renal failure progression in chronic kidney disease using integrated intelligent fuzzy expert

system." Computational and mathematical methods in medicine 2016, 2016.

[28] Farahani, Farzad Vasheghani, Fazel Zarandi, MH., and Ahmadi, A., "Fuzzy rule based expert system for diagnosis of lung cancer." In Fuzzy Information Processing Society (NAFIPS) held jointly with 2015 5th World Conference on Soft Computing (WConSC), 2015 IEEE Annual Conference of the North American, 1-6., 2015.

[29] Josefiok, Mirco, Tobias Krahn, and Jürgen Sauer. "A survey on expert systems for diagnosis support in the field of neurology." In Intelligent Decision Technologies, 291-300. Springer International Publishing, 2015.

[30] Naser, Samy S. Abu, and Mariam W. Alawar. "An expert system for feeding problems in infants and children.", 2016.

[31] Arsene, Octavian, Ioan Dumitrache, and Ioana Mihu. "Expert system for medicine diagnosis using software agents." Expert Systems with Applications, Vol. 42, No. 4, 1825-1834, 2015.

[32] Long, Hao. "Aircraft Oil System Fault Detection Expert System." 2015.

[33] Ravi, Vijay Kumar, Rahul, P. M., and Krishna Anand, S., "Designing an Expert System Using Association Rule Mining for Instant Business Intelligence." Middle-East Journal of Scientific Research, Vol. 23, No. 1, 88-93, 2015.

SELECTING RIGHT FPGA FOR THE RIGHT APPLICATION: A TECHNICAL SURVEY FOR XILINX FPGAS

Abdul Rafay Khatri[1], Nasreen Nizamani[1], Ehsan Ali[1], Abdul Sattar Saand[2]

[1]Deparements of Electronic Engineering, QUEST, Nawabshah, Pakistan.
[2]Deparements of Electrical Engineering, Technology, QUEST, Nawabshah, Pakistan.

ABSTRACT

Nowadays, the Field Programmable Gate Array (FPGA) is one of the most widely used components in the field of embedded system designs. Owing to its diverse advantages, it is used in the development of system on chip (SoC), Application Specified Integrated Circuits (ASICs), Reconfigurable ICs and Digital Signal Processors (DSPs). There are many vendors, which provide the FPGA with different capacities and functionalities. Xilinx Corporation is one of the major providers of FPGAs. The major families of Xilinx FPGA include Spartan, Virtex, Artix and Kintex. Each member of their family is different based on the capacity, features and capability to perform certain functions. In this paper, a technical survey about the Xilinx FPGA families is presented along with the technical analysis, which includes growth in capacity, clock rate, the suitability of an FPGA for a particular application. In the end, Open RISC-1200's ALU circuit is implemented on the Spartan-3E family of FPGA and simulated using Xilinx ISE, to give an idea of implementation of the circuit on FPGA.

Keywords: FPGA, Xilinx ISE, Look-up table, Spartan, Virtex.

I.INTRODUCTION

Field Programmable Gate Array is a breakthrough technology nowadays in the field of embedded system design. Owing to its remarkable features such as higher speed, parallelism, self-healing capabilities, cost effectiveness and reconfigurable capabilities [1], the FPGA becomes a heart of many embedded applications like aerospace, biomedical instrumentation, safety critical systems, satellite & communication applications and wireless sensor network applications during the last decade. It is also used as a processing element in many digital signal processing (DSP) applications. The FPGA is a fast growing field in order to implement embedded systems on a single FPGA chips i.e. System on Chip (SoC) design during the last decade. There are many vendors, which are working on this technology and produces different FPGAs for different applications, namely, Xilinx, Altera, Micro semi, lattice semiconductor to name a few. Xilinx Inc is one of the major providers, which produces various families of FPGAs. The major families are Spartan, Virtex, Artix and Kintex. Each new generation of FPGA devices have more density, faster speed large memory resources and compatible interfaces. The architecture of each FPGA families contains some common elements. The generic structure is described in Section II.

This paper gives the information about the most common parameter which one must consider while selecting the FPGA for a particular FPGA. We have considered the major FPGA provider i.e. Xilinx for the survey. The organization of this paper is as follows: The generic architecture and configuration technologies are presented in Section II. Section III gives the overview of FPGA vendors along with detailed introduction of Xilinx FPGA and their families. Section IV shows the implementation and simulation of OR1200 ALU on the Spartan FPGA. In the end, Section V concludes the paper.

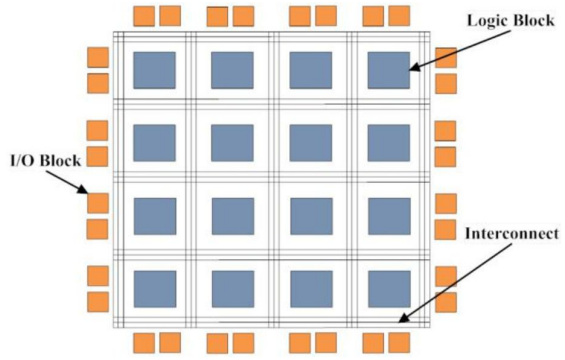

Figure 1. Simplified generic fabric of FPGA

II. FPGA ARCHITECTURE AND CONFIGURATION TECHNOLOGIES

The basic structure of the FPGA is known as fabrics. The architecture of the FPGA is divided into three main types, namely, Combinational Logic Blocks (CLBs) or Logic Elements (LEs), Routing channels or Interconnects and In-put/output Blocks (IOBs) [2]. The generic FPGA fabric is shown in Figure 1. Logic elements or CLBs are the smaller units consist of Look-Up Table (LUT) which,

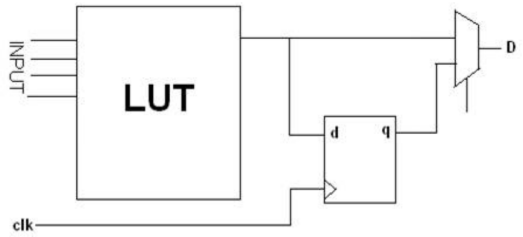

Figure. 2. Simplified structure of the FPGA LUT.

when combined, usually forms the functions of most logic circuits and designs as shown in Figure 2. CLB consists of four slices, state machine elements, combinatorial logic, controllers, and sequential circuits. The LEs are connected through interconnects that can be programmed. The FPGA has different types of interconnect depending in the distance between the logic elements to be connected [2]. The third element IOBs connects the design to the outside world. figured. There are three methods to configure the FPGAs,

1) SRAM based FPGAs
2) Flash
3) Antifuse

SRAM based FPGAs uses static memory to program or configure the FPGAs. This method is used for temporary configuration and needs to be programmed each time when power is on. The other two methods are used for permanent configuration of FPGAs. Modern FPGAs have some additional blocks that make the design easy, fast and efficient. In those FPGAs, embedded memories and embedded logic blocks are built-in to make easy interface and to perform arithmetic calculation, respectively [3]. Memory comes in different forms in new modern FPGA generation as, distributed memory is used for LUTs, FIFOs, single- and dual-port RAMs, and shift registers etc [4].

III. FPGA VENDORS AND THEIR FAMILIES

There are many vendors which provide FPGA integrated ICs, such as Xilinx, Altera, Micro-semi, Lattice semiconductor and many others. In this paper, the FPGAs from Xilinx and their families have been discussed.

Table. 1: XILINX FPGA SPARTAN FAMILY

Family	Members	# of Devices /member	System Gates	CLBs	IOBs/User IO	Block RAM bits	# of DCMs	Features/ Applications
SPARTAN	Spartan 2	6	15K-200K	96 - 1176	86-284	16K-56K	-	• Micro and Pico blaze embedded processor • Very low cost & high performance • High volume • Complete Xilinx ISE and web pack support
	Spartan 3	8	50K-5M	192-8320	124-633	72K-1872K	2-4	
	Spartan 3A	5	50K-1400K	176-2816	144-502	54K-576K	2-8	
	Spartan 3A DSP	2	1800K-3400K	4160-5968	469-519	1512K-2268K	8	
	Spartan 3AN	5	50K-1400K	176-2816	108-502	54K-576K	2-8	
	Spartan 3E	5	100K-1600K	240-3688	108-376	72K-648K	2-8	

Table.2: XILINX FPGA VIRTEX FAMILY

Family	Members	# of Devices /member	Logic cells	CLBs	IOBs/User IO	Block RAM bits	# of DCMs	Features/ Applications
Virtex	Virtex 2	6	-	-	-	-	-	• Micro and Pico blaze embedded processor • high performance • logic intensive applications • IP cores and SoC designs
	Virtex 4	17	12312-142128	-	320-896	648K-9936K	4-20	
	Virtex 5	26	-	-	172-1200	936K-18576K	2-12	
	Virtex 6	13	74496-758784	-	320-1200	5616K-39304K	-	
	Virtex 7	11	326400-1954560	-	300-1200	27M-67.68M	11	
	Virtex 7 3D	5		-	-	-	-	

A. Xilinx

Xilinx Inc, an American company, is known for developing and providing FPGA in a large scale. It is one of the major providers in this field. Xilinx FPGA products can be categorized into families, according to the different features each family provides. The main families are Spartan, Virtex, Kintex, Artix and Zynq series (SoC) [5].

1) Xilinx FPGA Spartan Family: The basic purpose of the Spartan family of FPGAs is cost sensitive in consumer electronics, high data volume applications and I/O intensive electronic applications. Each family is divided into members such as Spartan II family, Spartan 3, Spartan 3A, Spartan 3AN, Spartan 3A DSP, Spartan 3E and Spartan 6 etc. Each member consists of a number of devices with various features like number of logic cells, system gates and different features [6]–[10]. Table 1 shows the different parameters contained by each member in the family. Most application need to know the amount of LUT, system gates, CLBs, User I/O for their implementation.

2) Xilinx FPGA Virtex Family: Xilinx produces another family of FPGAs known as Virtex family. It is very well established and most widely used family from Xilinx. The Virtex family contains different members such as Virtex-II, Virtex-4, Virtex-5, Virtex-6 and Virtex-7 (Also Virtex-7 3D). Like Spartan, each member of the Virtex family consists of different devices and also sub families. Virtex 5 is the only family which is divided into 5 sub-families; remaining families are mostly divided into three sub families. This family is specifically designed for use in high performance FPGA applications. These family members are further divided based on the different platform used such as LXT, FXT, TXT, FXT etc [11]–[13]. Most of the members contain some special features such as, implementation of Power PC, High speed clock management circuitry, fast Ethernet to name a few. Table II shows the various features of Xilinx Virtex FPGA family members. The information of CLBs in Virtex family FPGAs is not directly seen but it is combined effect of slices and distributed RAM.

3) Xilinx FPGA Artix and Kintex Family*:* The basic purpose of these families is to apply these FPGAs in low cost (Artix) and mid range (Kintex) applications, respectively. These families contain only one member in each, e.g. Artix-7 and Kintex-7. Artix-7 contains 5 devices whereas Kintex-7 contains 7 devices [14].

IV. IMPLEMENTATION & SIMULATION OF OR1200 ALU ON FPGA

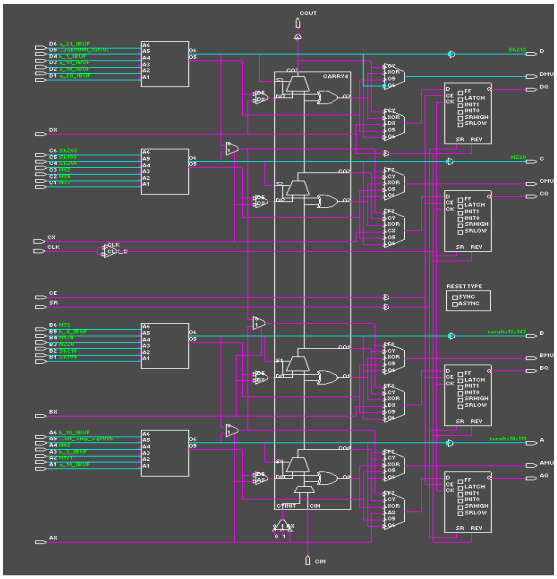

Figure. 3. Development of OR1200 ALU (FPGA editor).

The FPGA is configured and programmed into Hardware Description Languages (HDLs). The main HDL languages are Verilog and VHDL. When a program is written in these languages, number of steps are required to develop the de-signed for FPGA, such as synthesis which creates the netlist, translate, mapping on the particular device, place & route and bit file generation. A separate tool is required to do the specific task. All these tools are also provided by Xilinx, named as Xilinx ISE for these families of FPGAs [15]. Finally, IMPACT tool is used to download bit file into the target FPGA. User Constraint File (UCF) contains the information about the IOBs and the pins available on the FPGA chips. It connects the design with the outside connections. In this paper, a simple ALU from opencores.org for Open-RISC1200 processor is used and implemented on the one of the Xilinx FPGA from Spartan-3E family. This processor is written in the Verilog HDL. Using FPGA Editor tool, also provided in the Xilinx ISE, is used to visualize the implemented circuit under test as shown in Figure 3,whereas device utilization summary is shown in Table-3 for Spartan 3E 1600 device.

Table 3. Device utilization summary of circuit under test.

Logic Utilization	Used	Available	utilization
No. of slices	580	14752	3%
No. of 4 input LUTs	1046	29504	3%
No. of bonded IOBs	156	250	62%

In Table-3, the information about available device parameters and how much is used in the development and realization of a particular circuit is given. OpenRISC 1200 arithmetic and logic unit performs several operations. In this paper, some of the operations are simulated on the Xilinx ISIM simulator. The two 32-bit numbers are added (e.g. a +b) and subtracted (a-b) in this simulation. Results are shown in the Figure 4.

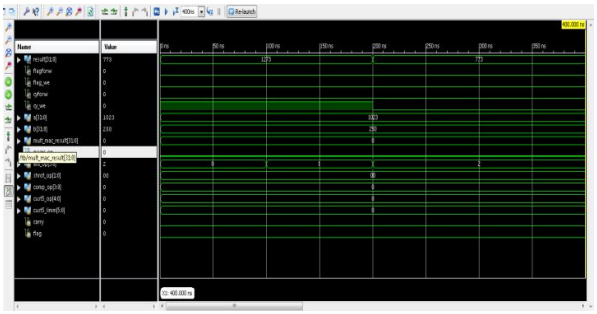

Figure 4: Simulation results for ADD/SUB commands

V. CONCLUSION

This paper presents the technical survey about the fast growing field in the development of embedded system design i.e. FPGA. It is used in the development of System on Chip designs. There are many manufacturers who are dealing with this field and provide us many types of FPGAs for various applications. The question is raised here, how do we select right FPGA for right applications? In this survey, we tried to find the answer about the Xilinx FPGAs. Xilinx is one of the biggest manufacturers of FPGAs and provides many families of FPGA for different purposes and applications. In the end, a simple design of the ALU is presented, implemented and simulated with the Xilinx tools. In this survey, various user guides and data sheets are studied from *www.xilinx.com* for each device mentioned here.

REFERENCES

[1] G. Corradi, R. Girardey, and J. Becker, "Xilinx tools facilitate development of FPGA applications for IEC61508," in 2012 NASA/ESA Conference on Adaptive Hardware and Systems (AHS), (Erlangen, Germany), pp. 54–61, IEEE, June 2012.

[2] Wayne Wolf, "FPGA Fabrics," in FPGA Based System design, ch. 3, pp. 105–164.

[3] C. Baumann, "Field Programmable Gate Array (FPGA)," in Embedded System Architecture, (Innsbruck), pp. 1–6, 2010.

[4] Pentek, "Selecting the right fpga for your application," 2016.

[5] Xilinx, "Xilinx fpga families," 2016.

[6] Xilinx, "Block in Virtex-5 FPGAs," 2010.

[7] Xilinx, "Device Package User Guide," 2010.

[8] Xilinx, "Spartan-3A DSP FPGA Family Data Sheet," pp. 1–101, 2010.

[9] Xilinx, "Spartan-3A FPGA Family," Xilinx, pp. 1–132, 2010.

[10] Xilinx Corporation, "Spartan-II FPGA Family Data Sheet," tech. rep., 2008.

[11] Xilinx Inc, "Summary of Virtex-4 Family Features System Blocks Common to All Virtex-4 Families," tech. rep., 2010.

[12] Xilinx Inc, "Summary of Virtex-5 FPGA Features," tech. rep., Xilinx, 2015.

[13] D. S. August, "Virtex-6 Family Overview Summary of Virtex-6 FPGA Features," tech. rep., Xilinx Inc, 2015.

[14] Xilinx Inc., "7 Series FPGAs Overview," tech. rep., 2015.

[15] A. R. Khatri, A. Hayek, and J. Borcsoek, "ATPG Method with a Hybrid Compaction Technique for Combinational Digital Systems," in IEEE SAI Computing Conference, (London, UK), July 2016.

SEGMENTATION AND CLASSIFICATION OF CALCIFICATION AND HEMORRHAGE IN THE BRAIN USING FUZZY C-MEAN AND ADAPTIVE NEURO- FUZZY INFERENCE SYSTEM

QAISAR JAVIAD *, MUHAMMAD ARIF**, SHAHNAWAZ TALPUR ***
*Department of Computer Science & SE, International Islamic University Islamabad, Pakistan
**Department of Computer Science, University of Gujrat, Gujrat, Pakistan
***Department of Computer Systems Engineering, Mehran University of Engineering & Technology, Jamshoro.
qaisar@iiu.edu.pk ,m.arif@uog.edu.pk, shahnawaz.talpur@faculty.muet.edu.pk,

ABSTRACT

In addition to the acquisition of excessive and false positive rates, radiotherapists tend to neglect a considerable number of deformities. The identification of features from images, along with their processing by using a pattern detection algorithm, is required in image processing. This work developed a method on the basis of the adaptive fuzzy c-mean (AFCM) method and adaptive neuro-fuzzy inference system (ANFIS). The developed method considers selective parameters, which present a major challenge in differentiating hemorrhage and calcification. ANFIS can be considered an extension of the artificial neural network family and it exhibits excellent learning skills and estimation competencies. Thus, ANFIS is a highly productive tool that can effectively manage ambiguities in any system. In medical descriptions used by radiologists, the newly recommended AFCM is desirable to offer extensive information for the early determination of a cure via surgery and radiation treatment. Desirable outcomes and useful information are most likely to be provided by fuzzy clustering segmentation methods. Irregular tissues in hemorrhage and calcification can be clearly identified with the aid of AFCM techniques. Generally, the recently recommended AFCM segmentation technique is applied to medical image segmentation. By applying this unsupervised segmentation algorithm, radiotherapists can reduce the effects of noise resulting from low-resolution sensors or/and from the movement of assemblies during data collection. The medical discipline benefits from the proposed system, especially through the identification of hemorrhage and calcification.

Keywords: Brain images, Calcification, Hemorrhage Fuzzy C-mean, Segmentation, ANFIS, Classification, Detection.

1. INTRODUCTION

The brain is a complex, delicate, and dominant part of the body that controls all bodily functions. Thus, the body is adversely affected by even the slightest brain injury. The skull protects the brain from injuries, but it prevents the brain from being directly observed for research. Hemorrhage exerts adverse impacts on the brain by altering the normal performance and structure of this organ. When abnormal cells and blood vessels in the brain are severed, brain hemorrhage normally occurs, and the functionality of the brain is affected by the presence of blood. In human beings, brain hemorrhage is the main cause of death related to solid tumor cancer [28].

The admission of calcium salts in necrotic tissue, in addition to the increase in calcified materials in local wounds, is described as a pathological calcification in the human body. Computed tomography (CT) systems generally reveal calcified wounds as high-density Hounsfield units containing phosphorus, calcium, potassium, silicon, zinc, and magnesium. Compared with routine magnetic resonance imaging (MRI), CT scanning performs better in spotting intracranial calcification as it functions on the basis of X-ray attenuation coefficients. The appearance of calcification, such as in T2-weighted (T2W) and T1-weighted (T1W) images, could not be positively defined by a common MRI sequence. The chemical process occurs at an extensive range of intensities[1, 2]. Traditional spin echo T1W and T2W images show calcification as low-intensity signals during

gradient echo acquisition; as a result, blood is displayed as a low signal and may thus cause confusion. The relatively low abundance of hydrogen protons in calcification compounds is the result of the low intensity of the calcification. A low signal is discharged by calcification, and thus, a low-intensity signal is observed in an image. An unusual hyper extreme appearance of calcification was reported by Tawil et al.[3] in a T1W image. The paramagnetic metal contents of a calcified material, which shortens the T1[3], are possibly the result of such an appearance. Calcification contents fluctuate, thus justifying the variable appearance of calcification in MRI. Given that Intra Cranial Hemorrhage (ICH) is a life-threatening condition, it must be quickly diagnosed and managed. Medical experts encounter challenges at times given that ICH is a dynamic process that exhibits several imaging attributes at the sub acute, hyper acute, and chronic stages[4].Accurately spotting calcification and brain hemorrhage is important because an erroneous diagnosis can exert adverse impacts. Moreover, the brain is a highly complex and integrated structure, and its exploration via surgery thus holds key significance[5]. An intricate connection apparently exists among brain cells. Essentially, the inner structure of the brain is not only complex but also delicate. In addition, brain chemistry cannot be examined through general laboratory tests[6][7].

To spot hemorrhage and calcification, doctors rely on varying structural evidence, various clinical frameworks, and diverse academic approaches available in the clinical domain. Establishing rule-based systems[8]often seems a difficult task. In the medical field, brain calcification and hemorrhage can be diagnosed by using MRI or computer-based methodologies. The congregate algorithm fuzzy c-means (FCM) was introduced to the examination of patients and to the diagnosis and classification of abnormalities. A new algorithm, known as the alternative FCM (AFCM),was recently developed by Wu and Yang[9].Comprehensive data can be acquired from medical images by using AFCM. The present study used AFCM segmentation techniques to distinguish hemorrhage and calcification in medical images of brains. Suitable information and desirable results are obtained through the AFCM segmentation methods.

The segmentation of medical images is a major step in clinical diagnosis. Different tissues can be clearly assessed from medical images through the successful application of clustering segmentation[10]. However, coinciding gray-scale intensities are always observed in most medical images of different tissues. Given the incomplete volume properties resulting from the low resolution of sensors and from the blur and noise during acquisition, suspicions across data obtained from MR images widely exist. Specifically, inherently vague memberships are found in boundaries, and tissues are not clearly delineated. Every point in a dataset is limited to just one cluster in traditional (hard) clustering techniques. Vague fitting labeled through a membership function (Mf) is delivered by frizzy sets. Consequently, medical images can be suitably segmented by using fuzzy clustering methods. In the present study, we focus on the use of FCM and AFCM techniques, in addition to the resolution of MRI segmentation ambiguity in ophthalmological scenarios.

2. RELATED WORK

Cocosco et al. proposed an adaptive method to segment brain MR images. A training set can be tailored using the pruning approach. The pathology of brain MRI and anatomical variability can be adjusted in this manner by using a segmentation method. Erroneously labeled samples delivered by previous tissue probability maps can be curtailed using minimum spanning tree. The k nearest neighbor(KNN) classifier[12]is used to group the tissues obtained from a brain MR image[11]. The major downside of this classifier is its inability to accurately classify tumors in the brain. El-Syed et al.[13] recommended the use of a hybrid technique to classify brain images as either normal or abnormal. This technique uses the discrete wavelet transform (DWT) method to extract the[13]features of brain MR images; these image features are subsequently condensed through principal component analysis (PCA). Finally, the features are classified as the final step. Classification basically includes two types of classifiers, namely, KNN and feed forward back propagation neural network. Zhang et al.[13] presented field models for the subdivision of brain MR images using the expectation–maximization algorithm and hidden

Markov random field[14].Subdividing a brain MR image is a completely mechanical and automated process. Threshold assessment is likely to drive this method, and this assessment is experimental in nature. Therefore, accurate results are obtained most of the time by using this method. The method proposed in[14]is costly. Saha et al.[15] proposed a fuzzy symmetry technique on the basis of the genetic clustering method for brain image segmentation. This technique uses fuzzy variable string length genetic point symmetry[15]for segmentation purposes. For membership role, a point symmetry-based distance is used instead of Euclidean distance. At this point, the basic goal is to regulate the optimum fuzzy partitioning of an MR image. Data are ideally separated by the maximum value of the FSym-index. A number of clusters can be formed, and a suitable fuzzy clustering of data can be achieved by using a genetic algorithm. In the current work, we suggest the use of fuzzy point balance-based cluster validity index to determine cluster quality. Dissimilar PD, T1, and T2 brain images have been used in certain experiments. This technique provides better output than the expectation–maximization algorithm and FCM. However, this technique does not properly segment brain images at times, and it does not consider spatial information. In addition, data sets containing similar points as a center for various clusters are not suitable for the application of this technique.

Ganesan et al.[16] proposed a fuzzy clustering method to divide brain MR images. In this method, the features of brain MR images are removed by the applying Haar wavelet transform of the images. We can obtain the approximate and detailed coefficients upon applying the Haar wavelet to a target image. In brain MR images, an imprecise coefficient is considered an attribute. Through brain segmentation, the application of these features can be observed. Experts use the clustering algorithm FCM for classification purposes. For each cluster, cluster centers are determined via FCM. The membership values for every data point in each cluster are assigned by the FCM. The cluster centers are iteratively reformed by the FCM to acquire the appropriate center within a dataset. The FCM aims to minimize objective functions. From the cluster center, the distance of any given data point is represented by the objective function. The data membership value point likely weighs the cluster center. Within an image, different objects can be easily classified using the Mf matrix. We can also use this matrix to reconstruct images. We can apply the Sobel edge detection technique for output image edge detection. The strength of the clusters can be revealed with the silhouette method. The result of the proposed method was graphically illustrated by Ganesan et al., although they did not quantitatively prove that their results are enhanced. In addition, they did not compare their results with those of other methods to validate their findings[15].

Li et al. developed an FCM algorithm with a membership constraint by integrating spatial information for image segmentation[17]. This proposed algorithm and the traditional FCM algorithm exhibit unique features. By using this new technique, we acquire enhanced MR images and their corresponding spatial data under different noise levels; the same outcome cannot be realized with the authentic FCM algorithm. For tumor extraction, Ahmed et al.[18] proposed the use of brain MR images for segmentation by integrating the Perona–Malik anisotropic diffusion model for image enhancement and the k-means clustering algorithm for grouping tissues. Desirable results are observed in the application of this method to segmentation. FCM clustering[19]has been successfully applied in various fields, such as in geology, astronomy, target recognition, medical imaging, clustering of image segmentation, feature analysis, and classified designs. Moreover, FCM is referred to as an unsupervised system. The quantitative evaluation of the results of any clustering algorithm is known as cluster validity. Wang and Wang[20] developed a modified FCM algorithm by adjusting the membership weight age of each cluster and by integrating the spatial data for brain MR image segmentation. They applied this method to different MR images and achieved valid results from the MR images under different noise types. A semi-automatic segmentation technique was proposed by Dubey et al. [21] for brain tumor observation in MR images. Compared with that in propagation, level set evolution is likely to be used by specialists in segmentation, as reported in[21]. Fuzzy clustering has been

comprehensively applied and studied in various fields[19, 22].For instance, Zadeh[23] proposed fuzzy sets and realized the idea of integrating Mfs in more than two sets described by an Mf. FCM clustering algorithm is generally applied to studies involving fuzzy clustering. In recent years, medical images have been segmented using the FCM method. Moreover, brain MRI is mostly observed using FCM segmentation techniques [24–26]. The present work focuses on the segmentation of calcification and hemorrhage in brain images.

3. MATERIALS AND METHODS

Our method was tested in 20calcified, 20hemorrhagic, and 20 hemorrhagic and calcified cases. The sample images are shown in Fig. 1.

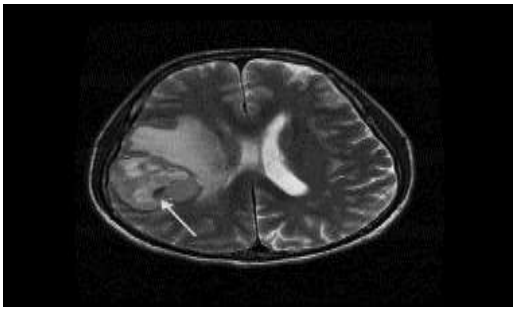

Fig. 1(a): Sample abnormal case showing hemorrhage in the MR image.

Fig. 1(b): Sample abnormal case showing calcification in the CT image

Fig. 1(c): Sample abnormal case showing hemorrhage and calcification in the CT image.

The main features of micro calcification include shape, contrast, energy, homogeneity, and correlation, which are considered in various techniques to automatically differentiate false positive and true positive measures. In addition, segmentation exerts a considerable effect on the acquisition of the abovementioned features and can ultimately assist in the classification and performance measurement. Our research work thus used segmentation to determine the precise outlines of hemorrhage and calcification and thereby maximize the information used for analysis and provide a basis for further analysis[27].

In the last few decades, the probabilistic neural network (PNN) classifier[28], artificial neural networks (ANNs)[29][30], LVQ+ANN[31],and back propagation network (BPN) classifier[32]have been widely utilized in medical image segmentation[30] and classification. In the segmentation of medical images, fuzzy clustering approaches can consider extensive mutual information related to an original image by using fuzzy membership; thus, these approaches can be used in a wide variety of applications. FCM clustering, which was established in the 1970s and later improved, assigns c membership grades and updates the membership matrix by using c × n member. Fuzzy memberships are used to update the centers that take a longer time to execute. A tight membership can be designated as pixels to update cluster centers in iterative steps and thus avoid the time and computational complexity in FCM.

1: For the p-dimensional input data, reorganize u_{ij} in the $d_1 \times d_2$ matrix, where d_1, d_2 are the input dimensions.

2: Set the new fuzzy membership functions as $u_{ij}^{\sim}$ and the label matrix as $L = \{L^1, L^2, \ldots L^c\}$, where L^k is the label matrix of the k[th] cluster in the present iteration.

3: Set all data points that are parallel to the L^k label matrix as I^K.

4: Describe $I^k = I_1^k, I_2^k, \ldots, I_{nc_k}^k$ for the k[th] cluster, where nc_k denotes the data points in the k[th] cluster.

5: Modify the center point of the k[th] cluster busing the following equation:

$$v_k^* = \frac{\sum_{j=1}^{nc_k} I_j^k}{nc_k}$$

The fuzzy cost and membership function is calculated with the following equation.

$$u_{ij}^{\sim} = \frac{1}{\sum_{k=1}^{c} \left(\frac{\|x_j - v_i^{\sim}\|}{\|x_j - v_k^{\sim}\|}\right)^{2/(m-1)}}$$

$$J_m^{\sim}(U^*, V^{\sim}) = \sum_{i=1}^{c} \sum_{j=1}^{n} (u_{ij}^*)^m \|x_j - v_i^*\|^2$$

We used the fast and accurate AFCM clustering algorithm to efficiently recognize hemorrhage and calcification.

Figs. 2(a, b, and c) show the intensity graph of the sample case of hemorrhage and calcification.

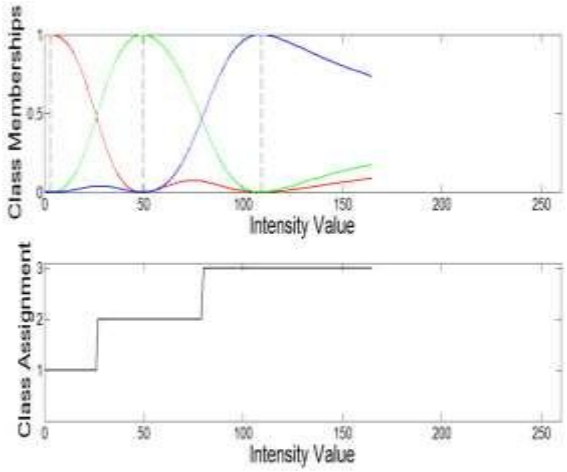

Fig.2 (a): Intensity graph of hemorrhage in an MRI image.

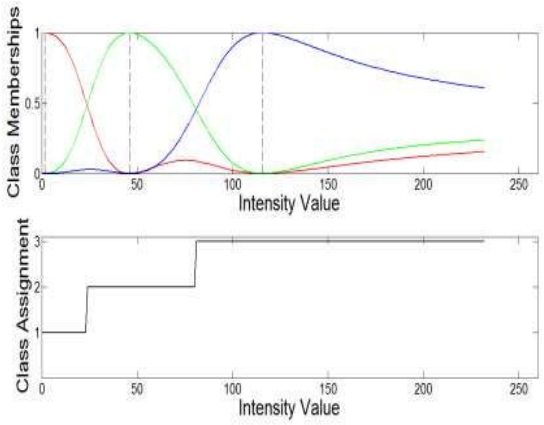

Fig.2 (b): Intensity graph of a calcification in a CT image.

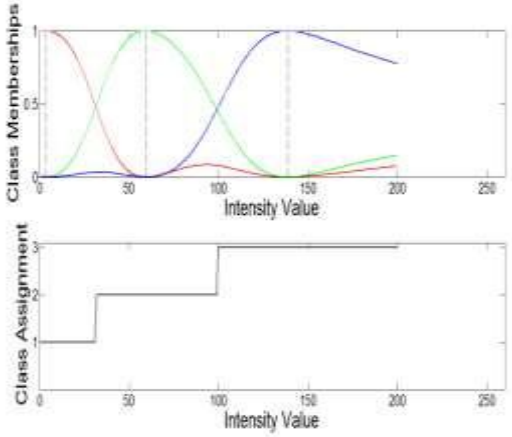

Fig.2 (c): Intensity graph of hemorrhage and calcification in a CT image.

Fig.3 shows the color segmentation of calcification and hemorrhage in brain medical images.

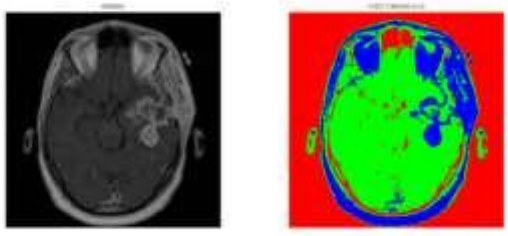

Fig. 3(a): Color clustering for hemorrhage

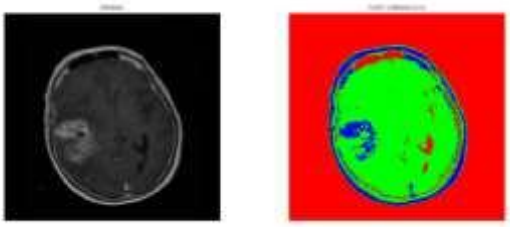

Fig. 3(b): Color clustering for hemorrhage images.

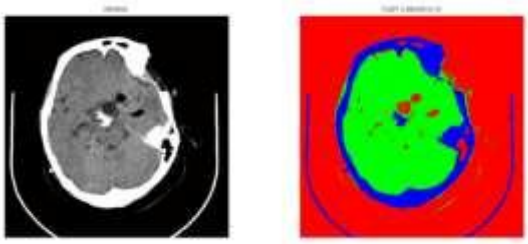

Fig. 3(b): Color clustering for calcification

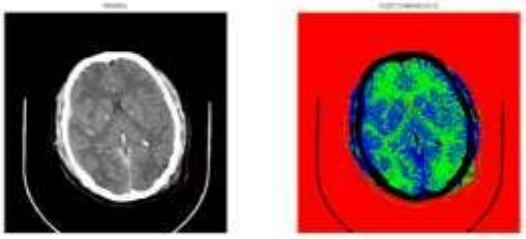

Fig. 3(d): Color clustering for calcification and hemorrhage images

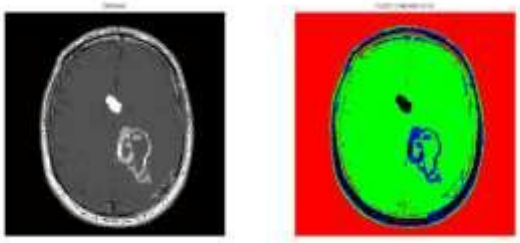

Fig. 3(e): Color clustering for calcification and hemorrhage images

We employed the AFCM on four images to show the clustering processing the calcification and hemorrhage cases.

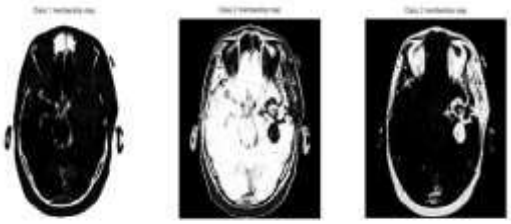

Fig. 4(a): Steps in a simple clustering of a sample hemorrhage case

Fig. 4(b): Clustering of a calcification case

Fig. 4(c): Clustering of a calcification case

Figs. 4a–cillustratethe AFCM results on the segmentation of hemorrhage and calcification cases. The succeeding step is aimed at reducing the dimensions of the AFCM results.PCA was performed to obtain the following results for dimension reduction.

GLCM was used for feature extraction after obtaining the reduction result for the AFCM dimensions. Feature extraction involves calculating the gray-level probabilities of pixels occurring in an obvious spatial association to pixels with a value j. The number of gray levels is used to determine the size of the GLCM in the whole image.

Table 1:GLCM offset values**.**

Offset	Angle
[0, D]	0
[−D, D]	45
[−D, 0]	90
[−D,−D]	135

We used the angles0°, 45°, 90°, and 135°and the distances 1, 2, 3, and 4to calculate the GLCM. The four offset values were assessed via various analyses and experiments using the stated database.

$$\sigma = \sqrt{\frac{1}{N}\sum_{i=1}^{N}(x_i - \mu)^2}$$

The following equation was used to calculate the standard deviation of the offset values mentioned above.

GLCM can be used to extract various statistics, which provide information on image texture. Tables 2 and 3 show the parameters used for the analysis in this part of our study. The outputs are hemorrhagic, calcified, or both hemorrhagic and calcified.

Table 2: Input and output parameters for hemorrhage and calcification segmentation

Inputs/Output	Parameter description
Input	
1	Contrast (Con)
2	Correlations (Corr)
3	Energy (Ene)
4	Homogeneity (Homo)
Output	
1	Hemorrhage
2	Calcification
3	Hemorrhagic and Calcification both

Table 3: Selected features for segmentation

Features	Description	Formulas
Contrast	The contrast feature quantifies the intensity of contrast between pixels and neighbors.	$\sum_{i,j} \lvert i-j\rvert^2 p(i,j)$
Correlation	The correlation feature quantifies the correlation between pixels and neighbors.	$\sum_{i,j} \frac{(i-\mu i)(j-\mu j)p(i,j)}{\sigma_i \sigma_j}$
Energy	The energy feature quantifies the aggregation of the squared elements in GLCM.	$\sum_{i,j} p(i,j)^2$
Homogeneity	The homogeneity feature quantifies the closeness of the distributions of elements from GLCM to GLCM diagonals.	$\sum_{i,j} \frac{p(i,j)}{1+\lvert i-j\rvert}$

Table 4 shows the evaluated features of 32 out of the 60 samples based on the selected features.

Table 4: Evaluated features of the sample images.

Input	Contrast	Correlation	Energy	Homogeneity
Image-1	10.47450426	0.556619373	0.114072025	0.187044719
Image-2	14.35417668	0.53538359	0.079166939	0.256324584
Image-3	11.12700305	0.479833457	0.11208159	0.198812244
Image-4	15.51959259	0.573584791	0.072812206	0.277135582
Image-5	11.6031588	0.565707397	0.109658119	0.207199264
Image-6	14.35412161	0.657738248	0.08843765	0.2563236

Image-7	13.37060501	0.660255513	0.102561135	0.238760804
Image-8	16.61253301	0.662841117	0.091158044	0.296652375
Image-9	12.93332844	0.647763718	0.101263616	0.230952294
Image-10	12.05911044	0.609394199	0.105968196	0.215341258
Image-11	9.32702551	0.564331884	0.11102797	0.166554027
Image-12	15.55630639	0.691493022	0.076347718	0.277791185
Image-13	14.35412161	0.671588661	0.090570847	0.2563236
Image-14	13.06093697	0.578486249	0.09795843	0.233231017
Image-15	8.927316171	0.449348687	0.109421862	0.15941636
Image-16	9.309806886	0.562464162	0.111650992	0.166246552
Image-17	7.960978409	0.43377205	0.105457546	0.142160329
Image-18	9.399166574	0.312201706	0.080297561	0.16784226
Image-19	15.28312301	0.688478787	0.081678311	0.272912911
Image-20	12.02222359	0.348558029	0.062117685	0.214682564
Image-21	8.763493303	0.436032965	0.111925123	0.156490952
Image-22	10.91152073	0.602611667	0.108936846	0.194848584
Image-23	10.1096182	0.313918928	0.075992211	0.180528896
Image-24	8.090069656	0.42263678	0.103549524	0.144348949
Image-25	10.52589251	0.527306407	0.11284473	0.188078126
Image-26	9.818632794	0.599843744	0.109656226	0.175332728
Image-27	12.5509036	0.646216833	0.10654619	0.224123279
Image-28	11.94982341	0.637584851	0.109515058	0.213389704
Image-29	14.02629571	0.66826515	0.095433116	0.250469566
Image-30	8.671252863	0.510581744	0.107901696	0.154843801
Image-31	9.7997867	0.485865631	0.110720101	0.174996191
Image-32	13.20666155	0.389669146	0.049584292	0.235833242

3.1. ADAPTIVE NEURO FUZZY INFERENCE SYSTEM (ANFIS)

Tissue segmentations classified into appropriate categories on the basis of ANFIS, which enhances the flexibility in training and is easily adaptable to the problem of emotion classification. ANFIS is an inference-based fuzzy system of neural networks that can be used to classify multi-class, nonlinear problems. In our methodology, we classified hemorrhage and calcification on the basis of the selected features with three hidden layers by using ANFIS. These layers contained 13, 9, and 5 neurons. Given the nature of neural networks, a standard method has not yet been developed to define the numbers of hidden layers and neurons. Therefore, the most effective architecture is usually selected. The input layer contains25 sensory neurons to match the length of the information vectors, whereas the output layer contains three neurons for classification according to seven different classes. The combination of the output neurons generates a three-digit binary sequence, and each sequence mapped to a class. The ANFIS network is trained using back propagation, which is a supervised learning technique that systematically updates the synaptic weights of multi-layer ANFIS networks. ANFIS combines all information on inputs and outputs and modifies all the information with the aid of the back propagation algorithm(Fig. 5). The ANFIS determines the target maximum velocity of the expression on the basis of the input and output training datasets. The FIS is trained and evaluated using a fuzzy logic toolbox in MATLAB.

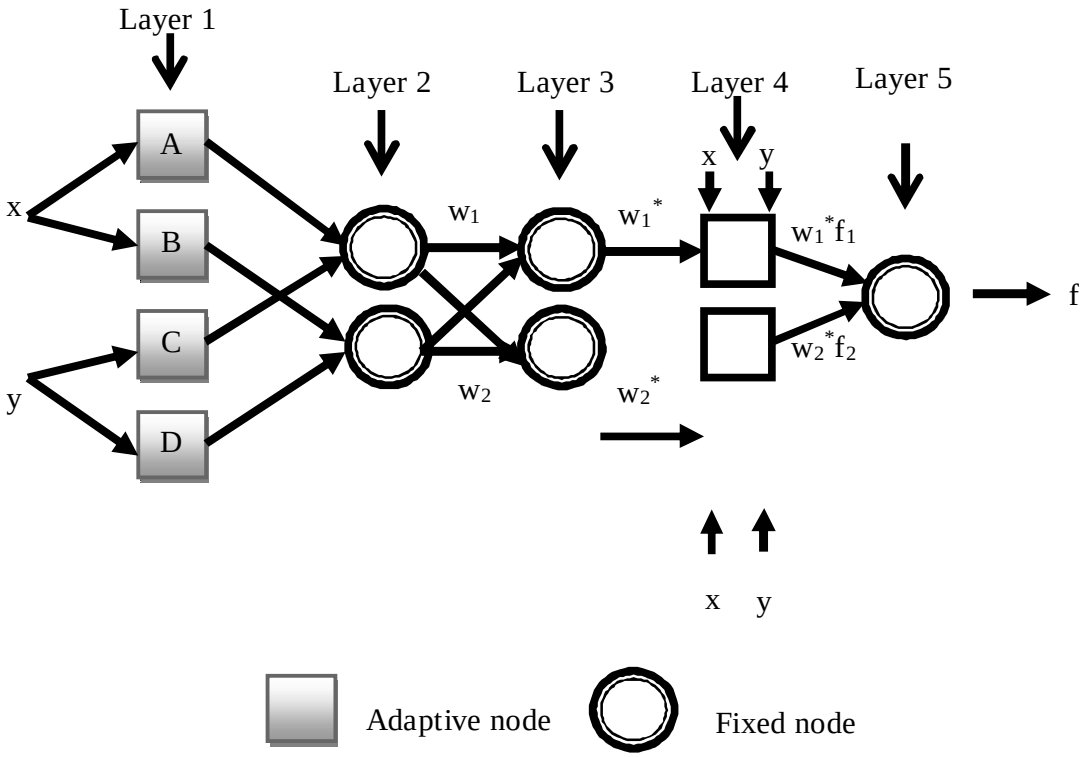

Fig. 5: ANFIS structure with two inputs, one output, and two rules

In our work, we used the first-order Sugeno model with two information inputs and the Sugeno and Takagi fuzzy rule:

$$\text{if } x \text{ is } A, \text{then } f_1 = p_1 x + t$$

The main layer in the ANFIS network comprises the Mfs and passes all information to the succeeding layer. The information is convincing textural information on hemorrhage and calcification. In this layer, every neuron is standardized with a neuron capacity.

$$0 = \mu(x, y, z)$$

Where $\mu(x, y, z)_i$ denote the Mfs.

In our work, the bell-shaped Mfs with the least and greatest equivalence of 0 and 1,respectively, were selected.

$$f(x; a, b, c) = \frac{1}{1 + \left(\frac{x-c}{a}\right)^{2b}}$$

The bell-shaped function depends on parameters a, b, and c. The b parameter is characteristically positive.

In ANFIS, the second layer verifies the weights of each Mf. It recognizes the information values from the first layer, sets the Mfs, and checks the fuzzy variable information. Every neuron in the second layer duplicates the approach, is non-adjustable, and sends an item to the succeeding layer, as presented in the following equation.

$$w_i = \mu(x)_i * \mu(x)_{i+1}$$

Every neuron outputs or indicates the firing strength or weight.

The third layer in the inference system is the rule layer. The nodes map the pre-situation fuzzy rules to calculate the activation levels of each rule and to determine whether the number of layers is equal to the number of fuzzy rules. In this layer, three nodes compute the normalized weights.

The third layer in ANFIS is non-versatile, and every neuron calculates the value of the principal finishing quality to complete the principal

terminating quality, as presented in the following equation:

$$w_i^* = \frac{w_i}{w_1 + w_2}$$

$$i = 1,2.$$

The output of the third layer is called the normalized weight or normalized terminating strength.

The fourth layer is called the de-fuzzification layer, which produces the output recovered from the third layer, known as the rule layer. Every neuron in this layer is known as a versatile neuron with a neuron capacity.

$$O_i^4 = w_i^* xf = w_i^* (p_i x + q_i y + r_i)$$

Where the parameters $\{p_i, q_i, r\}$located in the fourth layer denote the resulting constraints.

The fifth layer is known as the yield layer, which aggregates all the input summation from the fourth layer and alters the fuzzy grouping outputs into a binary. The single neuron in the fifth layer is not versatile, and it combines all information from the fourth layer and produces results.

$$O_i^5 = \sum_i w_i^* xf = \frac{\sum_i w_i f}{\sum_i w_i}$$

ANFIS is a hybrid algorithm that is used to differentiate the parameters in a given architecture. The algorithm and its variables are run until the final parameter is identified. This process continues up to the fourth layer.

4. RESULTS

The proposed technique was developed using the MATLAB software on a Core i7 with 2.6 GHz processor. Our experiments focused on brain MRI and CT images. Our data base included tumors, hemorrhage, calcification, and edemas of different locations, orientations, sizes, shapes, and types; border-enhancing tumors; and completely enhanced and non-enhanced tumors. The edema classification step presents the images as input to the segmentation phase. The segmentation phase of the proposed system precisely extracts the tumor region from these malignant brain images to a certain extent. Figs. 3 and 4 show the results of the segmentation phase. The effectiveness or correctness of the classifiers for every texture analysis was analyzed on the basis of the error rate. This error rate was depicted by the terms *true/false positive* and *true/false negative*.

TP (True Positive): The test result is positive for existent clinical abnormalities

TN (True Negative): The test result is negative for nonexistent clinical abnormalities.

FP (False Positive): The test result is positive for nonexistent clinical abnormalities.

FN (False Negative):The test result is negative for existent clinical abnormalities.

The dataset used in the testing state was provided to the proposed method to locate and classify the hemorrhage and calcification in the brain images. Evaluation metrics (specificity, accuracy, sensitivity, and overlap) were used to evaluate the obtained results. The following formulas were used to determine the values of these metrics in the brain images.

Sensitivity = TP/(TP + FN)

Specificity = TN/(TN+ FP)

Accuracy= (TN + TP)/(TN + TP + FN + FP)

As suggested by the above equations, sensitivity can be regarded as the amount of TPs correctly identified with the diagnostic test. It represents the adequacy of the test in detecting diseases. Specificity can be regarded as the amount of TNs correctly identified with the indicative test. It represents the adequacy of the test in identifying normal negative conditions. Accuracy is the amount of both TNs and TPs within a population. The exactness of a particular diagnostic test can be measured with accuracy. Specificity and sensitivity can be used to determine abnormal and normal cases, respectively. Correct accuracy and

classification of the proportion of correct classification to the total number of classification tests. The ANFIS classifier was tested by using some tested data and then evaluated using real data. We generated ANFIS architecture for hemorrhage and calcification detection. The ANFIS network was trained using the four extracted parameters. Fig. 6 shows the ANFIS architecture decision surface for calcification and hemorrhage detection and recognition of the four parameters, namely, contrast, energy, correlation, and homogeneity.

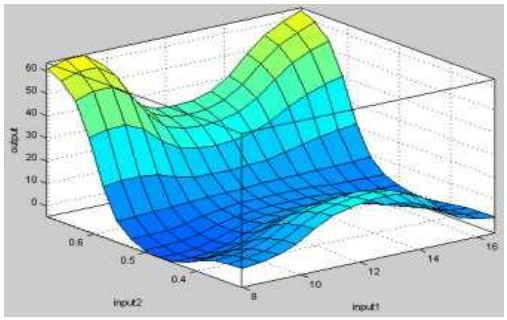

Fig: 6. (a) ANFIS decision surface for hemorrhage and calcification classification

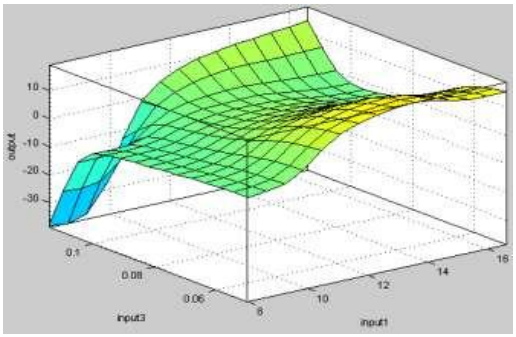

Fig: 6. (b) ANFIS decision surface for hemorrhage and calcification classification

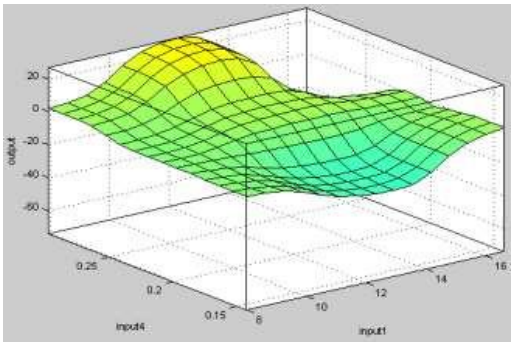

Fig: 6. (c) ANFIS decision surface for hemorrhage and calcification classification

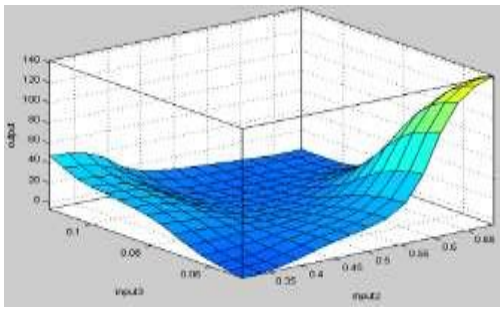

Fig: 6. (d) ANFIS decision surface for hemorrhage and calcification classification

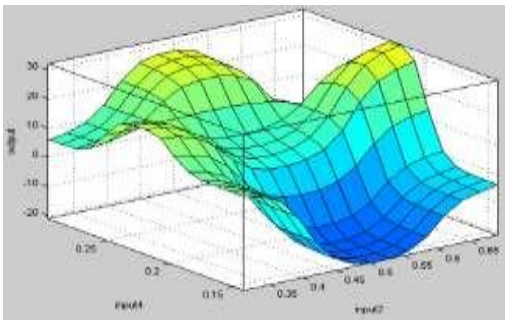

Fig: 6. (e) ANFIS decision surface for hemorrhage and calcification classification

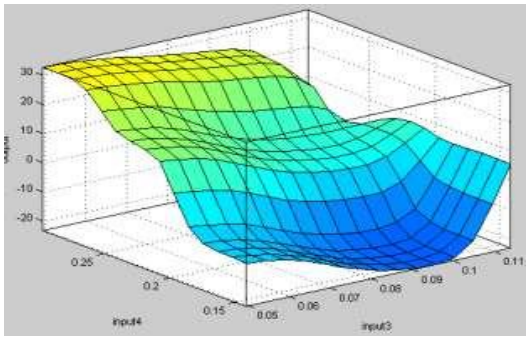

Fig: 6. (f) ANFIS decision surface for hemorrhage and calcification classification

ANFIS is useful in addressing the aforementioned issues despite the nonlinear characteristics of the diagnostic process. ANFIS method used to classify hemorrhage diagnosis by using the results for 60 records. The performance of the proposed approach under different resolutions is better than that of the other methods. It also performs better than the other algorithms when used in segmentation for dissimilar types of medical images, such as lungs, heart, and chest with single and multiple bleeding patterns.

Table 5: Performance classification of training and testing datasets by ANFIS.

Evaluation metrics	Proposed Method Training Dataset	Proposed Method Testing Dataset
TN	99	99
FP	98	99
TP	1	1
FN	2	1
Specificity	99.90	98.99
Sensitivity	99.99	99.99
Accuracy	98.90	98.60
Overlap	99.00	99.39

Table 6: ANFIS and other state-of-the art methods used in performance classification based on evaluation metrics.

Classifier	**Specificity (%)**	**Sensitivity (%)**	**Accuracy (%)**	**Overlap (%)**
ANN[29]	90.23	91.31	93.41	90.78
KNN[12]	90.34	89.23	92.34	91.76
PNN[28]	92.43	92.76	90.63	89.43
ANN+LVQ[31]	91.56	90.56	91.55	88.67
BPN[32]	88.23	93.45	92.33	92.13
DWT+PCA+ANN[13]	86.47	91.54	87.16	91.40
Proposed	98.99	99.99	98.60	99.39

To evaluate our proposed classifier, we compared our method with state-of-the-art classifiers, namely, ANN, KNN, PNN, ANN+LVQ, BPN, and DWT+PCA+ANN. For a supplementary analysis of the obtained results, the hemorrhagic and calcified regions of interest were manually marked by domain experts and served as ground reality. Table explains the specificity, sensitivity, accuracy, and overlapping of the hemorrhagic regions; the calcified regions were classified by means of ANN, KNN, PNN, ANN+LVQ, BPN, and DWT+PCA+ANN. The projected segmentation process was used to verify a dataset of 60 brain images and their dissimilarity with respect to the ground reality of the hemorrhagic and calcified regions of interest.

A quantitative assessment of the evaluation metrics was performed as a supplementary analysis of the results obtained with the proposed method. Table 5 shows that our method can generate desirable classification results with respect to ground truth regions. A dataset comprising 60 brain images was used to calculate these regions. Our method demonstrated the highest accuracy, sensitivity, and specificity. The result of the performance analysis shows the high accuracy of our method in hemorrhage and calcification segmentation. Tables 4, 5, and 6show the assessment results for the dataset consisting of 60 brain images. Table 6shows the sensitivity range (99.99–99.99) with an average value of 99.99, specificity range(99.90–98.99) with an average value 99.44, accuracy range (98.90–98.60) with an average value of 98.75,and overlapping range(99.00–99.39) with an average value 99.19.The results in Tables 5 and 6demonstrate that the proposed classification method significantly enhances hemorrhage and calcification detection in terms of evaluation metrics. The accuracy of our classification method is higher than that of the other state-of-the-art techniques.

5. CONCLUSION

A number of studies have been performed to detect hemorrhage. Some studies aimed to detect one or more of the three abnormal structures in brain images, namely, calcification, hemorrhage, or both. Some methods depend on the classification of brain lesions as either benign or malignant. The subjective analysis of brain images is influenced by issues caused by human errors, although it may also be affected by fatigue and other human-related factors. The present study investigated the systematic approach in hemorrhage and calcification segmentation by using the ANFIS strategy. A desirable outcome and useful information are most likely to be produced with fuzzy clustering segmentation methods. Irregular

tissues in hemorrhage and calcification can be effectively identified with the aid of AFCM techniques. The recently recommended AFCM segmentation techniques are generally applied to medical image segmentation. By applying this unsupervised segmentation algorithm ,radiotherapists can reduce the effects of noise resulting from low-resolution sensors or/and from the movement of assemblies during data collection. The most important parameters can be estimated by designing an ANFIS coordination scheme, which is an important criterion in overall diagnostics. Simulations were run in MATLAB, and the results obtained were observed on the corresponding output blocks.

REFERENCES

[1] Wu, Z., Mittal, S., Kish, K., Yu, Y., Hu, J., & Haacke, E. M. Identification of calcification with MRI using susceptibility-weighted imaging: a case study. Journal of Magnetic Resonance Imaging, 29(1), 177-182, 2009.

[2] Haussen, D. C., Gaynor, B. G., Johnson, J. N., Peterson, E. C., Elhammady, M. S., Aziz-Sultan, M. A., & Yavagal, D. R. Carotid siphon calcification impact on revascularization and outcome in stroke intervention. Clinical neurology and neurosurgery, 120, 73-77, 2014.

[3] Tawil, M., Wilson, J., & Wright, N. Intracranial lithography? The British journal of radiology, 75(894), 563-564, 2002.

[4] de Oliveira, D. F., de Lemos, R. R., & de Oliveira, J. R. Mutations at the SLC20A2 gene and brain resilience in families with idiopathic basal ganglia calcification ("Fahr's disease"). Frontiers in human neuroscience,2013.

[5] Creasy, J. L. Dating Neurological Injury:: A Forensic Guide for Radiologists, Other Expert Medical Witnesses, and Attorneys: Springer, 2010.

[6] Grannan, B. L., Yanamadala, V., Walcott, B. P., Stapleton, C. J., & Ogilvy, C. S. Repeated neurovascular imaging in subarachnoid hemorrhage when initial studies are negative. Journal of Clinical Neuroscience, 21(6), 993-996, 2014.

[7] Weishaupt, D., Froehlich, J., Nanz, D., Köchli, V. D., Pruessmann, K., & Marincek, B. How does MRI work?: an introduction to the physics and function of magnetic resonance imaging: Springer, 2008.

[8] Masulli, F., & Schenone, A. A fuzzy clustering based segmentation system as support to diagnosis in medical imaging. Artificial Intelligence in Medicine, 16(2), 129-147, 1999.

[9] Wu, K.-L., & Yang, M.-S. Alternative c-means clustering algorithms. Pattern recognition, 35(10), 2267-2278, 2002.

[10] Bharathi, K. K., Muruganand, S., & Periasamy, A.. Digital Image Processing Based Noise Reduction Analysis of Digital Dental Xray Image Using MATLAB. Journal of NanoScience and NanoTechnology, 2(1), 198-203, 2014.

[11] Vishnuvarthanan, G., Rajasekaran, M. P., Subbaraj, P., & Vishnuvarthanan, A.. An unsupervised learning method with a clustering approach for tumor identification and tissue segmentation in magnetic resonance brain images. Applied Soft Computing, 38, 190-212, 2016.

[12] Steed, T., Treiber, J., Patel, K., Taich, Z., White, N., Treiber, M., . . . Chen, C. Iterative Probabilistic Voxel Labeling: Automated Segmentation for Analysis of The Cancer Imaging Archive Glioblastoma Images. American Journal of Neuroradiology, 2014.

[13] El-Dahshan, E., Salem, A.-B. M., & Younis, T. H. A hybrid technique for automatic MRI brain images classification. Studia Univ. Babes-Bolyai, Informatica, 54(1), 55-57,2009.

[14] Zhang, Y., Brady, M., & Smith, S. Segmentation of brain MR images through a hidden Markov random field model and the expectation-maximization algorithm. Medical Imaging, IEEE Transactions on, 20(1), 45-57, 2001.

[15] Saha, S., & Bandyopadhyay, S. (2007). MRI brain image segmentation by fuzzy symmetry based genetic clustering technique. Paper presented at the Evolutionary Computation, IEEE Congress on 2007.

[16] Jaffar, M. A., Zia, S., Latif, G., Mirza, A. M., Mehmood, I., Ejaz, N., & Baik, S. W. Anisotropic diffusion based brain MRI segmentation and 3D reconstruction. International Journal of Computational Intelligence Systems, 5(3), 494-504.2012.

[17] Li, B., Chen, W., & Wang, D. An improved FCM algorithm incorporating spatial information for image segmentation. Paper presented at the Computer Science and Computational Technology, 2008. ISCSCT'08. International Symposium on. 2008.

[18] Ahmed, M. M., & Mohamad, D. B., Segmentation of brain MR images for

tumor extraction by combining kmeans clustering and perona-malik anisotropic diffusion model. International Journal of Image Processing,**2**(1): p. 27-34, 2008.

[19] Bezdek, J. C., Pattern recognition with fuzzy objective function algorithms. 1981: Kluwer Academic Publishers, 1981.

[20] Wang, P., & Wang, H.. A modified FCM algorithm for MRI brain image segmentation. in Future BioMedical Information Engineering, 2008. FBIE'08. International Seminar on. IEEE. 2008.

[21] Dubey, Y. K., Mushrif, M. M., & Mitra, K, Semi-automatic segmentation of MRI Brain tumor. ICGST-GVIP Journal,**9**(4): p. 33-40, 2009.

[22] Yang, M.-S., A survey of fuzzy clustering. Mathematical and Computer modelling,**18**(11): p. 1-16, 1993.

[23] Zadeh, L.A., Fuzzy sets. Information and control,**8**(3): p. 338-353, 1965.

[24] Phillips II, W., Velthuizen, R., Phuphanich, S., Hall, L., Clarke, L., & Silbiger, M., Application of fuzzy c-means segmentation technique for tissue differentiation in MR images of a hemorrhagic glioblastoma multiforme. Magnetic resonance imaging,**13**(2): p. 277-290, 1995.

[25] Lin, J.-S., Cheng, K.-S., & Mao, C.-W., Segmentation of multispectral magnetic resonance image using penalized fuzzy competitive learning network. Computers and Biomedical Research,**29**(4): p. 314-326, 1996.

[26] Suckling, J., Sigmundsson, T., Greenwood, K., & Bullmore, E, A modified fuzzy clustering algorithm for operator independent brain tissue classification of dual echo MR images.Magnetic resonance imaging,**17**(7): p. 1065-1076, 1999.

[27] Arif, M., Abdullah, N. A., Phalianakote, S. K., Ramli, N., & Elahi, M.Maximizing Information of Multimodality Brain Image Fusion Using Curvelet Transform with Genetic Algorithm. in Computer Assisted System in Health (CASH), 2014 International Conference on. IEEE.2014.

[28] Nanthagopal, A. P., & Rajamony, R. S., Classification of benign and malignant brain tumor CT images using wavelet texture parameters and neural network classifier. Journal of Visualization,**16**(1): p. 19-28, 2013.

[29] Varghese, T., Kumari, R. S., Mathuranath, P., & Singh, N. A. Discrimination between Alzheimer's Disease, Mild Cognitive Impairment and Normal Aging Using ANN Based MR Brain Image Segmentation. in Proceedings of the International Conference on Frontiers of Intelligent Computing: Theory and Applications (FICTA) Springer, 2013-2014.

[30] Dubey, Y. K., Mushrif, M. M., & Mitra, K., Segmentation of brain MR images using rough set based intuitionistic fuzzy clustering. Biocybernetics and Biomedical Engineering, 2016.

[31] Melin, P., Amezcua, J., Valdez, F., & Castillo, O., A new neural network model based on the LVQ algorithm for multi-class classification of arrhythmias. Information Sciences,**279**: p. 483-497, 2014.

[32] Rajakeerthana, K., Velayutham, C., & Thangavel, K., Mammogram Image Classification Using Rough Neural Network, in Computational Intelligence, Cyber Security and Computational Models., Springer. p. 133-138, 2014.

DETERMINATION OF ESSENTIAL STRUCTURAL ENGINEERING PROPERTIES OF NAWABSHAH CAMPUS SOIL

Ghulam Shabir Solangi*, Kanya L. Khatri*, , Zeenat M.Ali**[1], M.M Tunio***, Sadiq A. Shah****

ABSTRACT

This study was conducted for finding essential soil properties from structural engineering point of view in order to determine its suitability to receive the loads of super structure and transfer them to the underlying strata safely. For this purpose the site was selected between "B" and "C" sectors of Quaid-e-Awam University of Engineering, Science and Technology, Nawabshah, Sindh, Pakistan. Soil and water samples were collected at every 5-foot up to 80-feet depth from ground surface by using auger boring. Various laboratory as well as field tests were conducted to find out soil parameters. Also some field in situ tests were performed at site to know the bearing capacity of soil. The results show that a thin layer of cohesive soil with substantial "c-value" and shear strengths prevails the soil beneath it is sandy, the water table is high, but at a depth of about 10-feet below the surface of the soil may be termed as suitable to receive structural loads with a bearing capacity of about 0.5 kg/cm^2 or 5 tones/m^2.

***Keywords*:** *Properties of soil, QUEST, Nawabshah, bearing capacity of soil.*

1. INTRODUCTION

Soil exploration means technical investigation before any preliminary design is drawn or final plans prepared, by which the necessary information is obtained about geological, hydrological and soil conditions, geotechnical properties of soil at the prospective building site and the performance of the various soil types encountered when acted upon by structural and applied loads. This information is necessary as background upon which to base the design of a structure and to decide upon construction methods to be applied.

An engineering structures, however carefully designed is no better, than its foundation, supporting soil. In sufficient or inadequate information with respect to the character and bearing capacity of the underlying soil may result in serious structural damage or even collapse of the structure.

Soil exploration at the proposed building site is to be considered similar in purpose to the material survey, because soils are constructional materials in or on which or by means of which civil engineers build structure.

Soils are formed by the process of weathering of the parent rock. The properties of the soil materials depend upon the properties of the rock from which they are derived (Murthy, (1990). Soil is also a living natural body, formed by the interaction of environmental factors such as climate, parent materials, topography and living organisms. Nevertheless, this said soil which served as a sink to every matter on earth can be used for different purposes, but engineering purpose without proper evaluation of its present status it may result in soil degradation, rupture, structures collapse and alteration of the soil physical and chemical properties (Shepherd et al. 2002). The variety of soil materials encountered in engineering problems is almost limitless, at any given site, a number of different soil types may be present, and the composition may change over intervals of a little as a few inches (James, 1976). Similar combinations of soil-forming processes in different parts of the world have been found to lead materials of similar index properties and similar engineering characteristics (Taylor, 1990).

The bearing capacity of soil is the maximum average contact pressure between the foundation and the soil which should not produce shear failure in the soil. The the need for sort bearing capacity is based on the fact

*Department of Civil Engineering, MUET, SZAB Campus, Khairpur Mir's
**[1]Department of Chemical Engineering MUET Jamshoro
*** Energy & Environmental Engineering Department QUEST Nawabshah
**** Department of Mechanical Engineering, MUET, SZAB Campus, Khairpur Mir's

that foundations for different types of structure rest on soils. According to Bronick and Lai 2005, soil aggregation and its stability are dynamic processes because both are affected by many factors such as soil management practices, soil properties and soil environment such as soil moisture content. .In 1988, Salter said the performance of a highway pavement is influenced to a very considerable extent by the sub grade soil material. Furthermore, whereas, Oglesby and Hicks (1992) said that before 1920, attention was focused largely on the pavement surface, and little notice was given to the sub grade and base materials or to the manner in which they were placed or compacted. Later, increased vehicle speeds brought demands for higher design that resulted in deeper cuts and higher fills. In many instances, subsidence or even total failure of the roadway resulted. Study of these failures indicated that faults lay in the sub grade soil and not the pavement. This led to investigation of the properties of sub grade materials.

This would seem to be apparent that there would be no extra need to emphasize the importance of soil exploration. However, practice demonstrates that adequate soil exploration is frequently disregarded and even omitted. Lack of time in-sufficient to improper economy or to an attempt to save funds or time, the final cost of the structure exceeded every reasonable limit. The result may even be the failure of the structure itself, thus causing great troubles both to the builder and to the owner. This emphasizes the fact that it is the task of every civil engineer designing any construction work always to give first preference to the safety factor. In the light of safety, economic consideration should be regarded as secondary matter. This rule, however does not exclude the postulate of economical and safe structures. Besides timely and intelligently made soil explorations are relatively cheap as compared with the total cost of the structure or even as compared with the expenditure required only for the revision of the project and redesigning of the structure to fit the real soil conditions in order to avoid serious problems. Efficient, safe, economical design and construction can be achieved only through thorough evaluation of soil conditions under and adjacent to a proposed structure. This in turn, requires that adequate soil exploration at the proposed site should be made before any design of the foundations of a structure is started. It is best to pay proper attention to the bearing capacity and other geotechnical properties of the soil prior to the start of the construction activities or purchasing the land for construction purpose.

2. MATERIALS AND METHODS

For this study, soil as well as water samples at every 5-feet depth up to 80-feet below ground surface were collected by using auger boring. In order to determine the structural engineering properties of the studied soil, some laboratory as well as field in situ tests such as: water content, liquid limit, plastic limit, specific gravity, proctor's compaction test, sieve analysis, direct shear test, field bearing capacity by Proctor's needle method and vane shear tests were performed and their results are described in article 3.

3. RESULTS AND DISCUSSION

TABLE 3.1: Soil profile of study area up to 80- feet depth from ground surface

Depth (ft)	Type of soil	P.H value of water	Total Suspended Solids (ppm)
0-5	Silty-clay	---	---
5-10	Sandy	---	---
10-15	Sandy	---	---
15-20	Sandy	---	---
20-25	Sandy	---	---
25-30	Sandy	8.4	1477
30-35	Sandy	8.3	1372
35-40	Sandy	8.4	1423
40-45	Sandy	8.3	1344
45-50	Sandy	8.4	1456
50-55	Sandy	8.5	1680
55-60	Sandy	8.6	1897
60-65	Sandy	8.7	2136
65-70	Sandy	8.7	2380
70-75	Sandy	8.8	2464
75-80	Sandy	8.9	2828

TEST.3.1. Data and observation sheet for water content determination of 1st 5-ft depth soil by oven drying method

S.No.	Container No.	1	2	3	4
1	Wt.of empty container W_1 (g)	28.7	32.6	26	44.4
2	Wt.of container + wet soil W_2 (g)	166.5	151.1	148.7	182.7
3	Wt.of container + oven dried soil W_3 (g)	143.8	131.9	128.7	160.3
4	Wt.of water (W_2-W_3) g	22.7	19.2	20	22.4
5	Wt.of dry soil (W_3-W_1) g	115.1	99.3	102.7	115.9
6	Water content (%) = $\frac{W_2-W_3}{W_3-W_1}$ x 100	19.72	19.33	19.47	19.58
7	Average water content = 19.52%				

TEST.3.2. Data and observation sheet for specific gravity determination of 1st 5-ft depth soil by Density bottle method

S.No.	Container No.	1	2	3
1	Wt.of empty density bottle W_1 (g)	250	260	265
2	Wt.of bottle + oven dried soil W_2 (g)	449.6	460	464.7
3	Wt.of bottle + soil + water W_3 (g)	1390.4	1400.4	1405.5
4	Wt.of bottle + water W_4 (g)	1260.5	1270.5	1275.5
5	Specific gravity (G) = $\frac{W_2-W_1}{(W_2-W_1)-(W_3-W_4)}$	2.86	2.85	2.87
6	Average specific gravity (G) = 2.86			

TEST.3.3. Data and observation sheet for specific gravity determination of 15-ft depth soil by Density bottle method

S.No.	Container No.	1	2	3
1	Wt.of empty density bottle W_1 (g)	250.6	260	265
2	Wt.of bottle + oven dried soil W_2 (g)	450.6	460	465
3	Wt.of bottle + soil + water W_3 (g)	1371.8	1381.2	1386.2
4	Wt.of bottle + water W_4 (g)	1245.9	1255.9	1260.9
5	Specific gravity (G) = $\frac{W_2-W_1}{(W_2-W_1)-(W_3-W_4)}$	2.699	2.677	2.678
6	Average specific gravity (G) at 27^0C = 2.684			

TEST3.4. Determination of shear parameters by Direct shear test.

Specimen No.	1	2	3	4
Shear force divisions	50	70	90	110
Normal load (kg)	4	8	12	16
Shear force (kg)	4.5	6	7.5	9
c = 32.9Kg/cm^2 = 2.9/36 = 0.08 kg/cm^2 = 80 g/cm^2				
ϕ = 20^0				

Area of specimen = 6 x 6 cm^2 | Moisture content = 16% | Dry density = 1.81 g/cm^3

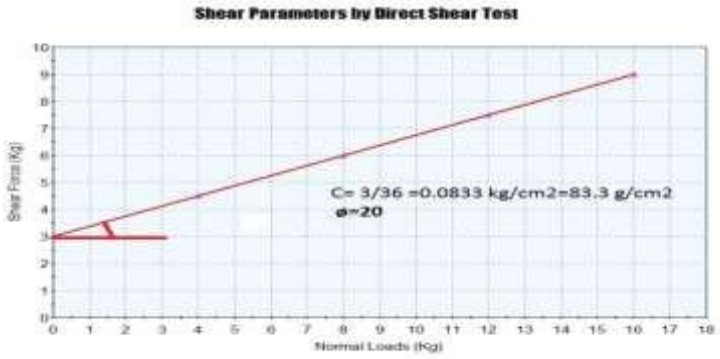

Fig.3.1 Graph between normal load and shear load

Test.3.5. Determination of liquid limit of 1st 5-ft depth soil

S.No.	Determination No.	1	2	3	4
1	No. of blows	57	63	12	19
2	Container No.	R	G	S	S
3	Wt.of container W_1 (g)	53.1	36.0	26.1	28.8
4	Wt.of container + wet soil W_2 (g)	60.6	53.8	39.2	43.9
5	Wt.of container + dry soil W_2 (g)	58.7	49.5	34.6	38.7
6	Water content (%)	34	31	54	53

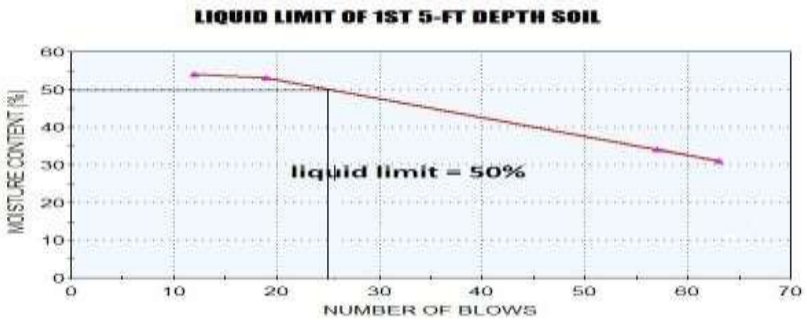

From graph, liquid limit at 25 blows = 50%

TEST.3.6. Determination of plastic limit and plasticity index of 1st 5-ft depth soil

S.No.	Determination No.	1	2	3
1	Wt.of container W_1 (g)	30	32.5	36
2	Wt.of container + wet soil W_2 (g)	31	34.4	38.6
3	Wt.of container + dry soil W_2 (g)	30.8	34	38.0
4	Water content (%)	25	26.66	30

Results:

(a) Average plastic limit = 27%

(b) Plasticity index = L.L – P.L = 50-27 = 23%

Test.3.7. Determination of compaction properties (bulk density, dry density and O.M.C) of first 5 feet depth soil by standard proctor's compaction test

(a) Density						
Determination No.	1	2	3	4	5	6
Wt.of mould W_1 (g)	4150	4150	4150	4150	4150	4150
Wt.of mould + compacted soil W_2 (g)	5950	6050	6100	6125	6110	6100
Wt.of compacted soil W = (W_2 - W_2) g	1800	1900	1950	1975	1960	1950
Bulk density (γ)	1.9	2.01	2.06	2.09	2.01	2.06
Dry density (γ/1+m)	1.7	1.76	1.8	1.7	1.65	1.7
(b) Water content						
Container No.	S	H	A	B	I	R
Wt.of container (g)	30	28.8	37.9	35.6	32.6	26.1
Wt.of container + wet soil (g)	80.5	100	96.4	121.7	93.9	115.8
Wt.of container + oven dried soil (g)	74.6	91	88.6	108.6	84.2	101.3
Water content (m) % =	13.2	14.5	15.4	17.8	18.8	19.3
O.M.C = 15.61 % ≈16% (from graph), Dry density = 1.80 g/cm^3						

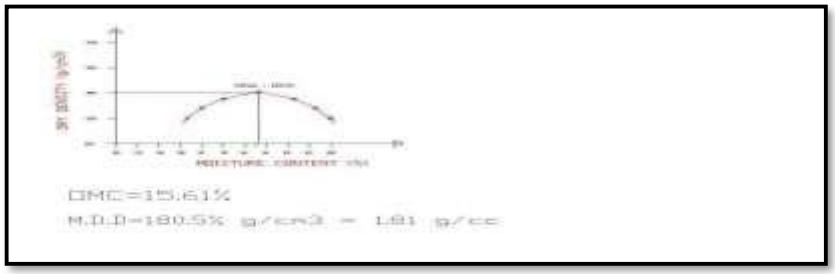

Fig.3.3 Graph between water content and dry density

Test.3.8. Determination of grain size distribution of 10-15 feet depth soil by sieve analysis

.

S.No.	Sieve size	Sieve opening	Wt. retained (g)	% retained	Cumulative % retained	Cumulative % finer
1	No.20	600 micron	10.1	1.01	1.01	98.99
2	No.30	485 micron	8.72	0.872	1.882	98.118
3	No.40	425 micron	6.00	0.60	2.482	97.518
4	No.50	300 micron	5.70	0.57	3.052	96.948
5	No.100	150 micron	5.00	0.60	3.652	96.348
6	No.170	90 micron	4.00	0.40	4.052	95.948
Total weight of soil sample = 1000 grams						

Result = Fine sand

TEST3.9. Determination of field bearing capacity of soil by Proctor's needle method

Observation No.	**1**	**2**	**3**	**4**	**5**
Ring readings	25	30	35	40	55
Load (kg)	12	14	16	18	55
Penetration resistance (kg/cm^2)	1.9	2.2	2.5	2.8	3.9
qu (average)	2.66 kg/cm^2 =	20.66 tones/m^2 = 37 lbs/in^2			
Diameter of needle head = 2.85 cm					
Area of bearing face = $\frac{\pi}{4} d^2 = \frac{\pi}{4} (2.85)^2$ = 6.4 cm^2					

TEST 3.10. Determination of cohesion apparent (c) of soil by Vane shear test

Determination No.	**1**	**2**	**3**	**4**	**5**
Height of vane (H) cm	10	10	10	10	10
Diameter of vane (d) cm	5	5	5	5	5
Torque (T) = Load x distance (kg x cm)	5x38=190	5x38=190	6x38=228	6x38=228	6.5x38=247
Value of "c"	0.4	0.4	0.5	0.5	0.54
Average cohesion apparent "c"	0.468 kg/cm^2 = 4.6 tones/m^2				
T = π d^2 c ($\frac{H}{2} + \frac{d}{6}$)		**c = $\frac{T}{458}$**			

TABLE 3.2 Summary of results of Silty- clay (1st -5 feet) soil of the study area

S.No.	Description	Data
1	**Natural water content**	19.525%
2	**Liquid limit**	50%
3	**Plastic limit**	27%
4	**Plasticity index**	23%
5	**Specific gravity**	2.86
6	**Maximum dry density**	1.81 g/cm^3
7	**Optimum moisture content (O.M.C)**	16%
8	**Angle of internal fraction "Φ"**	20^0
9	**Cohesion apparent "c" by vane shear test**	0.468 kg/cm^2
10	**Field bearing capacity by Proctor's needle method**	2.66 kg/cm^2 or 37 lbs/in^2

3. CONCLUSIONS

The soil investigation details of which presented in this study were aimed at finding the essential soil properties from structural engineering point of view in order to determine its suitability to receive the loads of super structure and transfer them to the strata safely. The properties show that a thin layer of cohesive soil with substantial "c-value" and shear strengths prevails the soil beneath it is sandy, the water table is high, but at a depth of about 10-feet below the surface of the soil may be termed as suitable to receive structural loads with a bearing capacity of about 0.5 kg/cm^2 or 5 tones/m^2.

Results obtained from this study will be helpful to analyze and predict the bearing capacity of soils with considerable reliability and will let the engineers make relatively accurate estimate of safe bearing capacity of soil under different ground conditions.

Acknowledgement
The authors are grateful to the Quaid-e-Awam University of Engineering, Science and Technology, (QUEST) Nawabshah for providing the research facilities.

5. REFERENCES

[1] Bowles, J. E., Foundation Analysis and Design, 5th edition.
[2] Bronick C, Lai R (2005), Soil structure and management. A review, Geaderma
[3] BS 1377 (1990), Methods of test for soils for civil engineering purposes, General requirements and sample preparation
[4] Dangnachew. D., (2011), Investigation Engineering characteristics of soil in Adama Town, Ethiopia
[5] Das, B.M. (1998), Principles of Geotechnical Engineering, 4th edition, PWS Publishing Company.
[6] Eni, et al., (2013), Evaluation of soil bearing capacity and its implication for foundation compatibility in Calabar, Nigeria, Journal of Social Science, Vol. 2(2), pp 34-37
[7] Head, K. H. (1992), Manual of Soil Laboratory Testing, Volume 1: Soil Classification and Compaction Test, 2nd edition, John Wiley and Sons.
[8] James K.M., (1976), Fundamentals of soil behaviour, University of California, Berkeley, John Wily and sons, Incl.
[9] Murthy, V.N.S., (1990), Geotechnical Engineering: Principles and Practices of Soil Mechanics and Foundation Engineering, Marcel Dekker, Incl., New York
[10] Oglesby, C.H and Hicks, R.G (1992), Highway Engineering, John Wiley and Sons, New York, 4th edition, 847 pp.
[11] Ola, S.A. (1978), Geotechnical properties and Behavior of some stabilized Nigerian Laterite Soil, Q.T.J. Engr. Geo. London Vol.III pp.144-160
[12] Quadri, et al., (2012), Investigation of the Geotechnical Engineering Properties of laterite as a Sub grade and Base Material for Road Constructions in Nigeria
.[13] Salter, R.J (1988), Highway Design and construction, Macmillan education limited, London, pp 341
[14] Soil Mechanics and Foundations Hand Book, Edited by Dr. B. C. Punmia
[15] Taylor R.M., (1990), Tropical Residual soils, The Quaternary Journal of Engineering Geology, London

METAL REMOVAL WITH CARBOXYMETHYL CHITOSAN USING SMALL COLUMNS

Zeenat M. Ali* Shuaib M. Laghari **, A. Jabbar Laghari*** M.M. Tunio****

ABSTRACT

Chitosan has reactive amino (NH_2)& hydroxyl (OH) groups on its skeleton, which could be used for chemical modifications under mild reaction conditions to alter its properties. In present work the alkylation method was opted for the preparation of carboxymethyl chitosan. The characterization of the compound was carried out via scanning electron microscopy, energy dispersive x-rays and fourier transformation infrared (FTIR) techniques. Five small columns were prepared each contained 2 gram carboxymethyl chitosan. The columns carried copper (lI), zinc (II), chromium (IIl), iron (II) and nickel (II) solutions having concentrations of 10-100 µg/L. When compared the order was Cu>Zn>Cr>Fe>Ni. The removal efficiency of over 86.4% - 95.1% and recovery of 100% was observed from wastewater for copper (132 mg/L), zinc (171 mg/L), chromium (118 mg/L), iron (353 mg/L) and nickel (96mg/L).

Key words: *efficiency, chitosan, columns, solution*

1. INTRODUCTION:

Many water-soluble derivatives have been prepared by quaternization or by introducing carboxyalkyl groups as carboxymethyl, carboxyethyl, carboxybutyl water-soluble Polymers in macromolecular chain of chitosan.In present work the carboxymethyl chitosan was prepared by modified direct alkylation method [**1**], because it utilized monochloroacetic acid for preparation of chitosan derivatives under optimum reaction conditions by soaking it into alkaline solution of pH 8–8.5 where only the amine groups were activated. The carboxymethyl group in present research work it was derivatized through O-chitosan [Fig. 1]. Wang et al [2]investigated crude oil for possiblemetal removal capacity by carboxymethyl chitosan using microwave technique. According to results the removal efficiencies of nickel and vanadium were 69.79%-93.66% at 60 °C with 500 mg/L dosage. Kannamba et al [3] reported preparation of cross linked xantate-chitosan for removal of Cu (II).Parameters for Cu(II) such as temperature, contact time,concentration, and pH wereexamined. Sepehran [4] et al reported Cu (II) and Ni(II) removal efficienciesfromsolutionsusing chitosan and modified chitosan at two values; pH 2.8 and pH 4.8 with 20 minute and 18 hours contact time. Gandhi et al [5] enhanced the sorption capacity of chitosan throughchange in beads of chitosan in order to remove copper. The Physical parameters studiedfor copper suggested nature if endothermic could follow Freundlich isotherms.Emaraa Adel [6]worked on derivatives ofchitosan for uptake of copper Cu(II) and concluded 0.461-0.572mmol/g concentration intake capacity at pH 5.6. Whereas polymer cinnamoylisothiocyanate examined wasbetter incomparison to other polymers for (Fe(lll), Cr(lll),Co(ll),Ni(ll)).

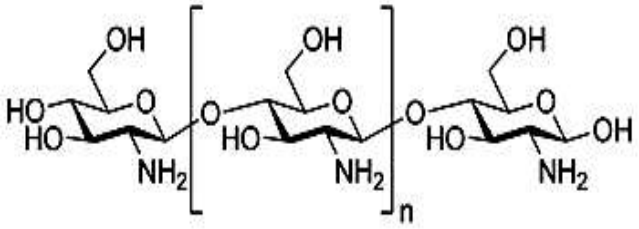

Figure:1 Chitosan-

* Assistant Professor, Chemical Engineering Department , MUET Jamshoro

** Civil Engineering Department, Universiti Teknologi PETRONAS, 31750 Tronoh, Perak, Malaysia

*** IARSCS/ HiTech RLs, University of Sindh, Jamshoro Pakistan

[1] Assistant Professor, Energy & Environment Engineering, QUEST, Nawabshah

2. PREPARATION OF CARBOXYMETHYL CHITOSAN:

Chitosan + Isopropanol (3gm/65ml) ⟹ NaOH + MCA* / Isopropanol 40% Sol (1:1m/m) ⟹ Carboxymethyl Chitosan

Chitosan−OH + **ClCH$_2$COOH** + **2NaOH** ⟶ **C**hitosan−O-**CH$_2$COONa**+ **NaCl**+ 2**H$_2$O**
(**C**hitosan) (MCA) (**SodiumHydroxide**) (**Carboxy**m**ethylC**hitosan)

*MCA = Monochloro acetic acid

3. RESULTS & DISCUSSION:

Organic modified material carboxymethyl chitosan when subjected to characterization proved satisfactory results. The techniques used for above studies were SEM, EDX & FTIR. The SEM with courtesy of Centre of Pure and Applied Geology University of Sindh Jamshoro, carried out on electron microscope model (JEOL 6490 LV – SEM by JAPAN).The prepared carboxymethyl chitosan showed crystal consisted of less than 10µm particle size. The scan prints suggest that it possessed crystalline surface. EDX studies were obtained byJSX-3400RII Energy-Dispersive X-ray model with Fluorescence Spectrometer detection system. .According to the results; the compound possesses 55.65%carbon, 34.36%oxygen, 5.30%nitrogen, 1.63% sodium and 1.91%chlorine. The compositions were determined from K shell under the particle size of 49.1nm- 62.5nm.

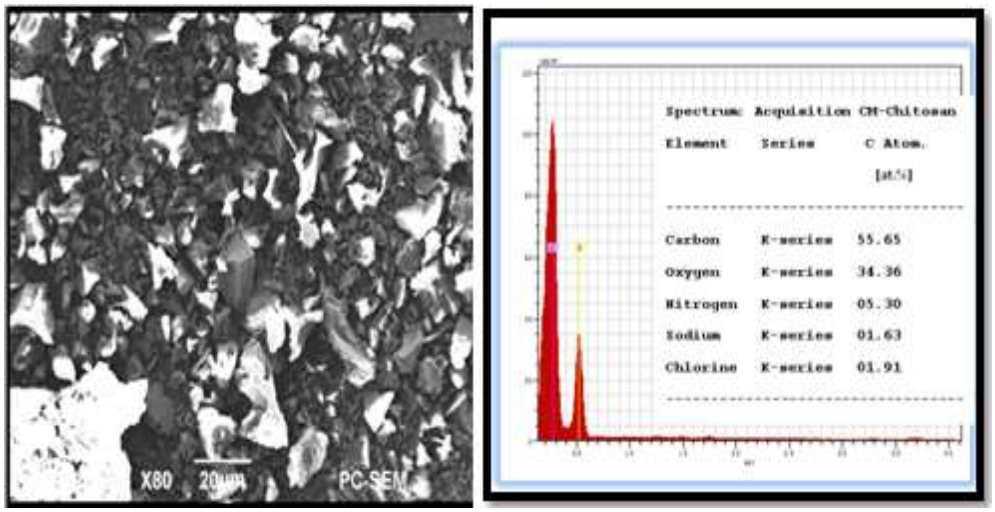

Figure.2: SEM &EDX Spectrumof Carboxymethyl Chitosan

Fourier transformation spectroscopy of carboxymethyl chitosan (fig.3), were conducted in Hitech Resources Laboratories, university of Sindh Jamshoro, Pakistan,byThermo Nicolet Avtar 330 FTIR (USA) with Zr-Se probe. Zeenat et al [7-9] reported FTIR of carboxymethyl chitosan having functional groups on skeleton. The band of spectrum at at 3436 cm^{-1}confirms stretching of O-H and N-H group. It further appears at 2900cm^{-1}due to stretching of C-H group. The band at 1634cm^{-1} appears due to asymmetrical stretching of C=O groups. Theband at 1420cm^{-1} suggests stretching of -CH_2 and -CH_3 groups.

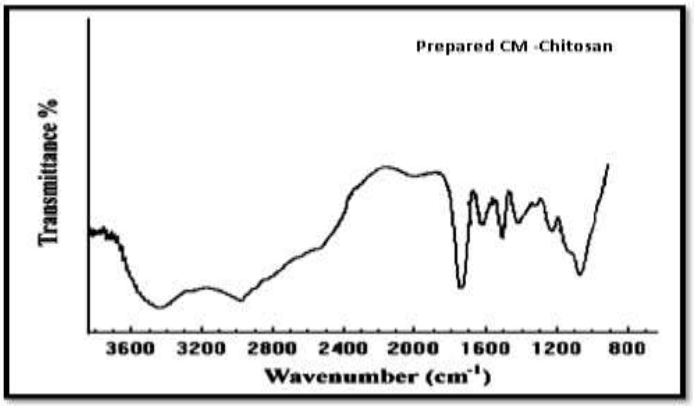

Figure 3: FTIR of Carboxymethyl Chitosan

4. METAL REMOVAL & RECOVERY BY COLUMN METHOD:

In present study five small columns were prepared each contained 2 gram carboxymethyl chitosan. The columns were eluted first with alkali solution of 10% NaOH. The columns were left for 2 hours then washed and neutralized at pH 7 with HCl diluted solution. The columns containing copper (lI), zinc (II),chromium (IIl), iron (II) and nickel (II) were examined for removal and recovery efficiencies from aqueous metal solutions with concentrations ranged from 10-100 mg/L. When compared the order of performance stood at Cu>Zn>Cr>Fe>Ni. On the contrary the ability of Cu(II) was foundbetter over other transition metals. During thiswork, the columns with 2 g carboxymethyl chitosan each for metals increased uptake capacity from 10-100 mg/L. Recovery of the metals was done with EDTA 84-100 % from industrial wastewaters (Table 2).

5. CALIBRATION CURVES OF METAL IONS BY ATOMIC ABSORPTION:

Calibration curves of metals were obtained using atomic absorption spectroscopy (AAS).The stock solution of 1000 mg/L of metals ions; iron, nickel, copper, chromium and zinc, were prepared from chloride salts of AR grade Merck (Germany). Appropriate dilutions were made for obtaining calibration curves [fig.4]. The above calibration curves of the metal ions were obtained by plotting absorbances on y-axis against concentration (µg/L) on x-axis [table.1].

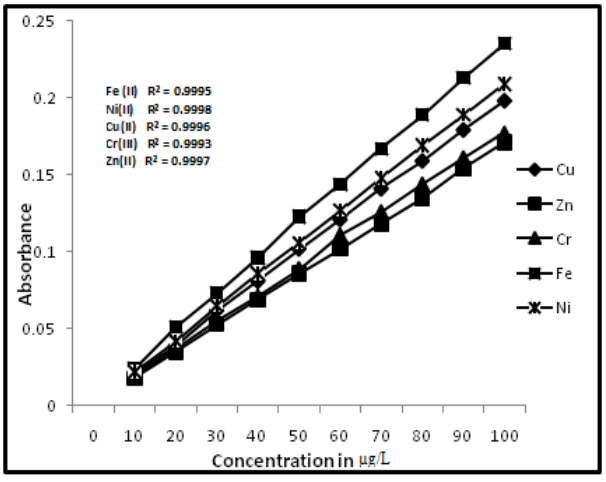

Figure 4: Calibration Curves of Metal ions by AAS

.

TABLE1: Recovery and removal efficiencies of metals against standard metal solutions (mg/l)

Metal Concentration (mg/L)	Cu(II)	Zn(II)	Cr(III)	Fe(II)	Ni(II)
20	99.8 ± 0.4	99.2 ± 2.1	98.1 ± 3.6	99.7 ± 1.1	96.2 ± 3.8
40	99.7 ± 0.3	98.9 ± 3.5	97.8 ± 3.3	99.3 ± 1.4	96.1 ± 4.7
60	99. 5± 0.7	97.3 ±2.6	96.7 ± 2.8	98.7 ± 1.9	95.4 ± 4.6
80	99.1 ± 1.1	96.9 ± 3.2	96.3 ± 3.2	98.2 ± 2.3	94.7 ± 3.9
100	99.1 ± 2.4	95.2 ± 3.4	93.1 ± 3.8	97.6 ± 2.9	94.2 ± 4.5

METAL ION REMOVAL AND RECOVERY FROM WASTE WATERS

The metal ions removal efficiency of over 86.4% - 95.1% and recovery of 100% was observed for copper (132 mg/L), zinc (171 mg/L), chromium (118 mg/L), iron (353 mg/L) and nickel (96mg/L) from waste water collected from phuleli dumping site off Mirza Mohallah Hyderabad, Pakistan. The metal intake capacity of carboxymethyl chitosan from waste water was remarkable. During present work it was found that 1.0 g carboxymethyl chitosan could adsorb from 0.5 to 1.3 mg of metal ions [table.2]. The pH was not adjusted in performing this work

Table 2 : Recovery and Removal Efficiencies of Metal Ions from Waste Waters

Metal Concentration (mg/L)	Cu(II)	Zn(II)	Cr(III)	Fe(II)	Ni(II)
	132mg/L	*171mg/L*	*118mg/L*	*353mg/L*	*96mg/L*
Metal Removal Efficiency (%)	93.1 ± 0.5	94.7 ± 1.3	95.1 ± 0.6	94.1 ± 1.0	86.4 ± 1.3

CONCLUSION

A new method based on small columns have been developed containing 2 grams of carboxymethyl chitosan and applied for removal and recovery of metal ions (mg/L); copper 132, zinc 171, chromium 118, iron 353 and nickel 96 respectively.

REFERENCES

[1] Abreu, F.; Campana-Filho, S.P. "Preparation and characterization of carboxymethylchitosan", Polímeros: Ciência e Tecnologia, volume15, number 2, pp. 79-83(2005)

[2] Wang, Shuangcheng; Xu, Xinru; Yang, Jingyi; Gao, Jinsheng 'Effect of the carboxymethyl chitosan on removal of nickel and vanadium from crude oil in the presence of microwave irradiation' Fuel Processing Technology" volume 92,number 3, pp.486-492(2011)

[3] Kannamba B, Reddy KL, Appa Rao BV "Removal of Cu(II) from aqueous solutions using chemically modified chitosan', Journal of Hazard Mater. volume175,number (1-3),pp. 939-48 (2010 Mar 15)

[4] Sepehran, M.; Nasernejad, B.; Edrissi, M "Selective Removal of Copper(II) and Nickel(II) from Aqueous Solution Using the Chemically Treated Chitosan: Factorial Design" Evaluation' Metallurgical & Materials Transactions. Part B; volume 39, number 6, pp. 905-908(Dec 2008)

[5] Rajiv Gandhi, M.; Kousalya, G.N.; Viswanathan, N.; Meenakshi, S."Sorption behaviour of copper on chemically modified chitosan beads from aqueous solution' *Carbohydrate Polymers*, volume 83, number 3,pp. 1082-1087(2011)

[6] Adel A.A. Emara, Mohamed A. Tawabb, M.A. El-ghamry ,Maher Z. Elsabee "Metal uptake by chitosan derivatives and structure studies of the polymer metal complexes"Carbohydrate Polymers, volume 83, number 1, pp. 192–202 (2011)

[7] Zeenat M. Ali, A. Jabbar Laghari, A. K. Ansari, M. Y. Khuhawar, "Extraction and Characterization of Chitosan from Indian Prawn (Fenneropenaeus Indicus) and its Applications on Waste Water Treatment of Local Ghee Industry" IOSR Journal of Engineering (IOSRJEN), Vol. 3, number 10, pp. 28-37 (October 2013)

[8] Zeenat M. Ali, A. Jabbar Laghari, A. K. Ansari M.Y.Khuhawar, "Synthesis and characterization

of Carboxymethyl Chitosan and its Effect on Turbidity Removal of River Water", IOSR Journal of Applied Chemistry (IOSR-JAC), volume 5, number 3, pp.72-79, (2013)

[9] Zeenat M. Ali, Moina Akhtar Mughal, A. Jabbar Laghari, A. K. Ansari, Hussain Saleem, "Polymeric Cellulose Derivative: Carboxymethyl-Cellulose as useful Organic Flocculant against Industrial Waste Waters", IJOART, volume 2, number 8, pp.14-20(2013)

OPTIMIZATION OF IRRIGATION FOR EFFICIENT WATER USE IN SURFACE IRRIGATED SOILS

Kanya L. Khatri[1], Sadiq A. Shah[2], Zeenat M. Ali[3], Ghulam S. Solangi[4],M.M Tunio[5]

ABSTRACT

The study was carried to simulate and optimize the furrow irrigation by using SIRMOD model for two different farm fields, one from Queensland, Australia and other Latif Farm from Tandojam, Pakistan. In this connection, the observed data for the advance times at different points along the furrow lengths for both fields has been collected. The advance trajectories were simulated using INFILT-V model, which are matching favourably with the measured curves and establish that the advance trajectories are passing through the advance point selected for the infiltration. Theirparameters were assessed and thereby cumulative infiltration was estimated using the INFILT-V model.The SIRMOD model was used to evaluate the performance of furrow irrigation for all selected fields using five different irrigation strategies. Irrigation application efficiencies under usual farm management for fields P and Q are obtained as 43.2% and 39% respectively. The simple optimization control strategy is feasible. From the computed irrigation efficiencies, it was found that this control optimised system may be used to make noteworthy improvements in irrigation performance over the actual farm management.Total volume of water used under ordinary farm management was 1595 m^3, however, under the optimized system it was computed using SIRMOD model is 963m^3, which shows a saving of about 40% that can be utilized for other crops. Hence, it is suggested that this study can be widely utilized for different soil typesand more benefits may be achieved from in the field of irrigation.

Keywords: Furrow Irrigation, Optimization, SIRMOD Model, Infiltration, Pakistan

[1] Associate Professor, Department of Civil Engineering, MUET, SZAB Campus, Khairpur Mir's
[2] Associate Professor, Department of Mechanical Engineering, MUET, SZAB Campus, Khairpur Mir's
[3]Assistant Professor, Department of Chemical Engineering MUET Jamshoro
[4] Assistant Professor, Department of Civil Engineering, MUET, SZAB Campus, Khairpur Mir's
[5]Assistant Professor, Energy and Environmental Department QUEST Nawabshah

Corresponding Author: Dr.ZeenatM.Ali **email : zeenat.ali@faculty.muet.edu.pk**

1.INTRODUCTION

Fresh water is in alimitedquantity, today the world uses 70% of all freshwater for irrigating 17% of the total cropped land resulting 40% of the overall agricultural outputs (ICID Congress, 2006). The aim is to have more crop yield using less water, we mean optimized irrigation with improved efficiencies which is only possible with the use of advanced technology.In Pakistan, Australia and other countries of the world, surface irrigation methods are commonly used for cultivating crops. In Australia, more than 70% of the irrigated area and in other countries like Pakistan, India and many other developing countries, over 90% of their cultivated lands are irrigated through these methods (Philip *et al* 2008, Khatri and Smith 2007).

Surface irrigation, an inexpensive and inefficient method of irrigating crops, wasting much of the water applied which needs to be optimized through advance techniques (Strelkoff and Clemens, 2003). In surface irrigation events, there are four phases i.e. advance, wetting or ponding, depletion and recession phases.The performance of furrow irrigation depends upon various parameters such as field design, soil infiltration characteristics, irrigation water management practices, etc. According to Anthony (1995), application efficiencies can be increased up to 90% in properly managed systems. The optimised irrigation system may surmount these spatial and temporal variations (Raine*et al.*, 1997, Smith *et al.*, 2005). In irrigation system, significant improvement can be made with optimised irrigation and optimisation of irrigation events individually. Total volume of water applied per irrigation can be saved substantially by implementation of a simple optimised irrigation system.Furrow irrigation method is considered to be a low efficient method having poorer irrigation efficiency usually around 70%. Actually it is not the method defect but it is because of poor management. In order to optimize the irrigation events of this system and achieving optimized and efficient irrigation; following research objectives are set forth:

(1) To calculate, infiltration rate on the basis of irrigation advance data for various furrow characteristics, advance and inflow rates; and

(2) To simulate the performance gains through various optimization strategies, using infiltrationcharacteristicsof soil and the above data.

2. MATERIALS AND METHODS

2.1. THE STUDY AREA

This study was carried out on two different farms, having cotton crops on both fields (see plate 1).

Plate 1: Cotton fields at both Tandojam Pakistan and Queensland Australia

For easiness above fields were designated as field P for Latif Farm, Tandojam, Pakistan and field Q for field of Queensland, Australia and their salient features are summarised in Table 1.

Table 1: Salient features of the fields P and Q

S. No.	Description	Field	
		P	Q
1	Irrigated Area in m^2	1000	**8160**
2	No. of furrows	10	**17**
3	Length of furrows in m	100	**240**
4	**Furrow spacing in m**	**1**	**2**

2.2 ADVANCE TRAJECTORIES

Data regarding inflow rate, cross sectional area and advance time measurement at various distances (m) and time (min) was collected/observed from the farms P and Q is shown in Table 2 and their

measured advance curves are shown in Figures 2 and 3 respectively.

Table 2: Advance Data for Field P and Q

Data Set Number	Field P		Field Q	
	Observation Points (Nos.)	Inflow rates (m^3/min)	Observation Points (Nos.)	Inflow rates (m^3/min)
1	4	0.41	4	0.0498
2	4	0.4	3	0.0498
3	4	0.4	4	0.0498
4	4	0.52	3	0.2244
5	4	0.37	4	0.0498
6	4	0.39	3	0.3126
7	4	0.50	4	0.3126
8	4	0.42	3	0.1566
9	4	0.42	3	0.4752
10	4	0.38	4	0.2700
11	4	0.50	4	0.1566
12	4	0.50	4	0.1566
13	4	0.48	4	0.2700
14	4	0.51	4	0.1134
15	4	0.51	3	0.2700

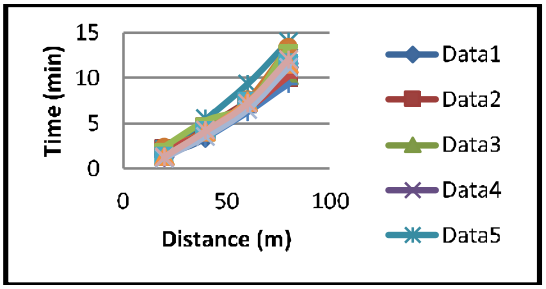

Fig. 2: Measured advance curves for field P

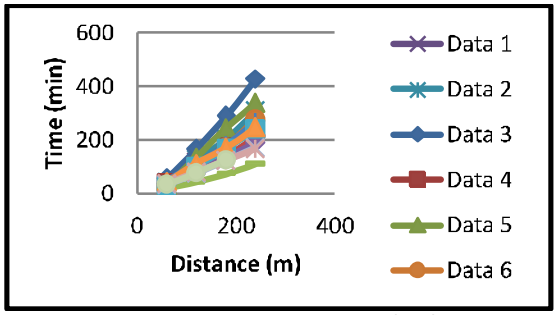

Fig. 3: Measured advance curves for field Q

From Table 2, three irrigation events such as advanced time and flow depth for both fields P and Q have been taken for simulation advance trajectories which have been described and analyzed in section 4.1.

2.3 PERFORMANCE MEASURES OF SURFACE IRRIGATION

The purpose of irrigation application is to apply the requisite amount of water efficiently and uniformly. However, various growers may furnish more or less importance on three relevant performance measures i.e. application and storage efficiencies as well as distribution uniformity, which are summarised in Table 3.

Table 3: Description of Efficiencies (%) and their Dependant Variables

Sr No	Efficiency Type	Equation	Depends upon variables	Expressed in %
1.	Application Efficiency (E_a)	$Ea = \frac{100\,W_s}{W_f}$ Michael (1999)	Volume of water stored in root zone (W_s) = W_f - (R_f + D_f) during irrigation to volume of water delivered in the field (W_f)	%age
2.	Storage Efficiency (E_s)	$Es = \frac{100\,W_r}{W_d}$ Michael (1999)	Water stored in root zone (W_r) during irrigation to water required in root zone (W_d)	%age
3.	Distribution Efficiency (E_d)	$Ed = \frac{100\,W_i}{W_a}$ Merriam and Killer (1999)	Average infiltration depth of water in lower quarter of field (W_i) to average infiltrated depth of water over the field (W_a)	%age

2.4 SIMULATION METHODOLOGY OF THE SIRMOD MODEL

In order to analyse the optimized control system, simulation trials were made for both fields by using the actual INFILT and the scaled infiltration parameters in the SIRMOD model. The simulated values were utilized to check the irrigation efficiencies in order to compute the performance of the farm irrigations through various strategies.

This model requires input data such aslength of field, slope, infiltration properties, target application depth, discharge, Manning's co-efficient of roughness*n* and geometrical parameters of furrowfor

simulation component (see Figure 4). After simulation process advance-recession trajectory, infiltrated water distribution, volume balance, run-off hydrograph, water distribution uniformity, water application efficiency and other efficiencies have been computed and their results are shown in Figure 5.

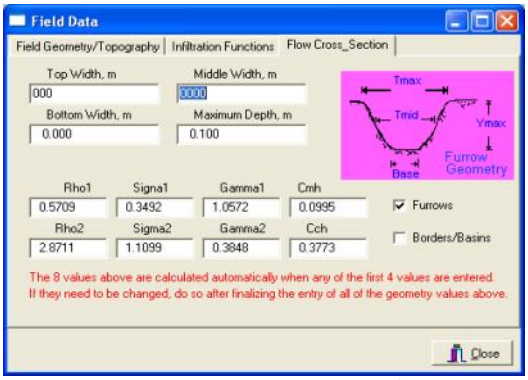

Fig. 4: SIRMOD screen showing the field geometry, infiltration functions and flow cross section

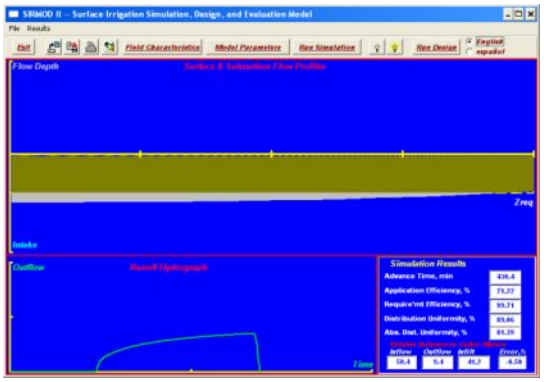

Fig. 5: Computed results shown on SIRMOD screen

3. SIMULATION MODEL STRATEGIES

For simulation purpose (05) strategies were developed to test irrigation system, which are explained as under:

Strategy 1: In thisstrategy, actual irrigation is simulated by taking the infiltration parameters (INFILT a, k, f_o),actual inflow rate (Q_o) and actual cut off time (t_{co}) under common practices.

Strategy 2: Under this strategy, each irrigation event was optimized by using INFILT parameters after changing the inflow rate and cut off time for maximum value of application efficiency.

Strategy 3: In this strategy, the cut off time is taken by90% of advance time and simulation is performed utilizing the INFILT parameters and actual flow rate.

Strategy 4: For this strategy, the cut off time is taken as 90% of advance time and inflow rate is taken same as that of strategy 3 and for simulation INFILT parameters are used.

Strategy 5: Under this strategy, INFILT infiltration parameters are utilizes by a fixed inflow rate while optimising only the cut-off time in order to attain the best irrigation.

4. RESULTS AND DISCUSSIONS

4.1 ADVANCE TRAJECTORIES AND COMMUTATIVE INFILTRATION

For both observed fields P and Q, INFILT-V model was used to simulate the advanced trajectories of both the selected fields P and Q. And data of simulated trajectories curves were compared with measured readings, some of them are represented graphically in Figures 6 and 7.

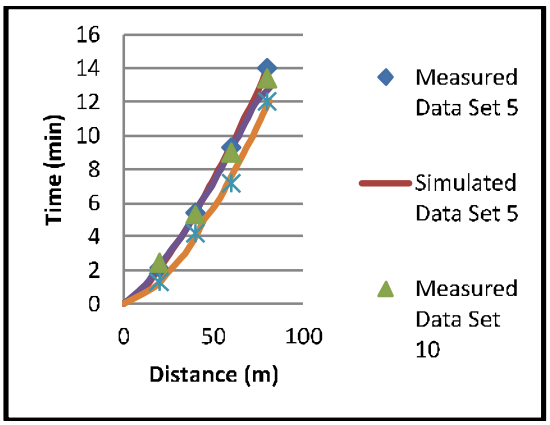

Fig. 6: Graphical representation of some measured and simulated advance trajectories for field P

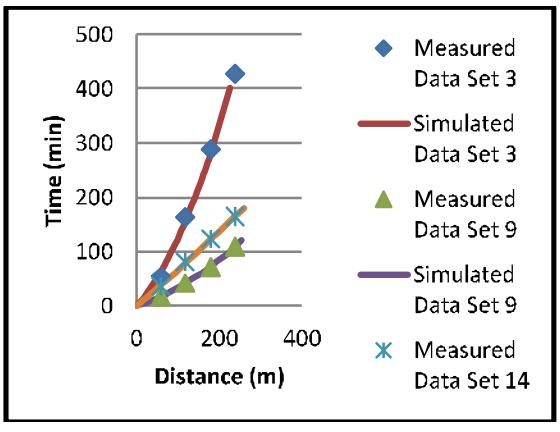

Fig. 7: Graphical representation of some measured and simulated advance trajectories for field Q

From above graphs, it is clear that there is similarity in between simulated advance trajectories and measured trajectories. But there is a small divergence between the advance trajectories and advance point selected for the infiltration in the end of the field for data set 10 of the selected field P.

4.2 IRRIGATION PERFORMANCE

The SIRMOD model was used to compute the application efficiency, storage efficiency as well as uniformity distribution for all strategies of fields P and Q. The average simulated irrigation performance for both fields is described in Table 4.

Table 4: Summary of irrigation performance under different modelling strategies

Management/ Model strategies	Field P (Average of 21 events)			Field Q (Average of 17 events)		
	E_a (%)	E_r (%)	DU (%)	E_a (%)	E_r (%)	DU (%)
Strategy 1 Actual irrigation	**43.2**	**93.6**	**82.6**	**39.1**	**97.9**	**80.2**
Strategy 2 Perfect management	**76.4**	**91.3**	**93.7**	**72.1**	**95.1**	**92.5**
Strategy 3 Simple recipe management (actual inflow)	**71.4**	**82.1**	**75.3**	**68.5**	**79.5**	**72.2**
Strategy 4 Simple recipe management (fixed inflow 6.5 lps)	**43.3**	**88.1**	**85.7**	**34.4**	**88.6**	**86.6**
Strategy 5 Real-time control (INFILT infiltration)	**73.4**	**84.3**	**89.3**	**70.2**	**81.3**	**88.5**

Strategy 1 (Actual irrigation - usual farm management)

From abovedescribed simulation results for fields P and Q, overall average (E_a) is 43.2% and 39.1%, (E_r) is 93.6% and 97.9% and DU is 82.6% and 80.2% respectively.

Strategy2 (Perfect Control and Management)

In this strategy irrigation events were optimized on the basis of INFILT parameters with varying inflow and cut off time to fit soil conditions and excellent performance was obtained for most of the events. The average overall performance (i.eE_a and E_r) for the fields P and Q are 76.4%, 91.3%, 72.1% and 95.1% respectively. In this strategy application of more advanced irrigation management practices is involved which is impracticable for the field. For this strategy, 6.5 lps as over all suitable dischargewas optimized that was considered in strategies 4 and 5 for further optimization in a simple way.not touch end of the furrow.

Strategy 3 and 4 (Simple Recipe Management actual and fixed)

For this, performance was improved by taking cut off time as 90% of the advance time but in most of the events the advance did not touch end of the furrowovercomethis difficulty, strategy 4 was applied by takingsame parameters as described in strategy 3 but rate of flowwas increased upto 6.5 lps. The simple recipe management indicated poorer results for both of fields P and Q, in both strategies 3 and 4. The advance was unable to reach the end of the field for many of the furrows and yet the fields were indicated to have low application efficiencies.

Strategy 5 (Optimized control)

From Table 4 it is clear that this strategy simulates an improved performance and clearedthat strategy 5 based on INFILT infiltration is closest to the observed results. Hence, this strategy is feasible having significant improvement which is also practicable for this strategy.

4.3WATER SAVING DUE TO OPTIMIZED CONTROL

Total volume of water applied to 27 furrows for both of fields P and Q under ordinary farm management has been observed. These 27 furrows cover an area of 0.916 hectares, which is comprised of 10 furrows having 100m length with spacing of 1m in case of field P and 17 furrows having 240 m length and spacing of 2 m for Q field. Under optimized control system, by using SIRMOD model, the quantity of water was computed which isdescribed in Table 5.

Table 5: Volume of water applied for the required time for various fields Q_0 = 6.5 lps

S.No.	Field P		Field Q	
	t_{co} (min)	Water diverted (m^3)	t_{co} (min)	Water diverted (m^3)
1	10	3.90	150	58.50
2	8	3.12	150	58.50
3	7	2.73	130	50.70
4	10	3.90	125	48.75
5	9	3.51	140	54.60
6	10	3.90	140	54.60
7	12	4.68	130	50.70
8	7	2.73	155	60.45
9	7	2.73	155	60.45
10	9	3.51	135	52.65
11	9	3.51	145	56.55
12	13	5.07	130	50.70
13	13	5.07	110	42.90
14	8	3.12	100	39.00
15	8	3.12	120	46.80
16	7	2.73	140	54.60
17	7	2.73	130	50.70
18	8	3.12	--	--
19	8	3.12	--	--
20	7	2.73	--	--
21	8	3.12	--	--
Total		72.15	--	--

However, by utilizing optimized control system, the summary of above values along with water saving is described in Table 6.

Table 6: Volume of water applied to both fields before and after optimization

Field	Actual Farm Management (AFM)(m^3)	Optimized Control(OC) (m^3)	Water savings due to OC (m^3)	%
Field P	104	72	32	30.77
Field Q	1491	891	600	40.24
Total	1595	963	632	39.6

However, by utilizing optimized control system, the summary of above values along with water saving is described in Table 6.

From Table 6, it can be seen that volume of water applied to various furrows of fields P and Q before optimization was 1595m^3; however, under optimized control system, it can be reduced to up to 963m^3, which prevails the potential savings of 632m^3 (0.632 million litres) of water during each irrigation over an area of 0.916 hectares.

Farmers while growing cotton crop, generally apply 10 to 11 irrigations which represents annual water saving of 1.73 to 1.90 ML/ha that may be constructively utilized to grow more crops and significant profits may be achieved in the field of irrigation

.

5. CONCLUSIONS

From this study, following conclusions are made:

- The data regarding different parameters for different points was observed and compared with the simulated advance trajectories and found that the advance trajectories were passing through the advance point selected for the infiltration
- By using the INFILT V model, the cumulative infiltration was also computed successfully.
- The simple optimized control strategy has the potential to bring significant improvements to enhance the irrigation performance, and
- By using the simple optimized control system, volume of water applied during irrigation may be significantly reduced which can be utilized to cultivate more farm lands.

6. RECOMMENDATIONS

From this study, it is clear that the irrigation performance may be significantly improved by adopting simple optimized control system. That optimized system was evaluated for two farm fields of different characteristics.

In continuation of this study, prototyping of the system may be considered as next step and research may be extended largely to achieve significant benefits in the field of irrigation.

ACKNOWLEDGEMENT

The authors are grateful to Institute of Water Resources Engineering and Management, MUET, Jamshoro for providing facilities regarding this study.

References

1. Anthony, D., "On-farm water productivity, current and potential: options, outcomes, costs", Irrigation Australia, Vol. 10, 1995
2. ICID, C., "Use of water and land for food security and environmental sustainability", Irrigation and Drainage, Vol. 55, 2006
3. Khatri, K.L., Smith, R.J., and S.R. Raine, "Toward a simple real-time control system for efficient management of furrow irrigation. Irrigation and Drainage", Vol. 58, 2007
4. Merriam, J. L., and Keller, J., "Farm irrigation system evaluation: A guide for management", Agricultural and Irrigation Engineering Department, Utah State University, Logan, Utah. 1978
5. Michael, A. M., "Irrigation: Theory and Practice", Vikas publishing house Pvt. Ltd Masjid road, Jangapura, New Delhi, India 1999
6. Philip K Langat, Steven R. Raine and KhatriKanya L, "Errors in predicting furrow irrigation performance using single
7. measures of infiltration", Journal of Irrigation Science, Vol. 26, 2008
8. Raine, S. R., McClymont, D. J., and Smith, R. J., "The development of guidelines for surface irrigation in areas with variable infiltration", Proceedings of Australian Society of Sugercane Technologists. Vol. 1, No. 4,1997
9. Smith, R. J., Raine, S. R., and Minkovich, J., "Irrigation application efficiency and deep drainage potential under surface irrigated cotton", Agricultural Water Management, Vol. 71, No. 2, 2005
10. Strelkoff, T. S., and Clemens, A. J., (2003), "Software for the design and management of surface irrigation systems" Retrieved 15 June, 2004, from http://www.uswcl.ars.ag.gov/publicat/index/ifm8.htm

A PROBLEM ANALYSIS METHOD BASED ON SOFT SYSTEM METHODOLOGY IN REQUIREMENTS ENGINEERING PROCESS

Rafia Naz Memon[1,*], Shah Zaman Nizamani[2], Farida Memon[3], Irfana Memon[4], Pardeep Kumar[5]

ABSTRACT

In order to perform Requirements Engineering (RE) process effectively and to extract the correct requirements, it is important to call the requirements engineers' attention to the benefits of focusing on the problem to be solved instead of directly moving to writing requirements from problem definition. However despite of the importance of problem analysis phase, it is difficult to find an appropriate method for performing problem analysis; hence novice requirements engineers find it difficult to perform problem analysis phase. This paper therefore focuses on the proposal of a method for performing problem analysis in RE based on the idea of Soft System Methodology (SSM). The proposed method used different RE techniques such as goals, scenarios, viewpoints etc along with SSM to make the process effective and easier to be used by novice requirements engineers. A prototype tool was also developed to automate the steps of the method. The application of method was shown by applying it on a case study. Finally the method was evaluated by the lecturers having experience of teaching RE course and researchers doing RE research through expert review method and evaluation results showed the positive acceptance of method by experts.

Keywords: *Requirements Engineering, Problem analysis, Soft system methodology.*

1 INTRODUCTION

Software requirements define the services that intended system should deliver and set out limitations on the intended system's operation [1]. A requirement is a statement of some class of user's or other stakeholder's need [2]. Many problems arise with these requirements such as the real needs of customers are not depicted by requirements, incomplete and/or inconsistent presentation of requirements, it is expensive to make changes to agreed requirements, there are misunderstandings between customers, requirements engineers and software engineers who have responsibility of developing and maintaining the system. The best way to reduce these problems is to improve the processes of eliciting, understanding, structuring, validating and managing system requirements [1]. Doing requirements well takes time, effort, and skills at the start of a project, but saves much more time later [2]. Very few organizations have an explicitly defined and standardized Requirements Engineering (RE) process. They simply define the result of process, namely requirements document. The people involved in the process are responsible for deciding what to do and when to do it, what information they need, what tools they should use, etc. [1]

In order to perform RE process effectively and to extract the correct requirements, it is important to call the requirements engineers' focus to the advantages of considering the problem to be solved instead of directly moving to writing requirements from problem definition. Yet without a means to discuss and inquire about problems in a precise, structured way, one can hardly be faulted for skipping problem analysis and leaping straight to the comforting rigor of design. Problem analysis is reported as an important aspect of RE by many researchers such as [3-7]. Methods and approaches that claim the title of 'problem analysis' usually prove, on closer inspection, to deal entirely with putative or outline solutions. The problem to be solved is neither stated in full detail nor explicitly analyzed; the reader must infer the problem from its solution [8]. User may not be able to imagine a new system or how they would use it, but they know what their problem is, and why they would like it fixed. They are expert in their own problem. [2] Experienced requirements engineers can perform the problem analysis using traditional RE methods with the help of their experience and observation. However the problems arise for beginners who have no experience of working on RE projects. It is very difficult for them to perform the activity without an appropriate method. A problem analysis method was therefore needed to be made

available to help novice requirements engineers in performing the process. This paper therefore focuses on the proposal of a method for performing problem analysis in RE based on the idea of soft system methodology (SSM) to be used by the novice requirements engineers. The application of method was presented through a case study. A prototype tool was developed to automate the steps of the method. Finally the method was evaluated through expert review method. It is expected that the proposed method will provide the explicitly defined RE process to perform the problem analysis process to novice requirements engineer.

In section 2 of the paper, background of the study is presented. In section 3 techniques used in the method are presented. Section 4 presents the proposed method. Section 5 presents the screen shots of prototype, section 6 presents the case study on which method was applied, Section 7 presents the evaluation of the method, and section 8 concludes the paper.

2 BACKGROUND

Problem is a situation where someone wanted something to be different from how it is and is not quite sure how to go about in making it so [9]. In RE, we are interested only in finding out the shape of the problem, not in how that problem will one day be solved [2]. The solution for the problem must come after the problem has been identified, documented, understood, and agreed on [10]. Problem reported by users can often be turned around into requirements. [2]

In RE, problem analysis is not explicitly performed but thought to be covered during requirements analysis phase using requirements analysis techniques such as goal-based requirements analysis methods, scenario-driven requirements analysis methods, structured Analysis and design methods, viewpoint analysis methods, object-oriented analysis methods etc. However requirements analysis methods should be used after some initial elicitation has been carried out. Problem analysis in RE covers initial understanding of the problem as well as analyzing and structuring the requirements. The two phases covered by problem analysis in RE are:

- Identifying what the problem really is or what the customer requires, and
- Refining and specifying the requirements on a desired system.

The structured methods of requirements analysis through which these two phases of problem analysis are normally thought to be performed, are not particularly useful for early stages of analysis where application domain, the problem and the organizational requirements must be understood. They are based on hard models of system, such as entity relationship models, data flow models etc. These models are inflexible and focus on automated systems. [11]

By contrast, soft systems methods can help in initial phases of software development as they rely on producing less formal models of the whole socio-technical systems. Soft System Methodology (SSM) is the best known of these approaches. SSM was not specifically designed as a technique of eliciting requirements for computer-based systems. Rather, it was developed to help apply 'system thinking' to problems within organizations. This perspective makes the approach usable in requirements elicitation. [11] Therefore it is proposed to use the concept of SSM for performing problem analysis in RE. SSM is briefly described in the following subsection.

2.1 SOFT SYSTEM METHODOLOGY (SSM)

SSM provides a means to understand abstract system requirements by analyzing organizational context, the problem to be solved and existing systems which are in place. SSM is more effective for helping to understand a problem, the organizational situation in which the problem exists and the constraints on the problem solution. [11]

SSM emphasizes on problem identification, problem structuring, and problem resolution, rather than on problem solution. SSM acts well when solving problems concerning complicated, interacting and dynamic group of processes in a situation, where a change is wanted to carry out somewhere in this continuum of processes. This is made by comparing the present real world situation of the system with those models of the system that are thought to make the system work in a more practical way. The seven stages of SSM are presented in Fig. 1.

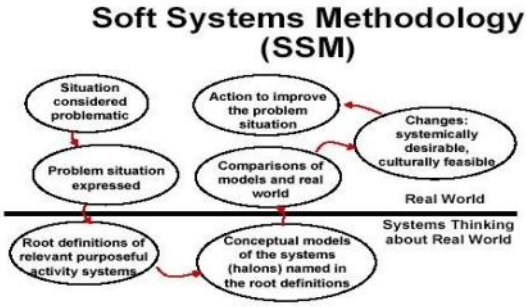

Fig. 1 The stages of SSM [12]

In SSM, systems thinker can look at an aspect of the world from a number of different viewpoints. The use of viewpoints can provide a better chance of discovering the

requirements. Some viewpoints that are particularly useful are listed here:

- How it is: the view of the world you are trying to understand
- What it is: the view of the meaning or the essence behind how things are done
- What it will be: the view of how things will work in the future, or the product you plan to build. [13]

3 TECHNIQUES USED IN THE METHOD

The proposed method used different RE techniques along with SSM to make the process effective and easier for novice requirements engineers. The selected techniques are presented below:

- SSM is selected as a front-end method because:
  - It is useful for the early stages of analysis. It is more effective for helping to understand a problem, the organizational situation in which the problem exists and the constraints on the problem solution. They produce abstract requirements for a system which need to be flashed out using other techniques [11].
  - The systems thinking approach that is, SSM, can be effectively used in requirements analysis. It provides techniques for observing and modeling the world for the purpose of understanding and tackling real-world problems. [13]
- The use of goals and scenarios in problem analysis. The goal-scenario combination is proved to be very effective for addressing different problems. Many researchers proposed to merge goals and scenarios together in order to overcome deficiencies of goal-driven and scenario-based approaches when used in isolation [14-18].
- The use of viewpoints for requirements analysis. Viewpoints are considered an efficient way to discover requirements from different perspectives, and can be proved more useful if combined with goals and scenarios.

4 TOWARDS A PROBLEM ANALYSIS METHOD

The proposed method consists of following elements:

- One should at least have general understanding of the application domain and the problem to be solved [11]. Therefore it is suggested that the user should have two inputs prior using our method that are: Customers' needs (initial informal problem statement of the customer) and Application domain knowledge (background knowledge of the area under study).
- In requirements analysis it will be easier for analyst to look at an aspect of world from a number of different viewpoints [13]. Therefore, concept of SSM is transformed into two main viewpoints:
  1. **What it is:** the view of the world you are trying to understand (real world thinking)
  2. **What it will be**: the view of how things will look in future, or the product you plan to build (System thinking)
- While the CATWOE (Customers, Actors, Transformation process, world-view, Owner (s) and Environmental factors) transformation (from SSM) will show that what needs to be changed (from first perspective) into what (from second perspective).

These ideas are depicted in Fig. 2.

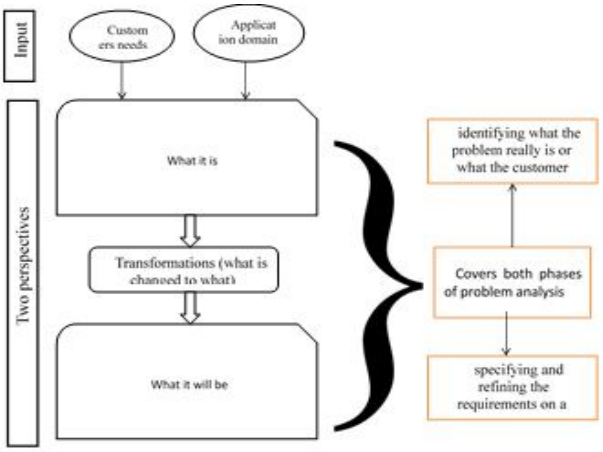

Fig. 2 Main elements of the proposed method

These three elements are presented in detail in the following subsections.

4.1 THE FIRST PERSPECTIVE: WHAT IT IS?

This is about understanding what the customer's problem really is. The activities performed in this perspective are presented at the left side of Fig. 3, while explanation and technique used to perform each activity are described at the right side of Fig. 3.

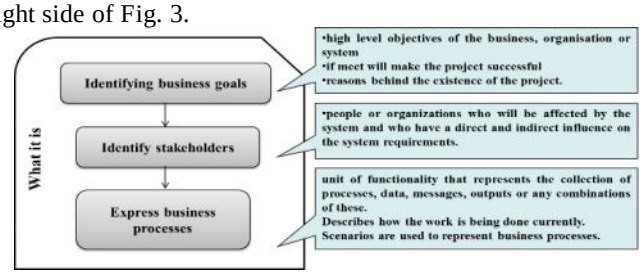

Fig. 3 The first perspective

From customer needs and application domain knowledge (inputs), the business goals and stakeholders are identified. The main step of this stage is identifying and expressing the business processes. These processes depict the way the work is done in the organizations and it is assumed that the problem occurs due the way these processes are currently performed; therefore steps in each business process are described in detail so that the problems can be identified.

4.2 TRANSFORMATIONS (WHAT IS CHANGED TO WHAT)

In this stage, each business process is analyzed in detail to identify the problem or the feature that needs to be changed to address the problem. This detailed analysis is performed through CATWOE analysis. CATWOE describes how the business processes are transformed into system processes and why.

CATWOE is a mnemonic for:

- Customers (and other stakeholders), i.e. people who are affected by transformation.
- Actors, i.e. the people who perform the activities in the transformation.
- Transformation process, stating what is changed and to what.
- World-view or perspective from which the transformation is meaningful.
- Owner(s), i.e. the person or people who control the transformation.
- Environmental / external factors, i.e. anything that constrains the transformation.

4.3 THE SECOND PERSPECTIVE: WHAT IT WILL BE?

It includes identifying the real requirements of the customer and refining those requirements. The activities performed in this perspective are presented at the left side of Fig. 4. While the explanation and technique used to perform each activity are described at the right side of Fig. 4.

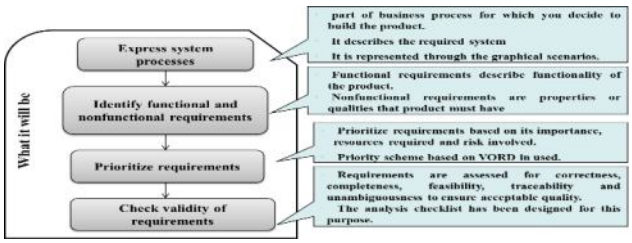

Fig. 4 The second perspective

In the first step of this stage, the system processes are described in detail. The transformation from business to system process is the key of the proposed method and the changes required to transform the business into system process are the requirements of the software. Therefore from system process the functional as well as non-functional requirements are identified. Functional requirements are what the user need for the system to work. Nonfunctional requirements are global, fuzzy factors or principles that relate to the system's overall success. [10]

The next two steps of the stage that is, prioritize requirements and check validity of requirements, are performed to refine the identified requirements. The priority scheme for calculating the priority of each requirement (based on [19]) is presented in table 1.

Table 1. The priority scheme

Weighing Factor	High (H)	Medium (M)	Low (L)
Importance	3	2	1
Resources required	1	2	3
Risk involved	1	2	3

The validity of requirements is checked using analysis checklists. The analysis checklist to validate each requirement is presented in table 2.

Table 2. Analysis checklist for individual requirement

1.	Is the requirement uniquely and correctly identified?
2.	Is the requirement in scope for the project?
3.	Is any necessary information missing from a requirement?
4.	Is the requirement as modifiable as possible?
5.	Is the requirement written in clear, concise, unambiguous language?
6.	Is the requirement free from content and grammatical errors?
7.	Is the requirement written in the customer's language, using the customer's terminology?
8.	Is the requirement acceptable to all stakeholders?
9.	Is the requirement a statement of stakeholder need, not a solution?
10.	If appropriate, is the requirement traceable?

4.4 THE PROPOSED METHOD

All elements presented from section 4.1 – 4.3 are combined to present the complete method (Fig. 5). Techniques used to perform each activity of the method are presented through cloud symbol.

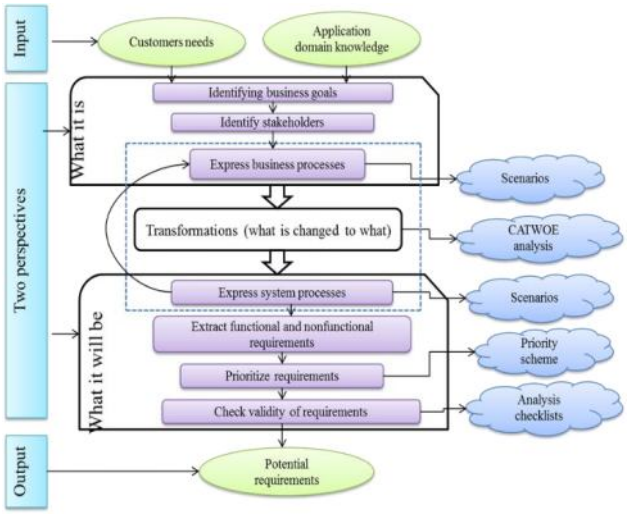

Fig. 5 The proposed method

The output of the method are potential requirements that are presented using requirements name, description, type and priority.

The proposed method is applied to a case study "Hospital management System" to show its application. A few steps of method application (until requirements extraction) of a few business processes are presented in section 6. In order to automate the process of the method, a prototype is developed using dot net framework. SQL server is used to design the back-end database.

5 A PROTOTYPE TOOL BASED ON PROPOSED METHOD

A prototype tool was developed based on the method in order to automate the steps of method. A few screen shots of the tool are presented in the section.

Fig. 6 presents the main screen of the tool. The steps of the method are shown at the left side of the screen.

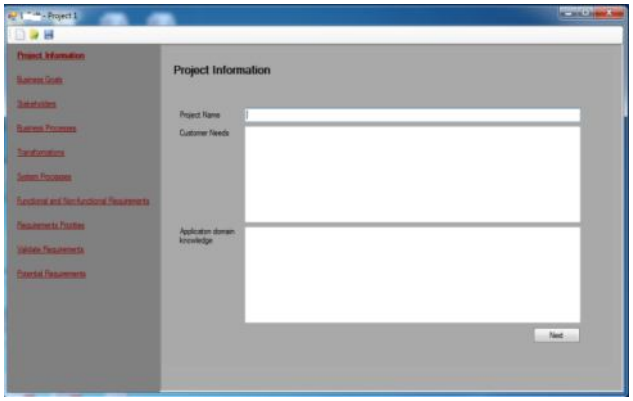

Fig. 6 Screen shot of main screen

Fig. 7 shows the screen shot of the page that ask the user to enter the stakeholders' information.

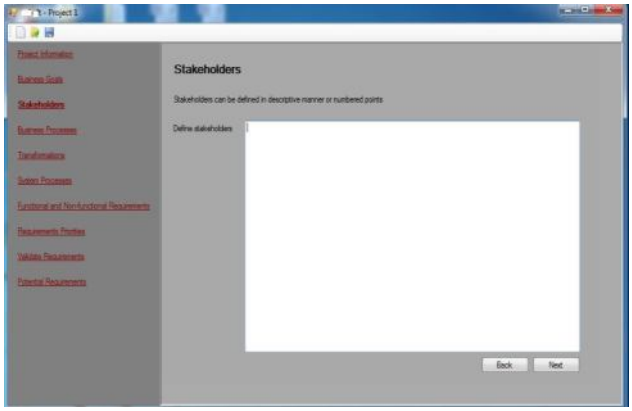

Fig. 7 Screen shot of stakeholders screen

Fig. 8 shows the screen shot of the page that allows the user to enter the functional/nonfunctional information.

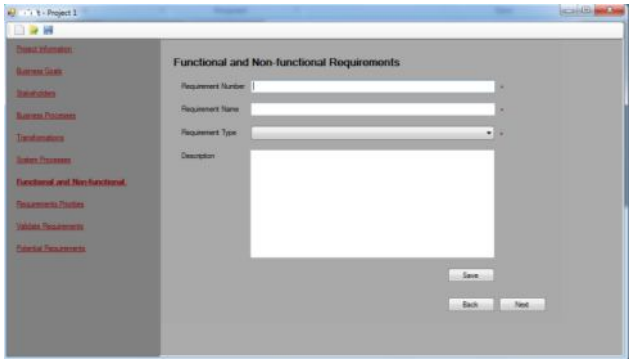

Fig. 8 Screen shot of requirements screen

Fig. 9 shows the screen shot of page that guide user in assigning priorities to the requirements.

Fig. 9 Screen shot of requirements priorities screen

Fig. 10 shows the screen shot of the page that allow the user to validate the requirements using analysis checklists.

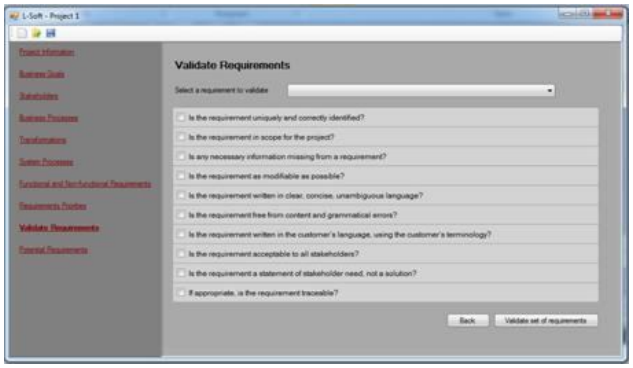

Fig. 10 Screen shot of validation screen

In the last page i.e., 'potential requirements', the set of requirements will be shown along with their associated information.

6 APPLICATION OF METHOD ON A CASE STUDY

The proposed method was applied on a case study to show its application on real world problems. The case study named Hospital Management System (HMS) is presented in the following sections.

6.1 CASE STUDY: HOSPITAL MANAGEMENT SYSTEM (HMS)

Customer needs:
The desired software product is the Hospital Management System (HMS). Currently most of the management operations are performed manually. The customer wants centralized hospital management system software that should be able to perform all the operations, such as system will be used to allocate beds to patients on a priority basis, and to assign doctors to patients in designated wards as need arises. Doctors will also use the system to keep track of the patients assigned to them. Nurses who are in direct contact with the patients will use the system to keep track of available beds, the patients in the different wards, and the types of medication required for each patient. The current system in use is a paper-based system. It is too slow and cannot provide updated lists of patients within a reasonable timeframe. Doctors must make rounds to pick up patients' treatment cards in order to know whether they have cases to treat or not. The intentions of the system are to reduce over-time pay and increase the number of patients that can be treated accurately.

Business goals:
Work Scheduling
Automation of patient's admissions and discharge operations
Automation of management services

Stakeholders:
Administrators: They all have post-secondary education relating to general business administration practices. They are responsible for all of the scheduling and updating day/night employee shifts. Administrators in the wards are responsible for assigning doctors and nurses to patients.
Doctors: All doctors have a medical degree. Some have further specialized training. Doctors will use the HMS to check their patient's list and duties schedule.
Nurses: All nurses have post-secondary education in nursing. Consulting nurses to whom patients give short descriptions of their conditions are also responsible for assigning patients to appropriate wards if the beds are available, otherwise putting patients on the waiting list. Nurses in wards will use the HMS to check their patient list and duties schedule.
Reception staff: They all have general reception and secretarial duties. Every staff has some basic computer training. They are responsible for patient's check-in or notification of appropriate people (e.g. notify administrator or nurse when an event occurs).

Processes:

- Patient registration
- Consultation
- Work scheduling
- Inpatient checkout
- Storing and retrieving information.

The application of first three processes have been provided in sections below.

6.2 PATIENT REGISTRATION PROCESS

Business process
Business process name: Patient registration
Stakeholders: Patient, reception staff

- Patient comes at reception desk and ask for medication
- Reception staff ask patient to fill in the form.
- Patient fills the form.
- Reception staff checks the form.
- Assign patient an identification number (ID) and make ID slip
- Patient receives ID slip.

Transformations:

- Customers: Reception staff, patient
- Actors: Developers, reception staff
- Transformation: From manual patient registration process to computerized registration process

- World-view: Every patient who visits the hospital has to get registered in order to get any consultation, treatment or investigations done.
- Owner: Owner of hospital.
- Environment: Every reception staff should have some basic computer training and should be provided training to operate the software.

System process

The graphical scenario of the required system process is shown in fig. 11.

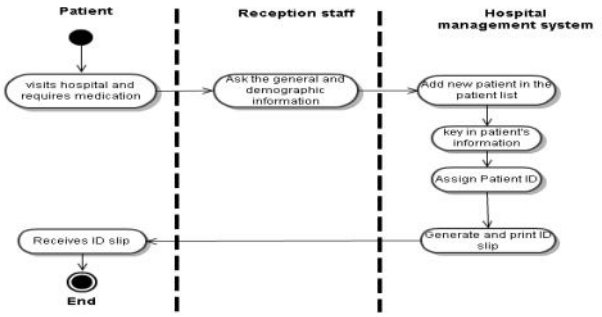

Fig. 11 Graphical scenario of system process of patient registration

Functional Requirements

- **R001 Add patients**

The HMS shall allow reception staff to add new patients to the system.

- **R002 Assign ID**

The HMS shall allow reception staff to give each patient an ID and add it to the patient's record. This ID shall be used by the patient throughout his/her stay in hospital.

- **R003 Assign ID**

The HMS shall allow reception staff to generate and print the registration slip with ID on it.

6.3 CONSULTATION

Business process

Business process name: Consultation
Precondition: Patient must have valid ID
Stakeholders: Patient, consulting nurse

- Patient explain the symptoms
- Consulting nurse checks the patient.
- Based on symptoms, the consulting nurse either refer patient to OPD (Outpatient Department) doctor or admit in the hospital (In Patient).
  - If Outpatient, the appointment is given based on availability of doctor and patient is asked to wait.
  - If Inpatient, nurse checks availability of bed in the specific ward
- If available , patient is admitted immediately
- If not available, the patient is put in the waiting list and admitted once bed is available

Transformation:

- Customers: Patient, consulting nurse
- Actors: Developers. Consulting nurse
- Transformation: From manual to computerized consultation service
- World-view: Consulting nurse do not have to go to the specific ward to check availability of bed, computerized records will help her to perform the process efficiently.
- Owner: Owner of Hospital.
- Environment: All nurses have post-secondary education in nursing; some nurses are computer literate while others should provide some training. Patient must have ID to enable him for consultation.

System process:

The graphical scenario of the required system process is shown in fig. 12.

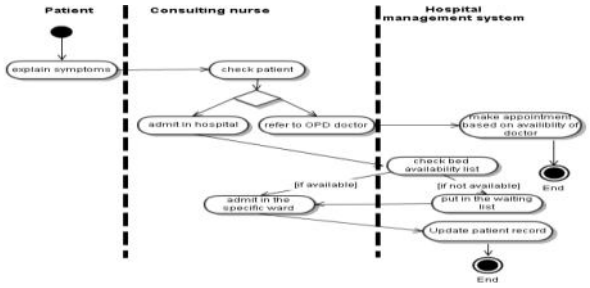

Fig. 12 Graphical scenario of system process of consultation

Functional Requirements

- **R004 make appointment**
  The consulting nurse shall use HMS to access the doctor's appointment lists and make appointments accordingly for Outpatients.
- **R005 Assign Ward**
  The consulting nurse shall use HMS to assign the patient to an appropriate ward.
- **R006 Assign to Waiting List**
  The consulting nurse shall use HPMS to assign Patient to a waiting list if no bed is available.
- **R007 Update patient's record**
  The consulting nurse shall use HMS to update Patient's record.

6.4 WORK SCHEDULING

Business process

Business process name: Work scheduling

Precondition:

Stakeholders: Administrative staff, nurses, doctors, reception staff.

- Administrative staff schedule weekend and day/night duties for doctor and nurses and other staff each week.
- Assign doctors and nurses to each patient
- Schedule surgery cases
- assign surgery room to patient
- Assign surgeon and nurses to patient
- Inform doctors, nurses and other staff about their duties.

Transformation:

- Customers: Doctors, nurses, patients, administration staff
- Actors: Doctors, nurses, patients, administration staff, developers.
- Transformation: From manual scheduling of duties to computerized work scheduling system.
- World-view: Increase efficiency by providing updated lists of patients within a reasonable time frame; doctors do not have to make rounds to pick up patients' treatment cards in order to know their condition.
- Owner: Owner of the hospital.
- Environment: All the staff should be equipped with computers and should be provided with training to use the software.

System process

The graphical scenario of the required system process is shown in fig. 13.

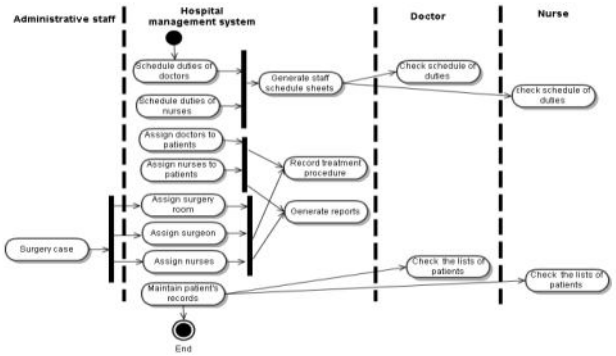

Fig. 13 Graphical scenario of system process of work scheduling

Functional Requirements

- **R008 Schedule Doctor's duties**
  The administrative staff in the ward shall use HMS to schedule day/night and weekend duties of doctors, nurses and other staff and generate schedule sheets.
- **R009 Assign Doctor**
  The administrative staff in the ward shall use HMS to assign a doctor to a given patient.
- **R010 Assign Nurse**
  The administration staff in the ward shall use HMS to assign a nurse to a given patient.
- **R011 Inform Doctors**
  The HMS shall inform doctors of new patients.
- **R012 Inform Nurses**
  The HMS shall inform nurses of new patients.
- **R013 Emergency Case**
  In an emergency case, the administrative staff shall use HMS to assign an emergency room, doctors and nurses to the patient immediately.
- **R014 Surgery case**
  In a surgery case, the administrative staff shall use HMS to assign a surgery room, surgeon and nurses to the patient.
- **R015 Generate Report (normal)**
  The HMS shall generate the patient's situation record every two hours for normal patients.
- **R016 Generate Report (Severe)**
  The HMS shall generate patient's situation record every half hour for severe patients.
- **R017 Record procedure**
  The whole treatment procedure for the patient shall be recorded by the system.
- **R018 Inform patient**
  The HMS shall automatically inform the patients who are on the bed waiting list of available beds whenever they become available.

7 EVALUATION OF PROPOSED METHOD

The preliminary evaluation of the proposed method is performed using expert reviews in order to evaluate the effectiveness of the method for performing problem analysis in RE. This section describes the participants, questionnaire; procedure used and results of the evaluation.

7.1 PARTICIPANTS

The lecturers having experience of teaching RE course and researchers doing RE research were selected as the participants of the study with the expectation that they can better assess the method due to many years of work experience. Total of six experts participated in the study. Of which two are from university of Malaya Malaysia, one from university of Putra Malaysia, one from university of Twente Netherlands and two from Mehran university of Engineering and Technology Pakistan. The average

experience of participants was 10 years of teaching/research.

7.2 QUESTIONNAIRE

The questionnaire included three categories of questions. In the first category, participants were asked to rate the effectiveness of processes of method, that are input, what it is, what is changed to what, what it will be and output of the method. In the second category, participants were asked to rate the applicability of techniques used in the method, that are scenarios, CATWOE analysis, priority scheme and analysis checklist. In the third category perception of experts towards the method were assessed through different questions, such as relevancy of theories and concepts chosen, efficiency of SSM as a front-end method, comprehensiveness of the method, effectiveness of the method etc. The scale used for all the three categories were very high-very low.

7.3 PROCEDURE

The lecturers and researchers from different countries were invited to participate in the study through emails. Those who agreed were sent all relevant documentation of the method including introduction, purpose, method itself, case study and tool setup along with the questionnaire. The responses were received in about one week time.

7.4 RESULTS

The results from first category of questions that are related to effectiveness of processes are presented in Fig. 14.

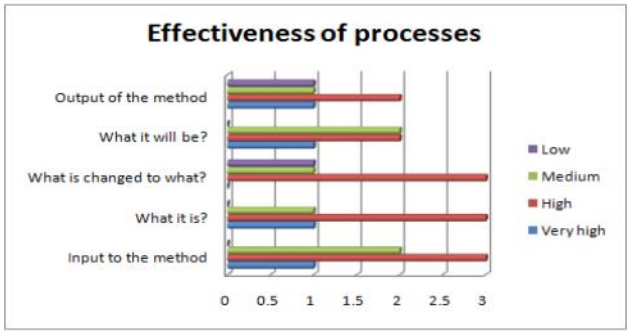

Fig. 14 Results of first category of questions

The results of second category of questions that are related to applicability of techniques used in the method are presented in Fig. 15.

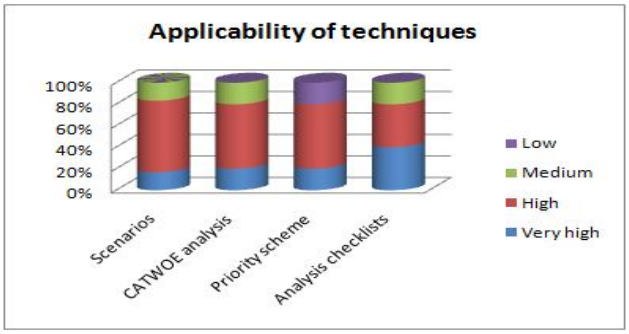

Fig. 15 Results of second category of questions

The results of third category of questions that are related to perception of experts towards method are shown in Fig. 16.

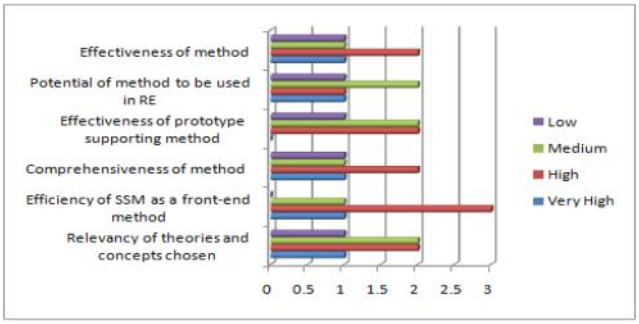

Fig. 16 Results of third category of questions

It can be noticed form the results that most of the experts have shown positive acceptance towards the method. Most of them also agreed with choice of processes and techniques of the method. Therefore it can be concluded that the method have a high potential of being used for performing problem analysis in RE.

8 LIMITATIONS OF STUDY

There are several limitations in this research. The proposed method is aimed at being easy to understand and apply RE method for performing the problem analysis process. However due to the complex nature of RE, one still need to perform a lengthy process and have to master many terms and concepts in order to cover the complete problem analysis process. In addition, the scope of the proposed method was limited to the problem analysis process only. Requirements engineers need to use requirements elicitation activities along with the proposed method in order to successfully apply the method and generate requirements. Also it does not cover complete RE process and needs to be accompanied with other RE processes and techniques.

The proposed method and tool have been developed only to make engineers perform the problem-based projects

(Problem-based projects start when a problem arise that demands a response). The blocking factors in their usage in production are they do not cover the complete RE process, plus they may not applicable to all domains. They only supports problem-based projects but not applicable to other types of projects such as contract-based or game development projects. This can also be seen as a limitation of proposed method.

9 CONCLUSION

The paper presented a method for performing problem analysis in RE to help novice requirements engineers in understanding and performing problem analysis process. The idea of using SSM in RE for problem analysis has been proposed. The method combined the concepts of SSM with RE techniques to improve its effectiveness in RE. A prototype application was developed to automate the steps of the method. The method is also applied to a case study to show its applicability in practice. The preliminary evaluation of the method was performed through expert reviews. However it is strongly needed to evaluate the method in practice by applying it on real projects. Therefore it is intended to perform an experimental validation study to assess its actual applicability and effectiveness in practice.

REFERENCES

1. Sommerville, I. and P. Sawyer, *Requirements engineering: a good practice guide*. 1997: John Wiley & Sons, Inc.
2. Alexander, I.F. and R. Stevens, *Writing better requirements*. 1 ed. 2002: Addison-Wesley Professional.
3. Gibson, J.P. *Formal requirements engineering: Learning from the students*. in *Software Engineering Conference Proceedings*. 2000. Australia: IEEE.
4. Daniels, M., et al. *Panel-Ill-structured problem solving in engineering education*. in *37th ASEE/IEEE Frontiers in Education Conference*. 2007. Milwaukee, WI: IEEE.
5. Smith, R. and O. Gotel, *RE-O-POLY: A Game to Introduce Lightweight Requirements Engineering Good Practices*, in *International Workshop on Requirements Engineering and Training*. 2007: India Habitat Center, New Delhi. p. 42.
6. Beatty, J. and V. Agouridas, *Developing Requirements Engineering Skills: A Case Study in Training Practitioners*, in *International Workshop on Requirements Engineering and Training (REET2007)* 2007: India Habitat Centre, New Delhi. p. 6-17.
7. Barnes, R.J., D.C. Gause, and E.C. Way. *Teaching the Unknown and the Unknowable in Requirements Engineering Education*. in *Requirements Engineering Education and Training*. 2008. IEEE.
8. Jackson, M., *Problem analysis and structure*. Engineering Theories of Software Construction, 1999: p. 3-20.
9. Badal, M.A., *Strategic management: problem structuring methods*, in *Informatics and Mathematical Modelling*. 2006, Technical University of Denmark.
10. Kulak, D. and E. Guiney, *Use cases: requirements in context*. Second ed. 2004: Addison-Wesley Professional.
11. Kotonya, G. and I. Sommerville, *Requirements Engineering Processes and Techniques*. 1998: John Wiley & Sons.
12. http://www.studycampus.com/PgD/itnfy/downloads/ITNFY_Lesson4.pdf. *Introduction to Soft Systems Methodology (SSM)*. 30/11/2015].
13. Robertson, S. and J. Robertson, *Mastering the Requirements Process- Getting Requirements Right*. 3 ed. 2012: Addison-Wesley Professional.
14. Anton, A.I., *Goal-based requirements analysis*, in *Second IEEE International Conference on Requirements Engineering (ICRE '96)*. 1996, IEEE: Colorado, USA. p. 136-144.
15. Rolland, C., C. Souveyet, and C.B. Achour, *Guiding goal modeling using scenarios*, in *IEEE Transactions on Software Engineering*. 1998, IEEE. p. 1055-1071.
16. Potts, C., K. Takahashi, and A.I. Anton, *Inquiry-based requirements analysis*. IEEE Software, 1994. **11**(2): p. 21-32.
17. Park, S., M. Kim, and V. Sugumaran, *A scenario, goal and feature-oriented domain analysis approach for developing software product lines*. Industrial Management & Data Systems, 2004. **104**(4): p. 296-308.
18. Sutcliffe, A., *Scenario-based requirements analysis*. Requirements Engineering, 1998. **3**(1): p. 48-65.
19. Firesmith, D., *Prioritizing requirements*. Journal of Object Technology, 2004. **3**(8): p. 35-47.